

University of Alberta

**Thermal Analysis and Pyrolysis Pathways of Coal-Related Ether
Compounds**

by

Wei Wei

A thesis submitted to the Faculty of Graduate Studies and Research
in partial fulfillment of the requirements for the degree of

Master of Science

in

Chemical Engineering

Department of Chemical and Materials Engineering

©Wei Wei

Spring 2014

Edmonton, Alberta

Permission is hereby granted to the University of Alberta Libraries to reproduce single copies of this thesis and to lend or sell such copies for private, scholarly or scientific research purposes only. Where the thesis is converted to, or otherwise made available in digital form, the University of Alberta will advise potential users of the thesis of these terms.

The author reserves all other publication and other rights in association with the copyright in the thesis and, except as herein before provided, neither the thesis nor any substantial portion thereof may be printed or otherwise reproduced in any material form whatsoever without the author's prior written permission.

Abstract

The stability of the ether bond affects coal dissolution during direct coal liquefaction and aliphatic ethers are reportedly the most reactive of the oxygenate classes during liquefaction. Some ether compounds are also persistent to high temperature during coal pyrolysis. The thermolysis of ether compounds using high-pressure differential scanning calorimetry (HPDSC) were performed to study the thermal decomposition of aliphatic and aromatic ethers. These results showed that the melting point of each ether sample is quite accurate compared to the literature data, and the high temperature decomposition could be determined. GC-MS results indicated that the ether compounds decomposed to a number of smaller and larger organic molecules. The detailed reaction pathways of the model ether compounds on their own and in the presence of a hydrogen-donor solvent were studied. These results help us to understand the role of autothermolysis of ethers versus induced thermolysis of ethers during coal liquefaction.

Keywords: Thermolysis, ether bond, Differential Scanning Calorimetry, coal liquefaction.

Acknowledgement

Firstly and foremost, I would like to say an enormous thanks to my supervisors Dr. Arno de Klerk and Dr. Rajender Gupta, for your great support and guidance. It was your encouragement that supported me to overcome challenges from the beginning of my master semester till the end of completing the thesis writing. I will always keep your valuable suggestions while I move forward in my future.

Secondly, I would like to thank Dr. Moshfiqur Rahman for your gracious help. You are not only a colleague to me, but also a dear friend. Thanks for your patience when I had trouble and I really appreciate everything you've done to me. Thanks Jun Zhao from Dr. Murray Grey's group, you are truly a good friend to me and your great support guide me through the darkest day. Thanks to all the group members of Dr. Arno de Klerk and Dr. Rajender Gupta, you guys are awesome and I enjoyed working with you guys very much.

Finally, I would like to give thanks to my whole family, thanks for your love and please always remember I love you guys very much.

Table of Contents

Chapter One: Introduction	1
1.1 Problem Statement	1
1.2 Objectives	2
1.2.1 General Objective	2
1.2.2 Specific Objectives	3
1.3 Justification	3
1.4 Reference	4
Chapter Two: Literature Review	5
2.1. Overview of Solvent Extraction of Coal	5
2.1.1. Coal Composition and Coal Rank	5
2.2 General Survey on the Solvent Extraction of Coal	8
2.2.1 Pre-treatment of Coal before Extraction	10
2.2.2 Extraction Temperature	11
2.2.3 Coal Properties	11
2.2.4 Solvents	13
2.3 Coal Liquefaction	14
2.4 The Role of Ether Groups during Coal Liquefaction	16
2.5 Chemistry of Ether Linkage	20
2.5.1 Review of Ether Compounds	21
2.5.2 Cleavage of C-O-C Bond	22
2.5.3 Pyrolysis of Ether	23

2.6 Thermolysis of Ethers during Coal Liquefaction	25
2.6.1 Coal Related Aryl Alkyl Ethers	25
2.6.2 Overall effect of coal-related model ethers on coal liquefaction	36
2.7 Remarks	36
2.8 Reference	38
Chapter Three: Heat Effects Study of Coal Digestion Using DSC	46
3.1 Introduction	46
3.2 Objectives	47
3.3 Experimental	47
3.3.1 Materials	47
3.3.2 Equipment	49
3.3.3 Procedures	51
3.4 Results	56
3.4.1 Cp measurement for solvent	56
3.4.2 DSC result for coal digestion	56
3.5 Discussion	57
3.5.1 Cp calculation for solvent	57
3.5.2 DSC analysis for coal digestion	58
3.6 Reference	59
Chapter Four: Thermal Study of Coal Related Ether Compounds Using DSC	61
4.1 Introduction	61
4.2 Objectives	61

4.3 Experimental	62
4.3.1 Materials	62
4.3.2 Equipment	64
4.3.3 Procedures	65
4.4 Results	
4.4.1 Thermal Analysis of Benzyl Phenyl Ether	66
4.4.2 Thermal Analysis of Dibenzyl Ether	70
4.4.3 Thermal Analysis of Diphenyl Ether	73
4.5 Discussion	75
4.5.1 Benzyl phenyl ether	76
4.5.2 Dibenzyl ether	77
4.5.3 Diphenyl ether	78
4.6 Conclusions	78
4.7 Reference	79
Chapter Five: Reaction Pathway of Coal Related Ether Compounds	81
5.1 Introduction	81
5.2 Experimental chemicals	81
5.2.1 Coal related ether compounds	81
5.2.2 Solvents	82
5.3 Experimental equipment	83
5.4 Experimental design	88
5.5 Experimental procedure	89
5.5.1 Reactor Feed and Loading	89

5.5.2 Reactor sealing and purging with nitrogen	89
5.5.3 Reaction	93
5.5.4 Product Recovery and Analysis	93
5.5.5 Validation of Experimental Method	95
5.6 Results	108
5.6.1 Reaction Network Pure Dibenzyl Ether (DBE)	108
5.6.2 Reaction Network Pure Benzyl Phenyl Ether (BPE)	116
5.6.3 Reaction of dibenzyl ether with solvents	123
5.6.4 Reaction of benzyl phenyl ether with solvents	133
Chapter Six: Conclusions and Recommendations	140
6.1 Conclusions	140
6.2 Recommendations for future study	141

List of Figures

Figure 2.1 Different forms of water/moisture associated with coal	12
Figure 2.2 Sample reaction network of ether cleavage with acid	19
Figure 2.3 Reaction pathways of benzyl phenyl ether	30
Figure 2.4 Reaction network for DBE thermolysis in supercritical water	34
Figure 3.1 Distillation profile of solvent sample obtain from Simdist	48
Figure 3.2 Cp calculation result for solvent	56
Figure 3.3 Calorigram of coal digestion process	56
Figure 3.4 DSC calorigram of coal digestion subtracted the DSC calorigram of solvent to study the heat effects of coal digestion	57
Figure 4.1 Temperature program for benzyl phenyl ether decomposition	67
Figure 4.2 Calorigram of benzyl phenyl ether thermolysis behavior	68
Figure 4.3 Temperature program for benzyl phenyl ether melting behavior	68
Figure 4.4 Calorigram of benzyl phenyl ether to determine melting behavior	69
Figure 4.5 Chromatogram obtained from benzyl phenyl ether thermolysis.	69
Figure 4.6 Temperature program for dibenzyl ether decomposition	71
Figure 4.7 Calorigram of dibenzyl ether thermolysis behavior	71
Figure 4.8 Temperature program for dibenzyl ether melting behavior	72
Figure 4.9 Calorigram of benzyl phenyl ether to determine melting behavior	72
Figure 4.10 Temperaturefor diphenyl ether thermal decomposition behavior	73
Figure 4.11 Calorigram of diphenyl ether thermal decomposition behavior	74
Figure 4.12 Temperature program for diphenyl ether melting behavior	74
Figure 4.13 Calorigram of diphenyl ether to determine melting behavior	75

Figure 5.1 Schematic of the micro reactor setup	85
Figure 5.2 Image of the sand bath	87
Figure 5.3 Schematic of the nitrogen cylinder setup	91
Figure 5.4 Internal reactor temperature as a function of time for a reaction with a sand bath set-point of 300 °C	96
Figure 5.5 Internal reactor temperature as a function of time for a reaction with a sand bath set-point of 350 °C	97
Figure 5.6 Internal reactor temperature as a function of time for a reaction with a sand bath set-point of 400 °C	97
Figure 5.7 Internal reactor temperature as a function of time for a reaction with a sand bath set-point of 450 °C	98
Figure 5.8 Overall comparison of the temperature profile	98
Figure 5.9 Mass balance of DBE reacted with different solvents at °C with DBE:Solvent=9:1	102
Figure 5.10 Mass balance of DBE reacted with different solvents at °C with DBE:Solvent=1:1	102
Figure 5.11 Mass balance of DBE reacted with different solvents at °C with DBE:Solvent=1:9	103
Figure 5.12 Triplicated experiments of DBE with mesitylene at 400 °C with ratio	104
Figure 5.13 Products distribution of DBE with mesitylene at 400 °C with ratio 1:1	105
Figure 5.14 Products distribution of DBE with tetralin at 400 °C ratio 1:1	106

Figure 5.15 Triplicated experiments of DBE with mesitylene at 400 °C 1: 1	106
Figure 5.16 Products distribution of DBE with naphthalene at 400 °C 1:1	107
Figure 5.17 reaction network of pure DBE at 350 °C.	110
Figure 5.18 Additional reaction of pure DBE at 400 °C experimental results	113
Figure 5.19 Additional reactions of DBE at 450 °C	116
Figure 5.20 Reaction network of pure BPE at 350 °C.	119
Figure 5.21 Additional reactions of DBE at 400 °C	122
Figure 5.22 Reaction network of DBE with Mesitylene at 350 °C	127
Figure 5.23 Reaction network of DBE with naphthalene at 350 °C	129
Figure 5.24 Reaction network of DBE with tetralin at 350 °C	130
Figure 5.25 Additional reaction network of BPE with mesitylene at 350 °C	136
Figure 5.26 Additional reaction network of BPE with naphthalene at 350 °C	137

List of Tables

Table 2.1 Classification of Coals by Rank	7
Table 2.2 Summary of selected solvent extraction processes	10
Table 2.3 Comparison of direct liquefaction, indirect liquefaction	15
Table 2.4 Ether studied prior to 1953	24
Table 2.5 Thermal cracking of diaryl ethers in tetralin	31
Table 2.6 Pyrolysis products of BPE and alkylaryl ether at 600 °C	32
Table 2.7 Pyrolysis products of diphenyl ether and dibenzofuran at 600 °C	33
Table 2.8 Coal minerals thermal treatment of benzyl ethers in tetralin	35
Table 3.1 Proximate analysis of the coal sample	48
Table 3.2 Temperature and caloric calibration of DSC	52
Table 3.3 DSC Experimental Conditions for coal digestion	54
Table 3.4 Parameters of Cp sapphire measurement	55
Table 4.1 Melting Point and Onset of Thermolysis of Ethers	75
Table 5.1 Detailed information of the ether compounds using for this study	82
Table 5.2 Detailed information of the solvents using for this study	83
Table 5.3 Determined GC-FID response factors of linear ethers	95
Table 5.4 Sample mass balance of DBE reacted with different solvents at °C with different ratios	101
Table 5.5 Triplicated runs of DBE with mesitylene at 400 °C with ratio 1: 1	104
Table 5.6 Triplicated runs of DBE with tetralin at 400 °C with ratio 1: 1	105
Table 5.7 Triplicated runs of DBE with naphtalene at 400 °C with ratio 1: 1	107
Table 5.8 Reaction product of DBE at 350 °C	109

Table 5.9 Reaction product of DBE at 400 °C	112
Table 5.10 Reaction product of DBE at 450 °C	115
Table 5.11 Reaction product of BPE at 350 °C	118
Table 5.12 Reaction product of BPE at 400 °C	121
Table 5.13 Reaction product of BPE at 450 °C	123
Table 5.14 Major products of DBE with solvents	125
Table 5.15 Major products of BPE with solvents at 350 °C	134
Table 5.16 Major products of BPE with solvents at 350 °C (Cont.)	135

Chapter One: Introduction

1.1 Problem statement

It has been commonly accepted that in coal there are 'bridge' bonds between oxygen and methylene (-CH₂-) groups and breaking of these bonds initiate thermal conversion and liquefaction of coal. Therefore, thermolysis of ethers modeling bridge bonds in coals has attracted extensive attention (Van Krevelen, 1980). Most investigations that have been done involved some model compounds such as benzyl phenyl and dibenzyl ethers. However, the goal of these investigations is limited to the study of specific experimental condition (e.g. the role of solvents, catalysts, initiators and stabilizers on chain conversion). In the literature that directly compared the reactivity of ethers, the degree of conversion served as the main criterion (Carson and Ignasiak, 1980; Takemura et al., 1981; Cassidy et al., 1982). However, the experimental conditions being different, no systematic comparison was possible.

Knowledge of the organic composition of coals, especially for the oxygenated functional groups, such as ether, is very important for understanding the basic chemistry involved in coal liquefaction, gasification and pyrolysis and for the potential development of new approaches to depolymerization. This kind of study is principally important in view of the hypothesis that cleavage of reactive ether linkages could be one of the most important

routes involved in coal depolymerization. Because of their relatively high concentration in subbituminous and bituminous coals and their high reactivity, these components are considered as key functional components in various studies. Particular emphasis has been placed on elucidating the thermal mechanisms leading to the formation of hydroxyaromatics and on ascertaining the nature and environment of the bonds cleaved and rearranged in this process (Siskin and Aczel, 1983).

The development of a basic understanding of the behavior of organically bound oxygen during the thermal decomposition of coal presents a special challenge. As we can see, the pyrolytic reactions of low rank coals are especially interesting because aromatic and aliphatic ethers are so prevalent in these materials. Thus, knowledge of the decomposition reactions of the coal related ethers is necessary for a better understanding of the basic chemistry involved in coal conversion processes.

1.2 Objectives

1.2.1 General objective

The main objective of the study is to carry out reactions of coal related model compounds (ethers) in the reactive regime of solvent extraction of coal to understand the role and fate of coal related ethers. Furthermore, it may be possible to find out the way in which ethers

decompose, and how it affects the product quality and liquid yield of solvent extraction processes.

1.2.2 Specific Objectives

- Systematically study the thermolysis of coal related ethers.
- Systematically study the reaction network of coal related ethers under different solvent environments over the temperature range from 300 to 450 °C.
- Thermal analysis of the coal digestion process: using DSC to analyze the thermal behavior of industrial solvents from the coal liquefaction process.

1.3 Justification

The present work is to set the basis to further understand the solvent extraction of coal mechanism, by establishing fundamental knowledge on the effect of the functional group, which is the ether linkage (R-O-R). This will allow rational selection of the most effective functional groups in the solvent used for liquefaction and the systematic evaluation of the combined properties of solvent mixtures. Once enough knowledge on the fundamentals of the solvent extraction of coal process is gained, an improved design may be proposed.

1.4 References

Carson, D. W. and Ignasiak, B. S. “Polymeric structure of coal. 3. Re-examination of the role of ether bonds in reduction of molecular weight of a low-rank vitrinite treated with hydrogen donor.” *Fuel* 62.11(1980): 757-761

Cassidy, P. I.; Hertan, P. A.; Jackson, W. R.; Larkins, F. P. and Rash, D., “Hydrogenation of brown coal. 3. Roles of hydrogen and hydrogen-donor solvents in systems catalysed by iron and tin compounds.” *Fuel* 61.10 (1982): 939-946

Siskin, M and Aczel, T., “Pyrolysis studies on the structure of ethers and phenols in coal” *Fuel* 62.2 (1983): 1321-1326.

Takemura, Y.; Itoh, H. and Ouchi, K., “Hydrogenolysis of coal-related model compounds by carbon monoxide-water mixture.” *Fuel* 60.5(1981): 379-384

Chapter Two: Literature Review

2.1. Overview of Solvent Extraction of Coal

2.1.1 Coal Composition and Coal Rank

Coal is composed of a complex mixture of organic and inorganic compounds. Figure 2.1 shows the elemental composition of a generic coal sample. Chemical composition of coal can vary over a wide range. The organic compounds in coal are composed of carbon, hydrogen, oxygen, nitrogen, sulfur, and trace amounts of a variety of other elements. The organic compounds in coal produce heat when coal is combusted; they can also be converted to synthetic fuels or may be used to produce the organic chemicals (Schweinfurth, 2009).

Harvey and Ruch did an over view of mineral matter in coals from different places in US. Although the mineral composition of coal varies based on the geological deposits of the coal, they stated that the most abundant minerals in coal are clay minerals such as kaolinite and smectite, oxidize such as quartz, and sulfide and carbonate such as pyrite and calcite. Many other minerals have also been found in coal. During coal gasification, the crystalline of almost all the minerals will be destroyed by the high temperature, and those “reacted” minerals are in the slag layer after the coal liquefaction (Groen and Craig, 1994). Some minerals are found to have catalytic effect during coal liquefaction. Pyrite in the coal is

found particularly active during coal liquefaction. With the presence of pyrite, hydrocracking of coal can be increased and hydrogenation of the product is enhanced (Hirano et al., 1999). Coal liquefaction can be conducted with or without catalysts, but catalysts can be used as an advantage to increase the yield. When there is mineral matter present in the coal, their catalytic effect can be beneficial. Also the presence of sulfur or pyrite in coal is related with an increase in coal conversion (Ishihara et al., 2004).

American Society for Testing and Materials (ASTM) provided a detailed table for coal by rank, which is shown in Table 2.1

Table 2.1 Classification of Coals by Rank

Class/Group	Fixed Carbon Limits (Dry, Mineral-Matter Free), %		Volatile Matter Limits (Dry, Mineral-Matter-Free), %		Gross Calorific Value Limits (Moist, and Mineral Matter Free Basis), MJ/kg		Agglomerating Character
	Equal or Greater Than	Less Than	Greater Than	Equal or less than	Equal or Greater Than	Less than	
Anthracitic:							Non-agglomerating
Meta-anthracite	98	-	-	2	-	-	
Anthracitic	92	98	2	8	-	-	
Semianthracitic	86	92	8	14	-	-	
Bituminous							Commonly Agglomerating
Low volatile bituminous coal	78	86	14	22			
Medium volatile bituminous coal	69	78	22	31			
High volatile A bituminous coal	-	69	31	-	32.56	-	
High volatile B bituminous coal	-	-	-	-	30.23	32.56	
High volatile C bituminous coal	-	-	-	-	26.74	30.23	
Subbituminous							Non-agglomerating
Subbituminous A Coal	-	-	-	-	24.42	26.74	
Subbituminous B Coal	-	-	-	-	22.09	24.42	
Subbituminous C Coal	-	-	-	-	19.30	22.09	
Lignite							
Lignite A	-	-	-	-	14.65	19.30	
Lignite B	-	-	-	-	-	14.65	

Lignite and subbituminous coal are called low rank coal, and bituminous and anthracite coal are known as high rank coals. According to the coal rank, the composition of coal varies; the sulfur content can vary from 1 wt. % to a very high concentration. The nitrogen content may be varying from 0.5 up to 2% (Wen et al., 1979). For bituminous coal, the structure generally consists of an aggregate of condensed aromatic and aliphatic rings linked by single bonds (Mayo et al., 1988).

For coal characterization, there are two different analysis methods commonly used, the proximate and the ultimate analysis. The proximate analysis determines moisture content, volatile matter content, ash content and fixed carbon (Berkowitz, 1979). The ultimate analysis determines the elemental composition of the coal, in which carbon, hydrogen, nitrogen, sulphur (organic) and oxygen are determined quantitatively (Berkowitz, 1979).

2.2 General Survey on the Solvent Extraction of Coal

Solvent extraction of coal has been performed effectively by numerous researchers (Bland et al., 2002). Coal partially dissolves in a number of solvents. A wide range of organic solvents can be used, but dissolution is never complete and usually requires heating to temperatures sufficient for some thermal degradation or solvent reaction to take place. Solvent extraction processes usually use liquids (often derived from the feed coal) as “donor” solvents, which are capable of donating hydrogen to the system under the

conditions of the reaction. General results show increased (relative to pyrolysis processes) amount of coal transformed to lower molecular weight, that is, solvent soluble products. Hydrogenation can occur if hydrogen can be introduced under pressure and 510 °C. This hydrogen can be generated from many unrelated coal or feed coal processes, or from by-product gases.

In solvent extraction processes, coal is mixed with a solvent that is capable of achieving the transfer of hydrogen from the solvent to coal (or from gaseous hydrogen to the coal) at temperatures up to 500 °C and pressures up to 34.5 MPa. (Braunstein, H.M. et al., 1986)

There are three different process configurations established for high-temperature solvent extraction processes:

- Extraction without hydrogen but using a recycle solvent that has been hydrogenated in a separate stage
- Extraction with hydrogen and with a recycle solvent that has not been previously hydrogenated
- Extraction with hydrogen and with a hydrogenated recycle solvent (Table 3.1)

In each of these configurations, the distillates of process-derived liquids have been used effectively as the recycle solvent that is recovered incessantly in the process.

Table 2.2 Summary of selected solvent extraction processes

Process	Developer	Reactor	Temperature		Pressure (MPa)	Residence Time (h)
			°C	°F		
Consol	Conoco	Stirred tank	400	750	1.0-3.1	<1
Synthetic fuel (CSF)						
Solvent-refined coal (SRC)	Pittsburgh and Midway Mining Co.	Plug flow	~450	840	6.9-10.3	<1
Solvent-refined lignite (SRL)	University of North Dakota Costeam	Plug flow	370-480	700-895	6.9-20.7	-1.4
Exxon donor solvent (EDS)	Exxon Research and Engineering Co.	Plug flow	425-480	795-895	10.3-13.8	0.25-2.0

Source: Braunstein, H.M. et al., Eds., *Environmental, Health, and Control Aspects of Coal conversion*, Oak Ridge National Laboratory, Oak Ridge, TN, 1977, Vol.1.

2.2.1 Pre-treatment of Coal before Extraction

It has been presented in the past that solvent extraction of coal can be enhanced with numerous kinds of pre-treatment, one of which is thermal pre-treatment.

Bland et al (2002) observed that when certain coals were heated to 200-400 °C in an inert atmosphere, cooled and extracted with solvents, the yield was higher than that of untreated coals.

2.2.2 Extraction Temperature

Bland et al. (2002) found that an increase in temperature can amplified the extent of extraction. Coal is decomposed into smaller molecular entities; this process is known as solvolysis, which refers to the action of solvents on coal. The temperature of slovolysis is at when the coal substance decomposes. In practice, it relates in particular to extraction at temperatures between 200 and 400 °C (390 and 750 °F). At temperatures below 350 °C (660 °F), the solvent power of the extracting liquid appears to be solely determined by the ability of the solvent to alter the coal physically (by swelling) prior to the onset of the degradation (depolymerization) process. At temperature excess of 350 °C (660 °F) the coal undergoes decomposition without the aid of the solvent but the solvent is necessary insofar as the radicals generated during the decomposition process must be prevented from forming higher-molecular-weight materials such as hydrogen-deficient chars or cokes.

2.2.3 Coal Properties

Moisture

Moisture is an important property of coal, since all coals are mined wet. Ground water and extraneous moisture is known as adventitious moisture and can be evaporated. Moisture within the coal is known as inherent moisture. Moisture may occur in four possible forms: surface moisture, hygroscopic moisture, decomposition moisture and mineral moisture. To

analyze the moisture, the mass loss between an untreated coal sample and the treated coal sample is defined as the moisture.

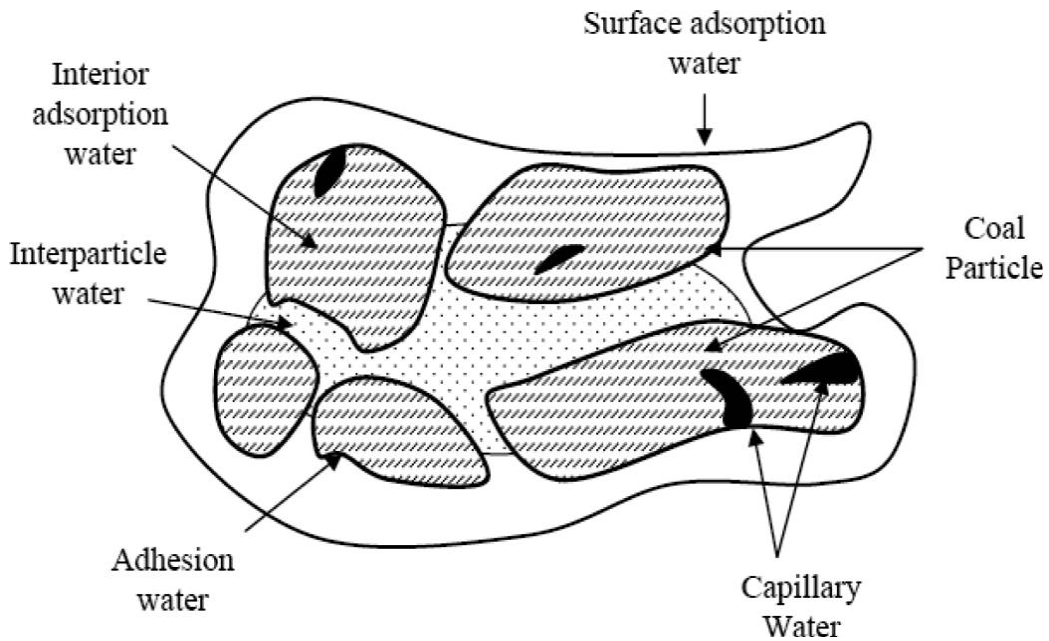


Figure2.1 Different forms of water/moisture associated with coal (Karthikeyan et al., 2009)

Volatile matter

Volatile matter refers to the components of coal, which are liberated at high temperature without air.

Ash content

Ash content of coal is the non-combustible residue left after coal is burnt. It represents the

bulk mineral matter after carbon, oxygen, sulfur and water have been fully burnt and the ash material expressed as a percentage of the original weight. It can also indicate the quality of coal.

Fixed carbon

The fixed carbon content of the coal is the carbon found in the material, which is left after volatile matters are removed. Fixed carbon is used as an estimate of the amount of coke that will be yielded from a coal sample.

2.2.4 Solvents

Based on Gadam's (1990) study, aromatic solvents are more effective than neutral aliphatic solvents. Whether the interaction of coal and solvent is physical or chemical in nature is uncertain. It is still in debate that certain organic liquids make more than a solvent action on coal. A sign of chemical interaction is found from the observation that the total weight of the products from time to time goes beyond that of the original coal. (Brand et al, 2002). It has been approved that nitrogen-containing compounds gave higher extraction yields than the other solvents and the nitrogen-to-carbon values of the extract were much higher when dimethylnaphthalene (DMN) and crude methylnaphthalene oil (CMNO) were used as extraction solvent. Yoshida et al. (2004) investigated the effects of the addition of polar

compounds to the extraction solvent. His study shows the addition of polar additives increased the extraction yields by 1%-7%, and when additives were used, the ash content in the extracts ranged from 0.039% to 0.071%.

2.3 Coal Liquefaction

Coal liquefaction is a process that converts coal from a solid state into liquid fuels, usually to provide substitutes for petroleum products. This process is a combination of physical and chemical processes to get liquid products from coal by using physical dissolution in a solvent or thermal decomposition in combination with a solvent. Liquefaction of coal is additionally achieved by incorporation of hydrogen into the coal structure through a hydrogenation process. The liquefaction processes are classified as coal pyrolysis, direct conversion to liquids processes and indirect conversion to liquids processes.

Pyrolysis involves the heat treatment of coal at temperature above 400 °C and low pressure to convert the coal into gases, liquids, and char. (Deepak and Michael, 1984) Direct coal liquefaction involves the conversion of solid coal to liquids without the process of producing synthesis gas as an intermediate step. In direct coal liquefaction, coal, a coal derived hydrogen donor solvent and molecular hydrogen gas react under temperature and pressure with or without catalysts to yield liquid hydrocarbons. Direct coal liquefaction should be the most efficient method of liquid production and this method makes it possible to obtain the highest oil

yield. Many technologies were developed for direct coal liquefaction, such as hydrolysis, pyrolysis in the presence of high pressure hydrogen and coal extraction using solvent and/or critical gas.

In indirect coal liquefaction, coal is first gasified in the presence of steam and oxygen to form syngas which contains carbon monoxide and hydrogen. The temperature can be very high (more than 1000 °C). Syngas is then converted to liquids by means of a catalyst in a syngas conversion process, such as Fisher–Tropsch (FT) synthesis. A unique characteristic of indirect liquefaction is the ability to produce a broad array of sulfur and nitrogen free products (Table 2.1).

Table 2.3 Comparison of direct liquefaction, indirect liquefaction and conventional crude oil conversion (King and de Klerk, 2011)

Description	XTL Conversion		Crude Oil
	Direct	Indirect	
Conversion Process			
Feed Properties Affect conversion Technology	Yes	No ^a	-
Feed Properties Affect Product Properties	Yes	No	Yes
Feed C-C Bonding Retained To Some Extent	Yes	No	Yes
Product Phase From Primary Feed Conversion	Liquid	Gas	Liquid ^b
Liquid Products Properties			
Contains Sulfur	Yes	No	Yes
Contains Nitrogen	Yes	No	Yes
Contains Oxygen	Yes	Yes	Yes

a. Some technology selection is affected by the nature of the feed, for example, gasifier type

Liquid products of direct liquefaction processes are much more aromatic than indirect liquefaction processes. DCL (Direct Coal Liquefaction) naphtha can be used to make very high octane gasoline component. DCL distillate is poor diesel blending component due to high aromatics, which results in low cetane number (include number) versus U.S. average of about 46. Raw DCL liquids still contain contaminants like sulfur, nitrogen, and oxygen, possibly metals and require extensive hydro-treatment to meet Clean Fuels Specifications.

The characteristics of Direct Coal Liquefaction

- Direct liquefaction carbon efficiency is higher than indirect technology.

One ton of a high volatile bituminous coal can be converted into approximately three barrels of high quality distillate synthetic crude for refinery upgrading and blending

- Direct liquefaction provides high octane, low sulfur gasoline and a distillate that will require upgrading to make an acceptable diesel blending stock.

2.4 The Role of Ether Groups during Coal Liquefaction

A lot of effort has been made in recent years to further understand the structure of coal and to achieve a fundamental understanding of the mechanism of coal liquefaction (Sternberg et al., 1971). Many models have been made to explain and correlate data obtained from liquefaction experiments. In most of those studies, species are lumped or grouped by

similarity were studied. However, the mechanism of coal liquefaction depends not only on operating parameters such as nature of the donor solvent, temperature and pressure but also on the characteristics and rank of the feed coal. Consequently, the chemical bonds of different coal compounds will affect the whole process and possibly the liquid yield.

The presence of labile linkages, such as ether groups, in the lattice networks would presumably hasten the combination of the coal matrix. The presence of ether bonds in coal has been inferred from alkali metal reduction studies (Sternberg et al., 1971; Ignasiak and Gawkak, 1977; Wachowska and Pawlak, 1977) in which the products were significantly more soluble in pyridine, were of a lower molecular weight and were of a higher phenolic content. Siskin and Aczel (1983) carried out a parallel study on coal pyrolysis and model compounds. By selectively blocking existing hydroxyl groups, they were able to determine the hydroxyl groups, which were generated by ether cleavage during pyrolysis.

In an earlier study it was reported that Wyoming coal (PSOC-521) had a slower conversion in spite of its higher number of cleavable ethers (Youtcheff and Given, 1982). The authors proposed two reasons for the observation: ethers constitute multiple cross-links that conversion of many THF-solubles requires cleavage of these ethers; the cleavage of ethers is slow. From its low apparent activation energy for conversion to THF-solubles and for unaccounted oxygen (oxygen from functional groups other than hydroxyl group) removal, it is inferred that this coal is extensively cross-linked by ether linkages. Similar changes in

activation energies were obtained with level of total conversion and extent of unaccounted oxygen removal for any coal up to more than 50% conversion. Since the removal of unaccounted oxygen consists of ether cleavage, ether cleavage continues to be important, not only in the earliest stages of coal liquefaction (Yotcheff et al., 1983).

Siskin et al (1993) studied the cleavage of diphenyl ether, 1-phenoxy-naphthalene, and 9-phenoxyphenanthrene in thermolytic and aquathermolytic conditions. They found that diphenyl ether was stable at 315 °C unless 15% sodium formate or 15% phosphoric acid were present. Thus, acidic condition might enhance ether cleavage under hydrolysis condition. Depending on the density of these ether linkages and their importance as crosslinks in the macromolecular structure of coals, solubility might be significantly improved solely by cleaving and capping ether bonds. Among the diaryl ether and dialkyl ether model compounds tested by pyrolysis at 600 °C, benzylic ethers are found to be the most unstable that they form hydrocarbon products and carbon monoxide during the pyrolysis, hence they have been implicated in the initiation of coal pyrolysis (Siskin and Aczel, 1983) and hydrolysis (Tanner and Bell, 1981). Arylation, the use of acids to cleave bonds in coals in the presence of aromatic rings to trap the consequent incipient carbonium ions, has a long history (Larsen and Kuemmerle, 1976). They provided an example reaction:

The importance of aromatic ether structures (Eds et al., 1982; Shah, 1982) in coal molecules has also been stressed and thermal cracking of several aromatic ethers has been studied by a few researchers (Schlosberg et al., 1981; Panelker et al., 1982), in order to elucidate the coal liquefaction mechanism. It is known that aliphatic ethers can be easily decomposed thermally, but diaryl ethers such as diphenyl ether are quite stable at temperatures as high as 450 °C. Kamiya et al (1986) stated that aryl ether is one of the key structures in coal liquefaction, so they thermally cracked several coal model diaryl ethers to study the effect of ring structure and effect of solvents. They found that some diaryl ethers with polycyclic aromatic nuclei could be cracked relatively easily at 450 °C. They also reported that the scission of phenyl-oxygen bond is the slowest reaction during thermal cracking of the diaryl ether they studied. The bond dissociation energy for the phenyl-oxygen bond is the higher than other aryl-oxygen bonds and that for other aryl-oxygen bonds decreases with increasing number of rings in the polycyclic nuclei (Kamiya et al., 1986).

2.5 Chemistry of Ether Linkage

2.5.1 Review of Ether Compounds

In contrast to alcohols with their abundant capacity for chemical reactions, ethers

(hydrocarbon compounds containing the C-O-C unit) are relatively non-reactive. This lack of reactivity makes them valuable as solvents in a number of synthetically important transformations. Unlike most ethers, epoxides (compounds which the unit forms of an O-containing three-membered ring) are very reactive substances. Sulfides (R-S-R') are the sulfur analogs of ethers.

Ethers are compounds of the general formula: R-O-R, Ar-O-R or Ar-O-Ar (where Ar is a phenyl or some other aromatic groups). As we can see in Figure 2.3, since the C-O-C bond angle is not equal to 180 degrees, the dipole moment of the two C-O bonds do not cancel each other out. Consequently, ethers possess a small dipole moment.

This weak polarity does not appreciably affect the boiling points of ethers, which are about the same as those of alkanes having comparable molecular weights, and much lower than those of isomeric alcohols with similar chemical formula. The boiling points of *n*-heptane (98 °C), methyl *n*-pentyl ether (100 °C) and *n*-hexyl alcohol (157 °C) are examples to illustrate the point. The hydrogen bonding, which holds alcohol molecules tightly together, is not possible for ethers, since the hydrogen they contain is only bonded to carbon.

The solubility of ethers in water is comparable to that of alcohols. For example, diethyl ether and *n*-butyl alcohol are both soluble to the extent of about 8g per 100g of water. This can be attributed the water solubility of the lower alcohols to hydrogen bonding between water molecules and alcohol molecules. The water solubility of ether arises in a similar

way. This occurs via the unshared electron pairs on oxygen. Thus, ethers can accept hydrogen bonds which are provided by water molecules.

2.5.2 Cleavage of C-O-C Bond

Ethers are comparatively non-reactive compounds. The ether linkage is quite stable towards bases, oxidizing agents, and reducing agents. Ethers undergo just one kind of basic chemical reaction: cleavage by acids.

Cleavage reactions of ethers can be classified into the following groups:

1. Cleavage by acidic reagents which involve some sort of a generalized oxonium salt intermediate.
2. Cleavage by nucleophilic reagents in the absence of acids.
3. Cleavage by alkali metals.
4. Cleavage by reaction involving heterogeneous catalysts.

The first three types of reaction, when described in terms of existing theories of the mechanism of organic reactions, are described primarily as bimolecular nucleophilic displacement reactions (S_N2). The cleavage of a carbon-oxygen bond in ethers has many points of similarity to the cleavage of the same bond in alcohols. One thinks of alcohols as being more reactive than ethers, but this is true only in terms of the ready cleavage of the oxygen-hydrogen bond of alcohols. Reactions involving the cleavage of carbon-oxygen

bonds occur at least as readily in ethers as in alcohols and in some cases more easily. Cleavage of this bond in ethers by nucleophilic reagents alone needs displacing species of very high nucleophilic potential. Since such species are normally very strong bases, they would eliminate a proton from an alcohol. The resulting alkoxide ion would be much less reactive in these reactions than would ether, owing to the negative charge on the alkoxide ion. (Robert, L. and Burwell, Jr., 1954)

2.5.3 Pyrolysis of Ether

Studies of the pyrolysis of organic ethers have been largely confined to the smaller molecules. Kineticists have conducted much research over the years in attempts to elucidate the nature of the elementary processes that occur in organic pyrolysis. The study of the thermal decompositions of simple hydrocarbons, simple aldehydes and ketones, as well as such ethers as dimethyl and diethyl ether, have generated a lot of information about the nature of free-radical reactions. (Patai, 1967)

Steacie (1954) summarized the work done prior to 1953 on the ethers listed in Table 2.5. In every case the overall mechanism is uncertain. Later work is equally fragmentary, with a few exceptions.

Table 2.4 Ether studied prior to 1953^a

Ether	Free radical present	Inhibited by nitric oxide
Methyl ethyl	Yes	Yes
Ethyl propyl	Yes	Yes
Dipropyl	Yes	Yes
Methyl butyl	Yes	Yes
Vinyl ethyl	Yes(above 537 °C)	No
Divinyl	Yes	—
Vinyl allyl	No	No
Diphenyl	Yes	—
Dibenzyl	Yes	—
Dioxane	Yes	Yes
Tetrahydrofuran	Yes	No
Dioxolane	Yes	Yes
2,2'-Dichlorodiethyl	(Probably)	—
Phenyl methyl	Yes	—

^a Brief summaries are given by Steacie (1954)

Elkobaisi and Hickinbottom (1959) thermally decomposed a series of aromatic ethers. The mechanisms are undoubtedly complicated as was evident from the variety of products. The pyrolysis were carried out by heating the ether (alone or in a suitable solvent) at 250-270 °C for periods ranging from 10 to 17 days in sealed tubes. Generally not all of the products could be identified. Benzyl phenyl ether yielded such major products as *o*- and *p*-benzylphenols and 2,4-dibenzylphenol with some phenol, toluene and 9-phenylxanthen.

Diphenylmethyl phenyl ether formed tetraphenylethane, phenol and some diphenylmethane, *o*- and *p*-tolyl, 2,4-dimethylphenyl and 2,6-dimethylphenyl benzyl ethers also produced toluene and the corresponding xanthenes. They established that the reactions proceed by a free-radical mechanism. Therefore in the presence of the solvent quinoline, benzyl phenyl ether yields benzyl and phenoxy radicals, since both benzyl and phenoxy substituted quinolines were found in the products (Elkobaisi and Hickinbottom, 1959).

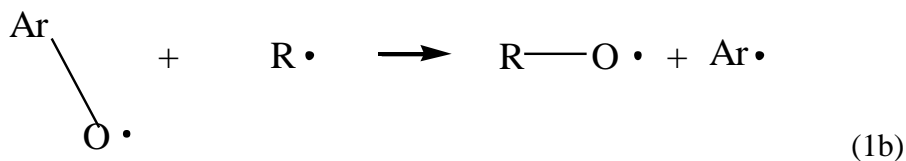
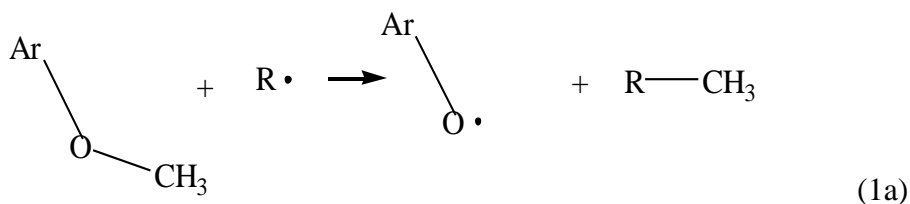
2.6 Thermolysis of Ethers during Coal Liquefaction

2.6.1 Coal Related Aryl Alkyl Ethers

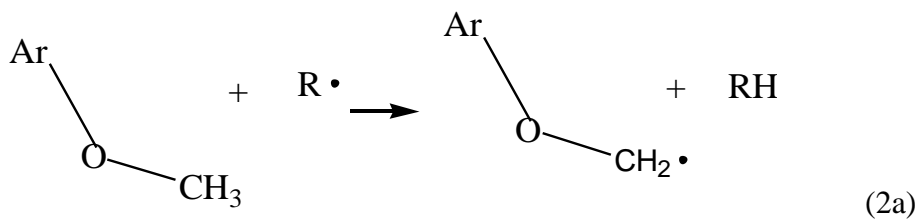
Siskin and Aczel (1983) found that phenols are formed by the scission of alkyl-oxygen bonds in the aryl alkyl ethers during pyrolysis at 600 °C. They used potassium to convert phenols originally in coal into potassium oxides, which would not give any liquids that boil when <600°C. That was how they separated the contribution to liquid pyrolysates of the phenolic functional groups already existing in coal and the contribution of same groups generated by ether cleavage during the pyrolysis. On the other hand, diaryl ethers and heterocyclic ethers such as dibenzofuran are stable and do not form phenols during pyrolysis at 600 °C. Notwithstanding, many uncertainties remain in these studies. The

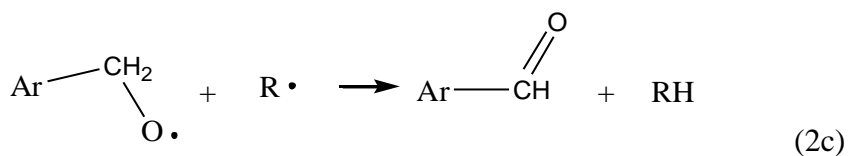
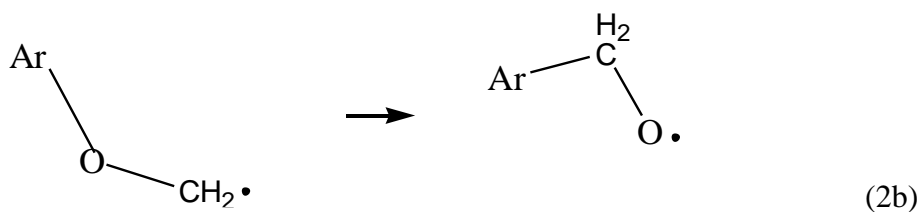
point is well demonstrated by the commentary on the modes of decomposition of the aryl alkyl ethers that are well-known to be constituents of lignites, subbituminous coals, and pure bituminous coals. Attention has been focused on the mechanism of decarbonylation of aryl methyl ethers, the simplest of the aryl alkyl ethers present in coal. These ethers are known to undergo thermal decarbonylation by two different mechanisms, as illustrated in Equations (1) and (2). Small amount of methane may be formed by other complex reaction sequences, but their contribution is not noteworthy.

Pathway A



Pathway B

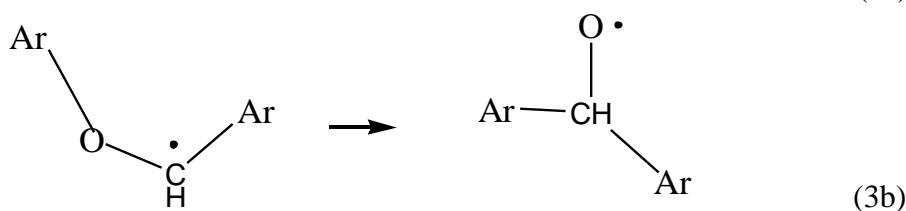
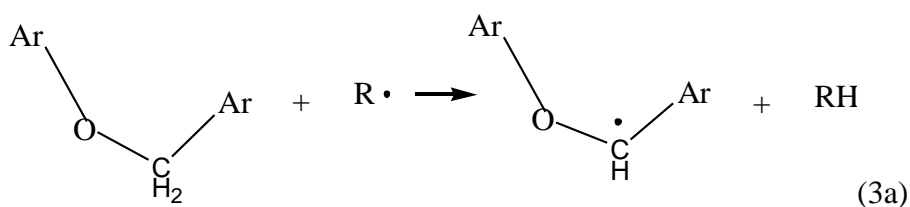


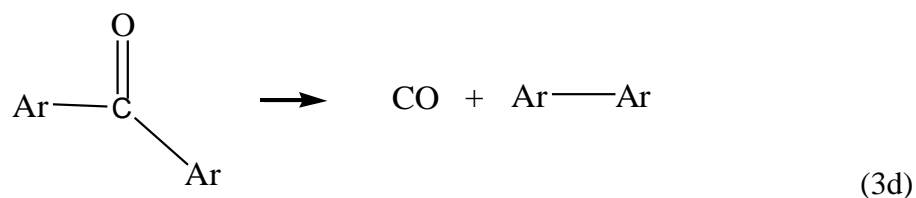
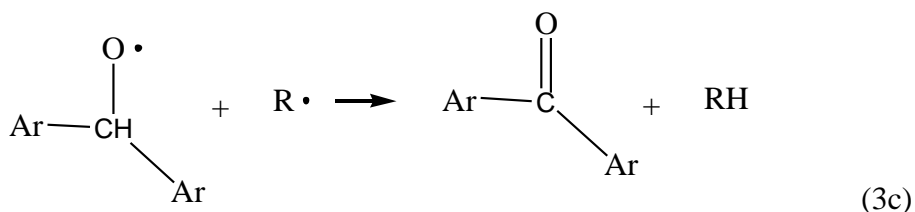


Reaction pathway A implicates two unimolecular processes. The first is the simple homolytic cleavage of the carbon-oxygen bond, and the second is a β -scission to form benzaldehyde. On the other hand, reaction pathway B is initiated by a bimolecular reaction in which a radical from coal, $\text{R} \cdot$, extracts a hydrogen atom from the ether to form phenoxymethyl radical. The reaction is followed by phenyl migration to form benzyloxy radical. This intermediate can undergo β -scission to form benzaldehyde, which decarbonylates (Kuntal et al., 1989). It is not possible to forecast which pathway will be dominant in coal pyrolysis because the key reaction in pathway A is unimolecular while the key step in pathway B is bimolecular. It is very hard to determine the relative importance of those processes within the coal matrix because the rate of bimolecular reaction depends upon the concentration and reactivity of the atoms and radicals present in the coal system (Kuntal et al, 1989). Work with pure compounds by Schlosberg et al. (1983) suggests that reaction pathway B might be especially significant.

It is evident that the aryl alkyl ethers produce carbon monoxide during coal pyrolysis (Detailed reaction network will be shown as examples in Chapter 5). Colussi et al. (1977)

found that the major decomposition pathway for these ethers is the basic carbon-oxygen bond scission with carbon monoxide being formed in the succeeding reaction of the phenoxy radical. The rate constant for the unimolecular decomposition reaction of the phenoxy radical in the gas phase has been assessed (Colussi et al., 1977) to be $10 \pm 5 \text{ s}^{-1}$ at $727 \text{ }^\circ\text{C}$. The decarbonylation reaction of the phenoxy radical happens in competition with hydrogen atom abstraction reactions and addition reactions that lead to condensation (Kuntal et al., 1989). Based on the pyrolysis experiments of Kuntal (1989), it is reported that carbon monoxide is produced predominantly from the ethers after the cleavage of the carbon-oxygen bond rather than via a hydrogen atom abstraction-rearrangement reaction. It is also interesting to notice that other aryl alkyl and aryl benzyl ethers with weaker carbon-oxygen bonds can undergo the hydrogen atom abstraction-rearrangement reactions, Equation (3), more promptly than the aryl methyl ethers.





Mulcahy et al. (1965) investigated peroxide radical-initiated anisole pyrolysis and Kislitsyn et al. (1970) reported phenol, toluene and benzaldehyde as major reaction products of the thermolysis of anisole at temperatures between 400 and 530 °C. No consistent mechanism was proposed in their study. It is reported that the reaction products from anisole pyrolysis include methane, carbon monoxide and small amounts of hydrogen and water in the gas phase and water, phenol, benzaldehyde, benzyl alcohol, toluene, benzene, biphenyl and other heavier species in the liquid phase (Richard et al., 1983).

Benzyl Phenyl Ether

The kinetics of the thermolysis of benzyl phenyl ether under hydrogen pressure in excess tetralin has been studied by Korobkov et al. (1988). The data they obtained made it possible to look into the reaction pathway. The experiment was conducted in a specially designed autoclave and hydrogen pressure in the autoclave was 8.5 MPa and tetralin was used in a

ten-fold weight excess. The coal liquefaction temperature was 410 °C. The reaction of benzyl phenyl ether is accompanied by a partial rearrangement into benzylphenol:

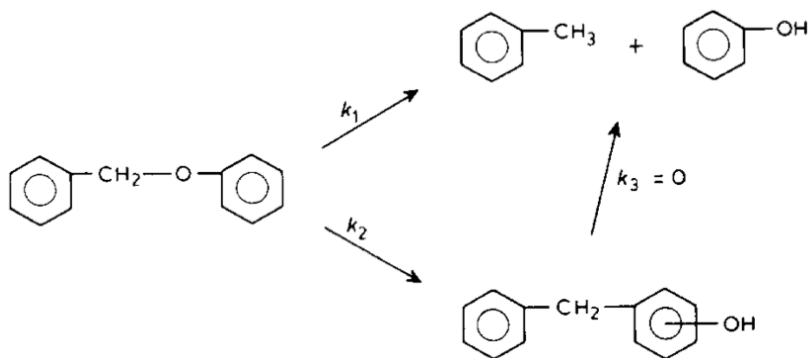


Figure 2.3 Reaction pathways of benzyl phenyl ether (Korobkov et al., 1988)

The calculations and experiments with *o*-benzylphenol have shown that benzylphenols do not undergo transformations under the experimental conditions. The value of k_1 is 5.1×10^{-3} , 2.4×10^{-3} , and 1.6×10^{-1} at 300, 325 and 350 °C, respectively; the value of k_2 is 1.1×10^{-3} , 6.0×10^{-3} , and 5.5×10^{-2} for the same temperatures. The activation energies of thermolysis is close to 204-212kJ/mol (48.7-50.5 kcal/mol), which points to direct homolysis of the alkyl C-O bond. (Korobkov et al., 1989).

Diphenyl Ether

Diphenyl ether is the organic compound with the formula $(\text{C}_6\text{H}_5)_2\text{O}$. The molecule is subject to reactions typical of other phenyl rings, including hydroxylation, nitration, halogenation and sulfonation. This simple diaryl ether possesses a variety of niche applications. Thermal cracking of nine diaryl ethers in a hydrogen donor solvent was studied kinetically by Kamiya et al. (1986). Nine diaryl ethers with phenyl, diphenyl,

naphthyl, phenanthryl and anthryl groups were treated in tetralin solution at 430 °C for 5 hours (Table 2.3). Diphenyl ether was extremely stable, but the 9-phenanthryl and 9-anthryl ethers showed high conversion values. The reason was because in general, the conversion rate constant of diaryl ethers increased with increasing number of rings in aryl structure. 9-phenanthryl and 9-anthryl ethers are three-ring aryl ethers.

Table 2.5 Thermal cracking of diaryl ethers in tetralin at 430 °C for 5 hours^a (Kamiya et al., 1986)

Ether	Conversion, %	K^b , $10^{-6}s^{-1}$	Relative value of k (k_T)	Product yield, mol%
Diphenyl ether	3.0	1.7	1.0	Phenol 0.84
4-Phenoxydiphenyl	7.6	4.4	2.6	Phenol 1.51 4-Phenylphenol 1.67
2-Phenoxy-naphthalene	12.8	7.6	4.5	Phenol 4.64 2-Naphthol 1.16
1-Phenoxy-naphthalene	38.0	26.6	15.7	Phenol 17.0 1-Naphthol 1.67
9-Phenoxyphenanthrene	53.0	42.0	24.9	Phenol 27.1 9-Phenanthrol 4.12
9-Phenoxyanthracene	>99.9	>3840	>2260	Phenol 72.8 Anthrone 0.53
2,2'-Dinaphthyl ether	39.2	27.6	16.3	2-Naphthol 12.8 1,2'-Dinaphthyl ether 4.7
1,2'-Dinaphthyl ether	57	46.9	27.8	2-Naphthol 19.5 1-Naphthol 4.6 2,2'-Dinaphthyl ether 2.2
2-Naphthyl-9-phenanthryl ether	66.1	60.1	35.5	2-Naphthol 19.1 9-Phenanthrol 4.4

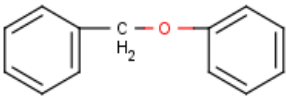
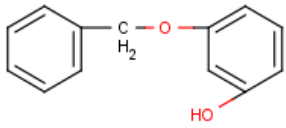
Experimental Conditions: Ether 5.0g, tetralin, 30 ml, initial pressure (H_2), $50kgcm^{-2}$
First order rate constant

The conversion rate of phenyl aryl ethers increased in the following order with respect to the second aryl group: phenyl < diphenyl < 2-naphthyl < 1-naphthyl < 9-phenanthryl <

9-anthryl (Kamiya et al., 1986).

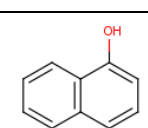
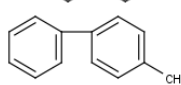
The pyrolysis of model oxygenated compounds at 600 °C was conducted by Siskin and Aczel (1983). It was found that phenols derive mainly from the cleavage of the alkyl C-O bond in alkylaryl ethers such as the benzyl phenyl ethers (a) and (b) in Figure 2.4 which form phenol and catechol, individually. There is an example shown in Figure 2.4, the second column indicates the percentage of phenols in the liquid product based upon reacted ether.

Table 2.6 Pyrolysis products of BPE and alkylaryl ether at 600 °C (Siskin and Aczel, 1983)

	Total volatile product (wt%)	Phenols in volatile products (wt%)
	78	63
	69	42

Diaryl ethers, such as diphenyl ether (c) and the cyclic diaryl ether, dibenzofuran (d) are stable, and do not form phenolic products when pyrolysed at 600 °C.

Table 2.7 Pyrolysis products of diphenyl ether and dibenzofuran at 600 °C (Siskin and Aczel, 1983)

	Total volatile product (wt%)	Phenols in volatile products (wt%)
	92	100
	95	100

Dibenzyl Ether

Dibenzyl ether (DBE) is a prototype model of certain aryl alkyl ether linkages believed to be important in coal. Townsend and Klein (1984) have studied dibenzyl ether as a probe into the supercritical fluid (SCF) solvent extraction of volatiles from coal with water. Thermolysis of dibenzyl ether in water at 374, 401 and 412 °C followed in prompt ether hydrolysis to benzyl alcohol, which in turn underwent significant secondary reactions to polymeric material. The observation implied that optimum use of SCF solvents in coal liquefaction could require the elaboration of kinetics, mechanisms and reaction pathways that involve the solvent. The primary hydrolysis pathway competed with a slower primary pathway to toluene and either benzaldehyde or benzyl alcohol, as detected in previous DBE pyrolysis either neat or with hydrogen. The experimental results indicate that DBE pyrolysis in water contains the reaction pathways summarized in Figure 2.6. The first

reaction pathway is hydrolysis of one mol DBE to two mol benzyl alcohol, and the second is identical to the neat thermolysis reported by Schlosberg et al. (1981) and also thermolysis in hydrogen donor noted by Simmons and Klein (1985). Benzyl alcohol and benzaldehyde both experience secondary reactions in Figure 2.6 and the GC-elutable oligomers formed from benzyl alcohol decomposition also react to unidentified polymeric material. Hydrolysis could enable manipulation of the yields of volatiles recovered from the reaction of coal in supercritical water.

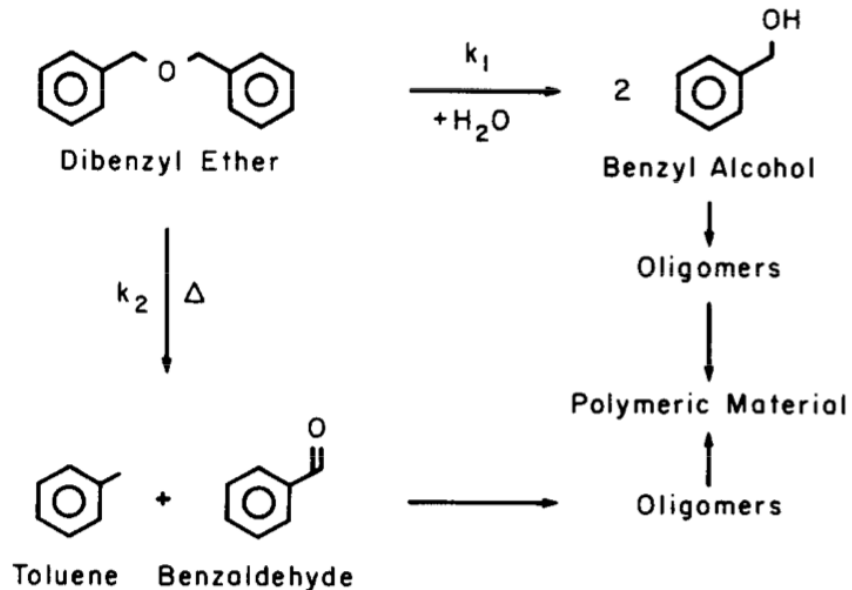


Figure 2.6 Reaction network for DBE thermolysis in supercritical water (Townsend and Klein, 1984)

The thermal decomposition of some model compounds representative coal structure, aromatic ethers has been carried out in tetralin solvent and the in presence of coal ash obtained by low temperature combustion (Kamiya et al., 1982). Thermal decomposition of

dibenzyl ether results in the formation of benzaldehyde and toluene. However, on the addition of coal minerals, the decomposition products were changed as shown in Table 2.7. The rate of reaction markedly increases, and the predominant product becomes benzyl tetralin. One mole of dibenzyl ether seems to yield almost two moles of benzyl tetralin, showing that coal minerals act as an alkylating catalyst.

Table 2.7 Effect of coal minerals on the thermal treatment of benzyl ethers in tetralin, residence time was 30 min (Kamiya et al., 1982)

Aromatic Ethers	Minerals, mg	Temp, C	Conversion		Product Yield ^c , mmol (mol%)
			mmol	mol%	
Dibenzyl ether	0 ^a	400	15.2	61.0	PhCH ₃ 16.1 (105.9), PhCHO 11.5 (75.5), PhH 3.0 (19.5)
	100 ^a	400	25.8	100	PhCH ₃ 1.3 (5.0), benzyltetralin ^d 39.8 (154.3)
	0 ^a	300	0	0	
	100 ^a	300	24.8	100	PhCH ₃ 1.0 (4.0), benzyltetralin ^d 40.3 (162.5)
Benzyl phenyl ether	0 ^a	400	27.2	100	PhCH ₃ 16.4 (60.3), PhOH 18.0 (66.2), benzylphenol 7.1 (26.5)
	100 ^a	400	27.2	100	PhCH ₃ 10.4 (38.2), PhOH 15.8 (58.0), benzylphenol 10.6 (39.0), benzyltetralin 3.7 (13.5)
	0 ^b	300	0.24	4.4	Trace of PhCH ₃ and PhOH
	50 ^b	300	3.42	62.8	PhCH ₃ 0.16 (4.7), PhOH 1.79 (52.3), benzylphenol 1.44 (42.1), benzyltetralin 1.13 (33.0)

^a Ether 5g, tetralin 20g, H₂ initial pressure 1.27MPa
^b Ether 1g, tetralin 5g, initial pressure 1.27 MPa
^c Values in parentheses are expressed in mol%
^d Benzyltetralin is a mixture of 1,2,3,4-tetrahydro-5-benzyl naphthalene and 1,2,3,4-tetrahydro-6-benzyl naphthalene

2.6.2 Overall effect of coal-related model ethers on coal liquefaction

The rates of ether-bridge cleavage have been studied using lots of different model compound systems. The results show that these bridges decompose under moderate conditions via an aromatic displacement reaction with atomic hydrogen. This class of reactions is vital in coal liquefaction processes since hydrogen-donating structures can release atomic hydrogen as they dehydrogenate. The reactions are fast and could be critical pathways for cleaving methylene bridges.

2.7 Remarks

- Solvent extraction is one of the most attractive aspects for converting coal into liquid fuels. Different aspects of coal liquefaction process have been investigated. From previous studies, certain bonds like ether linkage in coal are believed to rupture through free-radical mechanisms and the free radical fragments derived from the thermolysis is stabilized by hydrogen from the donor solvent. Other reactions which occur have not been established, nor have the reaction pathways involved (Benjamin et al., 1978).
- The reactivity of ether compounds is relevant to coal liquefaction chemistry because of the suspected prevalence of methylene and ether linkages between aromatic coal “Subunits” (Heredy and Fugassi, 1968) and the fact that bituminous

coals typically contain one phenolic hydroxyl group for every 20 carbon atoms (Abdel-Baset et al., 1978). A substantial fraction of the bond breaking in thermally promoted conversions of coals to lower molecular weight, lighter products is due to ether-bond thermolysis.

- Elimination of oxygen from coals is a critical and time-consuming step in donor solvent liquefaction processes (Whitehurst et al., 1977). Thus, elucidation of the mechanisms of conversion of these coal ether models could be of importance to the technology of coal liquefaction (McMillen et al., 1981).

2.8 References

Abdel-Baset, P. H. and Yarzab, R. F. "Re-examining of the phenolic hydroxyl content of coals." *Fuel* 57 (1978): 95-98

ASTM Standard D388, 2003, "Standard Classification of Coals by Rank," ASTM International, West Conshohocken, PA, 2003, DOI: 10.1520/D0388-12, www.astm.org.

Benjamin, B. M.; Vernon F. R.; Paul H. M.; Lloyd L. B. and Clair J. C., "Thermal cleavage of chemical bonds in selected coal-related structures" *Fuel* 57 (1978):
269-272

Berkowitz, N. "In an introduction to coal technology." Academic Press Inc.: New York, 1979

Colussi, A. J.; Zabel, F. and Benson, S. W., "The very low-pressure pyrolysis of phenyl ethyl ether, phenyl allyl ether, and benzyl methyl ether and the enthalpy of formation of the phenoxy radical". *Int. J. chem. Kinet.* 9 (1977): 161-178

King, Hsiang-Hui, and Leon M. Stock. "Aspects of the chemistry of donor solvent coal dissolution: The role of phenol in the reaction." *Fuel* 61.11 (1982): 1172-174.

Elkobaisi, F. M. and Hickinbottom, W. J. "372. Molecular Rearrangements. Part III. The thermal rearrangement of aryl benzyl ethers." *J. Chem. Soc.* (1959): 1873-1876

Gorbaty, J. W.; Larsen and Wender, I., Eds "Chapter 4" *Coal Science*. Volume 1, Academic Press. 1982

Groen, J., and J. Craig. "The inorganic geochemistry of coal, petroleum, and their gasification/combustion products." *Fuel Processing Technology* 40.1 (1994): 15-48.

Harvey, R.D, Ruch, R.R., "Overview of mineral matter in U.S. coals" ACS Div. Fuel Chem. Prepr., 29 (4) (1984), pp. 2-8

Hirano, K.; Kouzu, M; Okada,T.; Kobayashi,M.; Ikenaga, N.; Suzuki,T.; "Catalytic activity of iron compounds for coal liquefaction", *Fuel*, 78. 15. 1999, 1867-1873

Ignasiak, B. S. and Gawlak, M. "Polymeric structure of coal. 1. role of ether bonds in constitution of high-rank vitrinite" *Fuel* 56 (1977): 216-222

Ishihara, A.; Sutrisna, I. P.; Finahari, I.; Qian, E. W.; Kabe, T. "Effect of demineralization on hydrogen transfer of coal with tritiated gaseous hydrogen" *Fuel Processing Technology* 85 (2004): 887-901

Kamiya, Y., Nagae, S. and Oikawa, S. "Effect of coal minerals on the thermal treatment of aromatic ethers and carbonyl compounds." *Fuel* 62.1 (1982): 30-33

Korobkov, V. Y., Grigorieva, E. N., Byrov, V. I. and Kalechitz, I. V. "Mechanism and kinetics of thermolysis of ethers modeling the oxygen-methylene 'Bridge' bonds in coal organic matter." *Journal of Analytical and Applied Pyrolysis* 16 (1988): 57-73

Kuntal C.; Leon, M; Stock and Zabransky, R. F; "The pathways for thermal decomposition of aryl alkyl ethers during coal pyrolysis." *Fuel*, 68 (1989): 1349-1354

King, D. L. and de Klerk, A. "Overview of feed-to-liquid (XTL) conversion", *ACS Symp. Ser.*1084 (2011): 1-24

Larsen, J. W.; Kuemmerle, E. W. "Alkylation and depolymerization reactions of coal: a selective review with supplementary experiments" *Fuel* 55 (1976): 162-169

Mulcahy, M. F. R.; Tucker, B. G.; Williams, D. J.; and Wilmshurst, J. R.; "Decomposition and rearrangement of free radicals from alkyl phenyl ethers." *Chem. Comm.* 23 (1965): 609-610

Marty, R. A. and De Mayo, P. "Flash thermolysis: The formation of aldehydes from anisole derivatives." *Chem. Comm.* (1971): 127-128

McMillen, D. F.; Ogier, W. C.; and Ross, D. S.; "Coal structure cleavage mechanisms: scission of methylene and ether linkages to hydroxylated rings" *J. Org. Chem.* 46 (1981): 3322-3326

Patai, S. "The Ether Linkage" John Wiley & Sons Ltd. 1967

Panelker, S. V.; Shah, Y. T.; and Cronauer, D. C.; "Hydrogen transfer reactions of model compounds typical of coal" *Ind. Eng. Chem. Fundamentals* 21 (1982): 236-242

Mayo, F. R.; Pavelka, L. A.; Zevely, J. S.; Hirschon, A. S. "Extractions and reactions of coals below 100-degrees-C .3. Comparison of extraction products of Illinois No-6 Coal."

Fuel 67 (1988): 607-611

Muthusamy, K. and Wu. Z. "Low-rank coal drying technologies-current status and new developments" *Drying Technology* 27 (2009): 403-415

Robert, L. and Burwell, Jr. "The cleavage of ethers." *Chemical Reviews* 54 (1954): 575-711

Richard H. S.; Paul F. S.; Gerald D. D.; Jeffrey A. D.; Argo K.; Terrence R.; Ashe and William N. Olmstead. "Pyrolysis studies of organic oxygenates" *Fuel* 62 (1983): 690-694

Steacie, E. W. R., *Atomic and Free Radical Reactions*, Reinhold Publishing Corp., New York, 1954: 196-198

Sternberg, H. W.; Delle Donne, C. L.; Pantages, P.; Moroni, E. C. and Markby, R. E. "Solubilization of an Ivb coal by reductive alkylation." *Fuel* 50 (1971): 432-442

Schlosberg, R., T. Ashe, R. Pancirov, and M. Donaldson. "Pyrolysis of benzyl ether under hydrogen starvation conditions." *Fuel* 60 (1981): 155-57.

Shah, Y. T. "Chapter 2" *Reaction Engineering in Direct Coal Liquefaction*. Addison Wesley 1981

Schlosberg, R. H.; Davis Jr. W. H. and Ashe, T. R. "Pyrolysis studies of organic oxygenates. 2. benzyl phenyl ether pyrolysis under batch autoclave conditions" *Fuel* 60 (1981): 201-204

Schlosberg, R. H.; Dupre, G. D.; Kurs, A.; Szajowski, P. F.; Ashe, T. R. and Pancirov, R. J. "Pyrolysis studies of organic oxygenates. IV. naphthalene methyl ether pyrolysis under batch autoclave conditions." *Liquid Fuels Technology* 1 (1983): 115-126

Siskin, M and Aczel, T., "Pyrolysis studies on the structure of ethers and phenols in coal" *Fuel* 62.2 (1983): 1321-1326.

Siskin, M., A. Katritzky, and Balasubramanian, M., "Aqueous organic chemistry 5. diaryl ethers: diphenyl ether, 1-phenoxyphenanthrene and 9-phenoxyphenanthrene." *Fuel* 72.10 (1993): 1435-444.

Schlosberg, R. H.; Szajowski, P. F.; Dupre, G. D.; Danik, J. A.; Kurs, A.; Ashe, T. R. and

Olmstead, W. I. "Pyrolysis studies of organic oxygenates: 3. High temperature rearrangement of aryl alkyl ethers." 62 (1983): 609-694

Simmons, M. B. and M. T. Klein. "Free-radical and concerted reaction pathways in dibenzyl ether thermolysis." *Ind. Eng. Chem. Fundam.* 24 (1985): 55-59

Schweinfurth, S. P. "Chapter C: An introduction to coal quality." *The National Coal Resource Assessment Overview*, 2009

Tanner, K. I. and Bell, A. T. "Conversion of solvent-refined coal to liquid products in the presence of Lewis acids" *Fuel* 60 (1981): 52-58

Thakur, D. S. and Thomas, M. G. "Catalyst deactivation during direct coal liquefaction: a review" *Ind. Eng. Chem. Prod. Res. Dev.* 23 (1984): 349-358

Wachowska, H. and Pawlak, W. "Effect of cleavage of ether linkages on physicochemical properties of coals." *Fuel* 56 (1977): 422-426

Wen, C. Y.; Lee, E. S.; and Dutta. S.; "Coal conversion technology." Addison-Wesley

Publishing Company: Reading, Massachusetts, 1979.

Whitehurst D. D; Farcasiu .M; Mitchell, T.O. and Dickert, Jr. Annual Report, Feb 1977, for Electric Power Research Institute, Contract No. EPRI AF-480.

Youtcheff, J. S. and Given, P. H. "Dependence of coal liquefaction behaviour on coal characteristics. 8. Aspects of the phenomenology of the liquefaction of some coal" *Fuel* 61 (1982): 980-987

Youtcheff, J. S.; Given, P. H.; Baset, Z.; Sundaram, M. S. "The mode of association of alkanes with coals" *Organic Geochemistry* 5 (1983): 157-164

Chapter Three: Heat Effects Study of Coal Digestion Using DSC

3.1 Introduction

Coal pyrolysis is one of the most important aspects the coal conversion chemistry in all major coal conversion processes. It has been extensively investigated in laboratory studies (Bland, B. et al, 2002). Specific energy (heat involved in coal digestion) is an important design aspect of coal liquefaction reactors, because it determines the adiabatic temperature change during reaction.

DSC is the method of choice to determine thermal quantities, study thermal processes, and characterize or just simply compare materials. Sample preparation is easy and requires only small amounts of material. The technique is ideal for quality control, material development and material research. DSC can be used to analyze and study polymers such as thermoplastics, thermosets, elastomers and adhesives, foodstuffs, pharmaceuticals and chemicals in general. The method yields valuable information relating to processing and application conditions, quality defects, identification, stability, reactivity, chemical safety and the purity of materials.

The specific heat capacity C_p is a characteristic material property of a substance. It describes the amount of heat required to increase the temperature and is thus an important property for the calculation of thermal processes in chemical industry.

3.2 Objectives

The aim of this study is to acquire a better understanding of the solvent extraction process by studying heat flows involved in this process. The following objectives can be emphasized in this regard:

- Analyze heat effects of solvent extraction process to obtain information regarding the heat effects and dominant reactions over time in the solvent extraction of coal process.
- Experimentally obtain the specific heat capacity C_p of an industrial solvent that will be used during design to obtain a more precise energy balance for commercial process.

3.3 Experimental

3.3.1 Materials

- Coal Sample

The Bainfait Lignite coal sample was obtained directly from industry. The proximate analysis was conducted by TGA701 from LECO. The experimental method was ASTM D7582 MVA in Coal.

Table 3.1 Proximate analysis of the coal sample

	Proximate analysis (wt. %)						
	Moisture	Volatile	Ash	Fixed	Volatile	Ash	Fixed Carbon
				Carbon	Dry	Dry	Dry
Coal (Run 1)	10.33	33.91	16.94	38.82	37.82	18.89	43.30
Coal (Run 2)	10.23	34.04	16.94	38.79	37.92	18.84	43.21
Coal (Run 3)	10.27	33.82	16.95	38.96	37.69	18.89	43.42
Average	10.28	33.92	16.94	38.86	37.81	18.87	43.31
Standard deviation	0.05	0.11	0.01	0.09	0.12	0.03	0.11

- Solvent Sample

The solvent sample we were using was obtained directly from industry and it is hydrotreated coal liquids. Varian 1200L MS/MS and CP-3800GC was employed to analyze the coal liquid sample provided by Sherrit Technology.

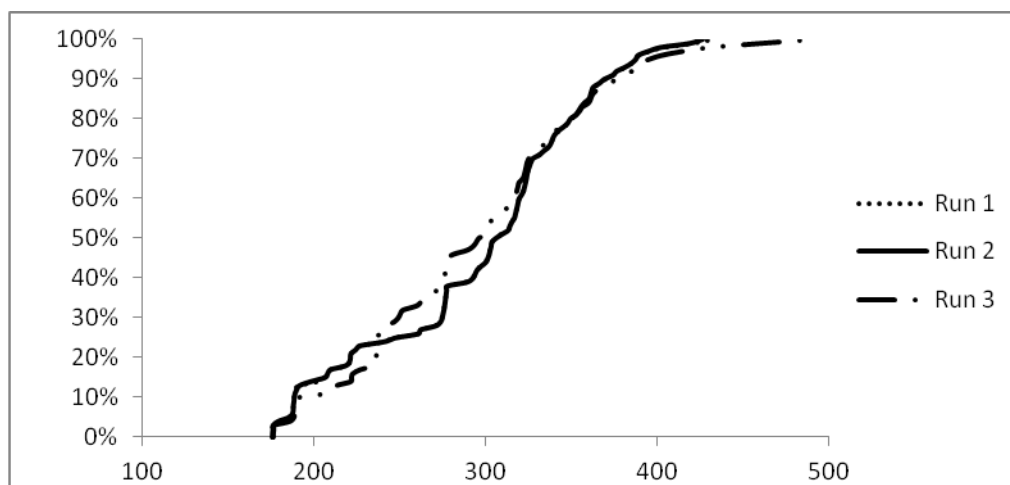


Figure 3.1 Distillation profile of solvent sample obtain from Simdist

Three individual runs were carried out for statistical accuracy. As we can see, Run 1 and Run 3 match each other very well. The initial boiling point of the sample is about 180 °C, and the final boiling point is around 450 °C. Almost no residues could be found, which means the sample fairly light. This data is good for comparison purpose for other coal liquids.

3.3.2 Equipment

- Balance

Three balances are prepared for all the weighting in the experiments:

- AL104, by METTLER TOLEDO Company, accuracy to 0.01mg; weighing range 0.01mg to 500mg, used for weighing HP crucibles and sapphire.

- APX 200, by DEVER Instrument Company, accuracy to 0.1mg; weighing range 0.1mg to 1000mg, used for preparing the sample, weighing the mixer of coal and solvent.

- Thermo-Gravimetric Analysis (TGA)

The approximate analyses were carried out by TGA701 from LECO, complies with ASTM methodology.

- Simdist (Varian 1200L MS/MS and CP-3800G)

Column: 10m, 0.53mm ID, 2.65µm Rtx-2887

Injection: Direct injection, 1.0µL of a 0.1 to 0.01 wt% hydrocarbon standard in carbon

disulfide.

Oven Temperature: 35 °C to 360 °C at 15 °C/min. (hold 5 minutes)

Injection and detector Temperature: 360 °C

Carrier Gas: N₂ 112cm/sec. (15mL/min.)

- Differential Scanning Calorimetry (DSC)

The DSC tests were carried out with DSC1 from Mettler Toledo.

Sensor type: FRS5

Pans: 40 µL Al pans with lid and without pin

30 µL HP stainless crucibles with lid, gold-plated sealing and without pin

Carrier gas: Nitrogen

Temperature Program: specified for each sample in section 3.5

- Ultrasonic Bath

An ultrasonic bath (Model 150HT Aquasonic Bath from VWR Scientific) was used in this study to provide an ultrasonic environment for the mixture of coal and solvent. This bath has a capacity of 5.7L and provides the frequency 60Hz.

3.3.3 Procedures

- Calibration of DSC

Temperature and caloric calibration of DSC was accomplished using the high purity reference materials provided by Mettler Toledo. The onset temperature of melting was employed for temperature calibration and the heat of melting was employed for caloric calibration. Bui (2013) conducted a detailed calibration showed in Table 3.2. The temperature measurements were corrected for the heating rate (β) by performing the temperature calibration at different heating rates and extrapolating to close-to-zero heating rate ($\beta \rightarrow 0$). The heating rate correction ($dT/d\beta$) was determined for each calibration substance. Temperature values were corrected for heating rate ($dT/d\beta$) at different temperature. In the table, “x” is the average value and “s” represents the standard deviation. Corrected sample standard deviation was employed, denoted by s:

$$= \sqrt{\frac{1}{N-1}} \sqrt{\sum_{i=1}^N (xi - \bar{x})^2}.$$

Table 3.2 Temperature and caloric calibration of DSC (Based on the melting point (T_m) and heat of melting (ΔH_m) of standard calibration materials provided by Mettler).

Material	Experimental T_m (°C)		Experimental ΔH_m (J/g)		Literature values		$dT/d\beta$ (K/K.min ⁻¹)
	x	s	x	s	T_m (°C)	ΔH_m (J/g)	
In	156.70	0.08	29.3	0.22	156. 60	28.6	0.03
Sn	231.95	0.10	59.6	0.31	231. 93	60.3	-0.01
Pb	327.41	0.11	23.4	0.18	327. 47	23.0	0.04
Zn	419.49	0.15	109.8	0.87	419. 53	108.6	-0.01

- Sample preparation

The coal sample and the solvent sample were weighed and put into a glass beaker, stirred and then put into ultrasonic bath for 30 minutes to ensure the sample was well mixed. For the samples loaded inside the glove box, the HP crucible, gold-plated sealing and the sealing equipment were transferred into the glove box. The glove box provided an argon atmosphere to avoid oxidation during the sample preparation. High purity argon was circulated inside the glove box to maintain an anaerobic environment. Water and oxygen content was constantly kept below 0.1 ppm. The crucible and the gold-plated sealing were weighed before loading the sample. The sealed crucible was weighed afterwards to calculate the weight of sample inside the crucible.

- Choose the experimental condition

According to the industrial application, the temperature range we were chosen was 25 °C to 425 °C, which is the reaction temperature using by industry. The effect of temperature is most marked for benzene-type solvents. With neutral tar oils, a sharp rise in yield from less than 3% at about 200 °C to more than 50% at between 350 °C and 400 °C has been reported by Shell. The heating program is 10 °C per minute which is the common procedure.

- Run the experiments

After sample preparation, the sealed crucible was placed inside the DSC chamber along with the reference crucible (a sealed empty crucible). Open the nitrogen cylinder to maintain the purge system. Set the method in STAR^e software then starting running the experiments.

All the DSC (Mettler Toledo) experiments were carried out using the conditions shown in Table 3.4, considering the physical properties of samples used in our experiments.

Table 3.3 DSC Experimental Conditions for coal digestion

Sample	coal+LH-1007		
Solvent to coal ratio (mass ratio)	2.5:1		
Treatment	BL coal and solvent well mixed according to the coal to solvent ratio, and stay in ultrasonic bath for 30mins.		
Exp. No	Exp.1	Exp.2	Exp.3
Sample Mass	12.68mg	13.08 mg	12.18 mg
Temp Range/°C	25~425		
Sample Pan	High Pressure crucible, stainless steel sealed with gold-plated sealing without pinhole		
Atmosphere	All the crucibles are closed under hydrogen atmosphere		
Purge Gas	Nitrogen @100 ml/min		
Heating Procedure	The sealed crucible was kept at room temperature for 5 minutes and then heated to 425 °C with a heating @10 °C /min followed by isotherm for 5 minutes at 450 °C.		

- Cp sapphire measurement

Cp sapphire measurement is advisable when more exacting demands are placed on the accuracy of the results. In addition to the actual sample and blank curve, for the sapphire method a sapphire measurement must be performed. The known heat capacity of sapphire is used in the calculations. Even more accurate results are obtained when the temperature range under investigation is not simply scanned linearly, but divided into short dynamic segments with isothermal pauses.

The detailed information about Cp procedure is listed in Table 3.4. All the experiments are

carried out by DSC 1 from Mettler Toledo.

Table 3.4 Parameters of Cp sapphire measurement

Experiment step	1 st Blank curve	2 nd Sapphire	3 rd sample
content	Empty crucible	Add Sapphire crystal	Add Solvent LH-1006
Temperature program	Isothermal at -30 °C for 30mins, then heat it up to 150 °C at heating rate 10°C/min, then isothermal at 150 °C for 30mins.		
Sampling	All the sampling steps are prepared in the glove box under argon atmosphere, to exclude any possible reaction.		
Purge Gas	Nitrogen @ 100 ml/min		

In each measurement, three steps are followed in Table 3.4. Two parallel measurements are obtained for further discussion.

3.4.5 Cp calculation for Solvent

Definition:

$$\text{Equation Cp: } = \frac{dH}{dt} * \frac{1}{\beta_{s+mo}} \quad (3.1)$$

Where dH/dt = heat flow to the sample (corrected by blank curve)

B_s = heat rate in the sample

M_o = sample mass

Cp as a function of sample temperature is obtained as the result in J/g.K. The deflection of the DSC curve of the sample is compared with that of sapphire and Cp determined from this. An isothermal step has been measured before and after the dynamic segment, correction for the isothermal drift is done.

3.4 Results

3.4.1 Cp measurement for solvent

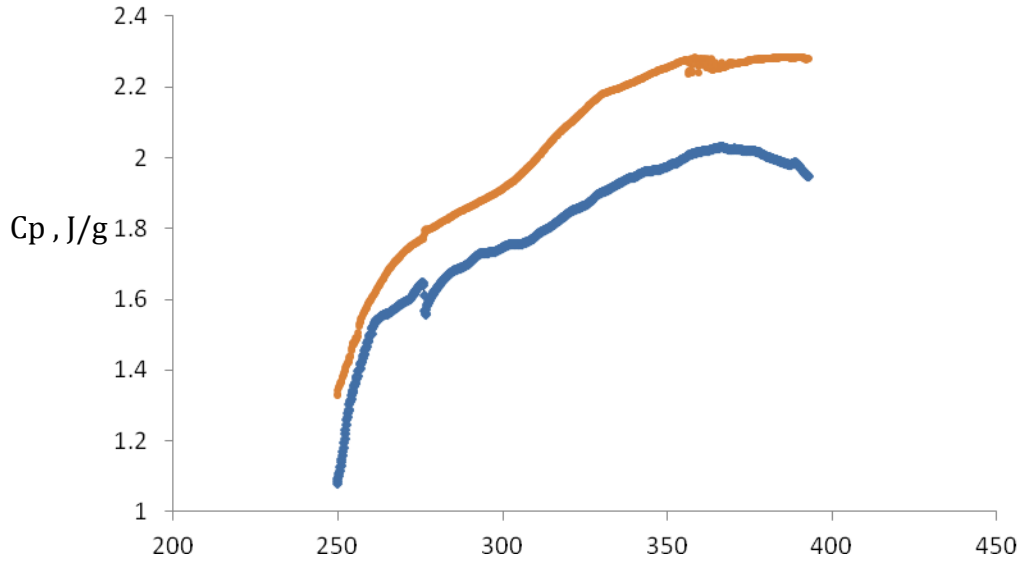


Figure 3.2 Cp calculation result for solvent

3.4.2 DSC result for coal digestion T, K

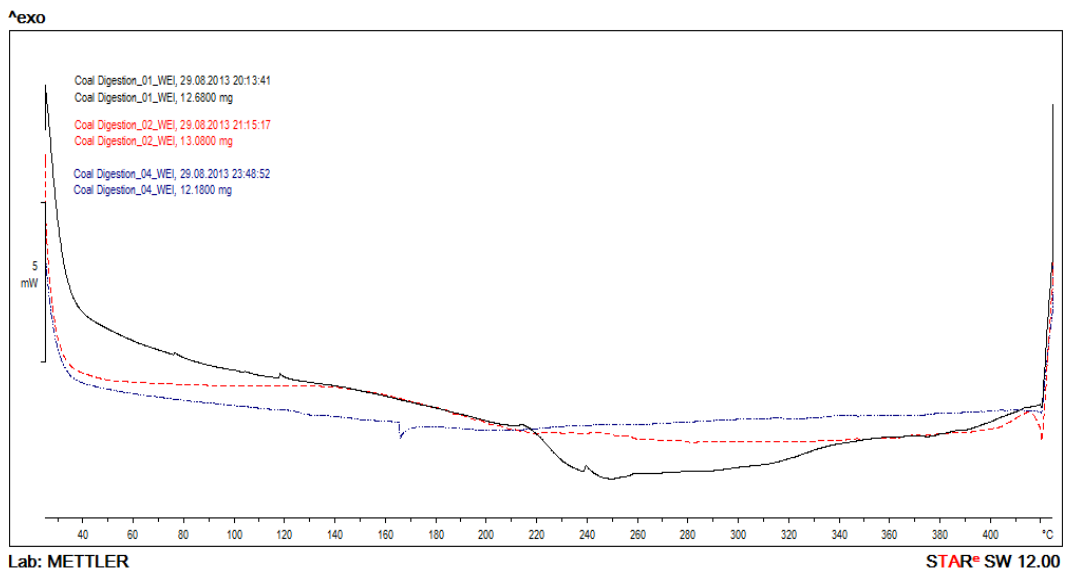


Figure 3.3 Calorigram of coal digestion process (heating +25 to +425 °C).

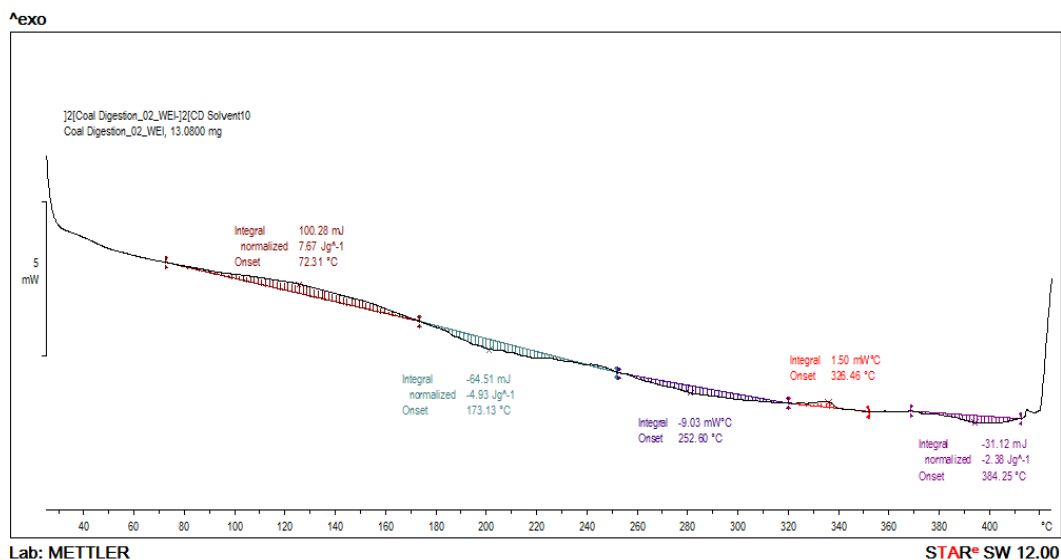


Figure 3.4 DSC calorigram of coal digestion subtracted the DSC calorigram of solvent to study the heat effects of coal digestion.

3.5 Discussion

3.5.1 Cp calculation for solvent

The heat capacities, C_p , for the solvent was measured over the temperature range 250-400K. As we can see from figure 3.2, the results are showing great difference at two separate measurements. Part of the problem is the nature of the solvent. From the direct observation of human eyes, there are a lot precipitate in the bottom. The sample itself is not homogeneous. Since the DSC measurement just takes a single drop of the solvent to do the experiment, the composition of every drop of sample can be very different, thus the C_p can be very different from one to another, but the data obtained can be used as reference for

industrial study.

3.5.2 DSC analysis for coal digestion

Figure 3.3 was the results obtained from three DSC experiments for coal digestion. The measurement is repeated three times to ensure the accuracy of the experiment. The X-axis represents time; the Y-axis represents the heat flow. Figure 3.3 shows the DSC calorigrams of coal and solvent mixture. The thermal decomposition of coals was found to be an endothermic process. From the DSC curves, three experiments have the same trend. The curves are relatively smooth.

To further study the reaction of coal digestion, the DSC calorigram of solvent was obtained by performing the experiment by the same method as coal digestion. Then the calorigram of coal digestion was subtracted by the calorigram of solvent to eliminate the heat effect of solvent during coal digestion (Figure 3.4). A baseline was established after the subtraction. There's an exothermic peak with onset temperature is 72.3 °C, the heat flow is 7.67 J/g which is quite small amount. This might be the dissolution of coal into solvent. At this stage, the viscosity increased. The second event is a flat endothermic peak came right after the first peak with onset temperature is 173.13 °C. The heat flow is -4.93 J/g. This can be the start of chemical reaction of coal and solvents. The third peak is an endothermic peak with onset temperature is 252.6 °C. This should also be the reaction between coal and solvent. At 326.46 °C, a very small and sharp exothermic peak occurred and this should be

the depolymerization of large coal molecules. At last, a flat endothermic peak with onset temperature 384.25 °C, this should be coking because after the experiments, the crucible was opened and examined, the residue was lighter than original sample which shows the decrease of viscosity, also there was black chunk of solids which shows coking was taken place as well.

The data obtained from this study can be further used as comparison with industrial process.

3.6 Reference

Bui, Ly, H. “Alkali Metal C1-C12 n-alkanoates”, Graduate Thesis, University of Alberta, Department of Chemical Engineering, Edmonton, Alberta (2013)

Bland, B.; Stansberry, P. G.; Stiller, A. H.; Zondlo, J. W.; Chen, C. and Fenten, D. *Design, construction, and evaluation of coal extraction pilot plant to manufacture coal-based carbon pitch*, Department of Chemical Engineering, West Virginia University, Morgantown (2002)

Gadam, Shishir Dattatrayarao. “Coal upgrading under mild conditions using

supersolvents”, Graduate Thesis, West Virginia University, Department of Chemical Engineering, Morgantown (1990)

Chapter Four: Thermal Study of Coal Related Ether Compounds Using DSC

4.1 Introduction

From the earlier study, there is some consensus that cleavage of open ether linkages (R-O-R) plays an important role in early stages of liquefaction of coal into lighter products (Whitehurst et al., 1982). In this study, benzyl phenyl ether, dibenzyl ether and diphenyl ether have been chosen as model compounds representing ether linkages in coal liquids. Melting points of each compound have been investigated and well established. In this chapter, melting points have been re-examined and compared with literature. The thermal decomposition temperature of each compound was established and can be used as a reference for further study.

4.2 Objectives

To study the thermal behavior of model compounds, DSC 1 from Mettler Toledo was employed. Melting points and thermal decomposition temperature should be obtained from this process.

4.3 Experimental

4.3.1 Materials

- Benzyl phenyl ether

Manufacturer: Sigma Aldrich

Purity: 98%

Color: White

Form: Powder

Use: as model compound

- Dibenzyl ether

Manufacturer: Sigma Aldrich

Purity: >98% (GC)

Color: Colorless

Form: Clear, Liquid

Use: as model compound

- Diphenyl ether

Manufacturer: Sigma Aldrich

Purity: 99%

Color: White

Form: Crystalline

Use: as model compound

- Acetone

Manufacturer: Caledon

Purity: 99.5%

Color: Colorless

Form: Liquid

Use: To wash the crucible

- Dichloromethane

Manufacturer: Fisher

Purity: 98%

Color: Colorless

Form: Liquid

Use: To wash the crucible thoroughly

- Nitrogen

Manufacturer: Praxiar Inc.

Purity: 99.998 % ($O_2 < 5$ ppm, $H_2O < 3$ ppm)

Color: Colorless

Form: Gas

Use: Purge gas for DSC 1

4.3.2 Equipment

- Differential Scanning Calorimeter (DSC)

Manufacturer: Mettler Toledo

Model: DSC 1

Sensor type: FRS5

Pans: 40 μ L Al pans with lid and without pin

30 μ L HP stainless crucibles with lid, gold-plated sealing and without pin

Carrier gas: Nitrogen

Temperature Program: Specified for each sample in section 4.4, 4.5, 4.6

- Glove Box

Manufacturer: UNIlab workstation from MVraun Incorporated

Purge gas: Argon (Avoid oxidation during the experiments)

- GC-MS

Manufacturer: Varian Inc.

Model: Saturn 2200 (GC model: CP 3800)

Carrier gas: Helium 1 mL/min

Auto injector: Varian CP-8410

GC Column: factor four capillary column (30 m x 0.25mm i.d.)

GC Temperature program: initial T =50°C, holding time 10 min; ramp= 10°C/min, final

T= 320°C, holding time 10 min; injection T= 320°C, FID T= 320°C, TCD T= 220°C

GC Detectors: Front FID/ Middle TCD

MS mass range: 50-350 m/z

MS ionization mode: starts at 3.5 min

4.3.3 Procedures

- Calibration of DSC

The detailed calibration of DSC was included Table 3.1 in chapter 3.

- Sample Preparation

For the samples loaded inside the glove box, the HP crucible, gold-plated sealing and the sealing equipment were transferred into the glove box. The glove box provided an argon atmosphere to avoid oxidation during the sample preparation. High purity argon was circulated inside the glove box to maintain an anaerobic environment. Water and oxygen content was constantly kept below 0.1 ppm. The crucible and the gold-plated sealing were weighed before loading the sample. The sealed crucible was weighed afterwards to calculate the weight of sample inside the crucible.

- Run the experiments

After sample preparation, the sealed crucible was placed inside the DSC chamber along with the reference crucible (a sealed empty crucible). Open nitrogen cylinder to maintain

the purging system. Set the method in STAR^e software then starting running the experiments.

- Sample Collection and Analysis

After the experiments, the sealed crucible was carefully opened and the residue inside the crucible was collected by glass pipette. The thermolysis decomposition products were characterized to determine the nature of the decomposition.

4.4 Results

4.4.1 Thermal Analysis of Benzyl Phenyl Ether

The following information is obtained from literature, using as reference for this study.

Chemical Name: Benzyl phenyl ether

CAS Registry Number: 946-80-5

Type of Substance: Isocyclic

Molecular Formula: C₁₃H₁₂O

Molecular Weight: 184.238

Melting Point (Shah et al., 2005): 39-40 °C

Boiling Point (Yaws et al., 2012): 286.5 °C

The DSC results are shown as follows. Figure 4.1 is the detailed method for studying benzyl phenyl ether decomposition and figure 4.3 is the detailed method for studying

benzyl phenyl ether melting behavior. The calorigrams of benzyl phenyl ether are shown to illustrate the evaluation of melting point (Figure 4.2) and thermolysis (Figure 4.4). The detailed GC-MS chromatograph of pyrolysis products of benzyl phenyl ether after 450 °C was shown in figure 4.5.

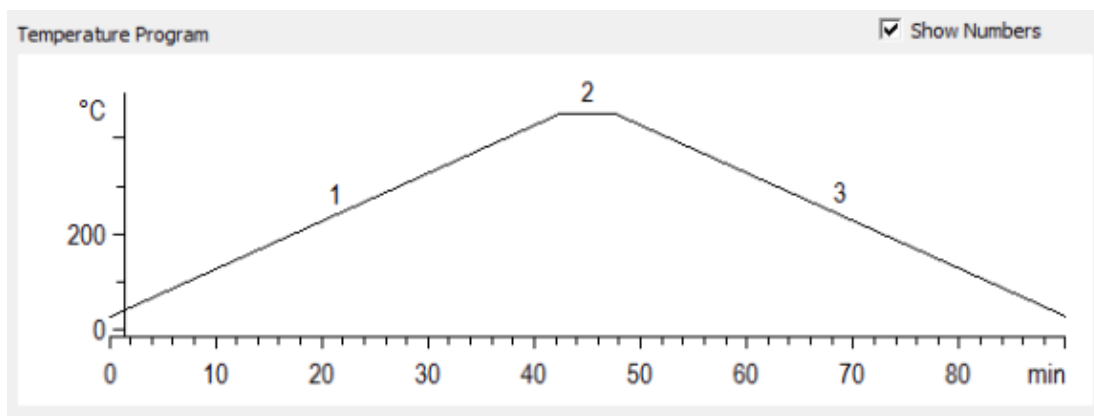


Figure 4.1 Temperature program for benzyl phenyl ether decomposition. (heating rate 10 °C/min, cooling rate 10 °C/min)

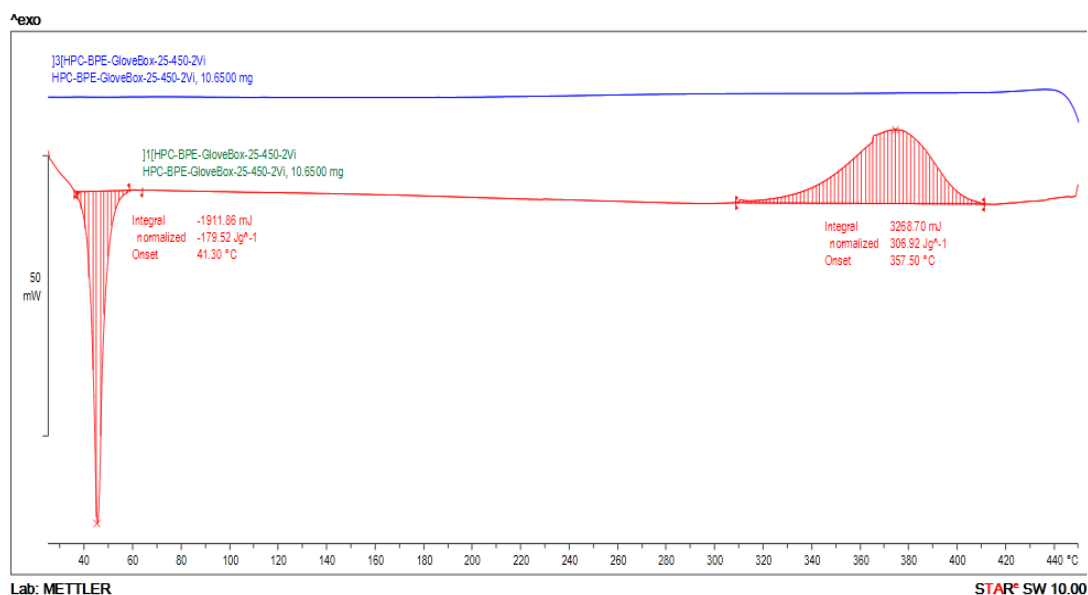


Figure 4.2 Calorigram of benzyl phenyl ether thermolysis behavior (heating +25 to +450 °C below; cooling above).

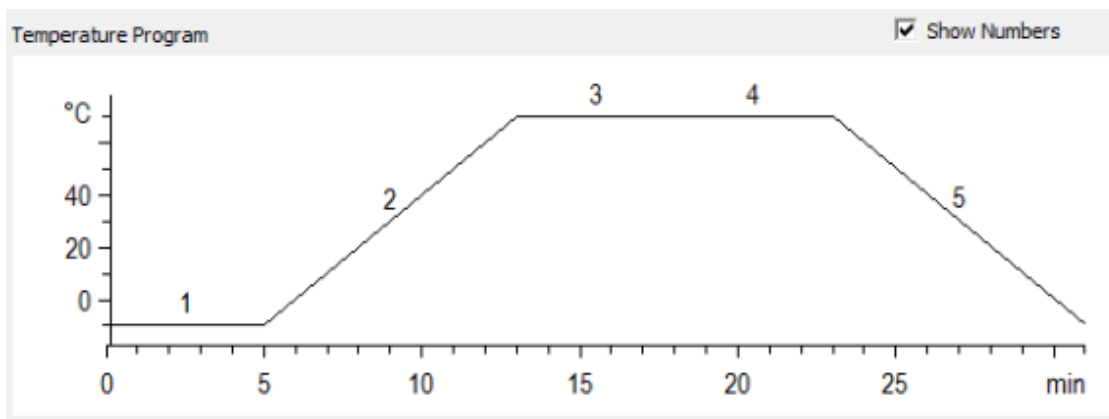


Figure 4.3 Temperature program for benzyl phenyl ether melting behavior. (heating rate 10 °C/min, cooling rate 10 °C/min)

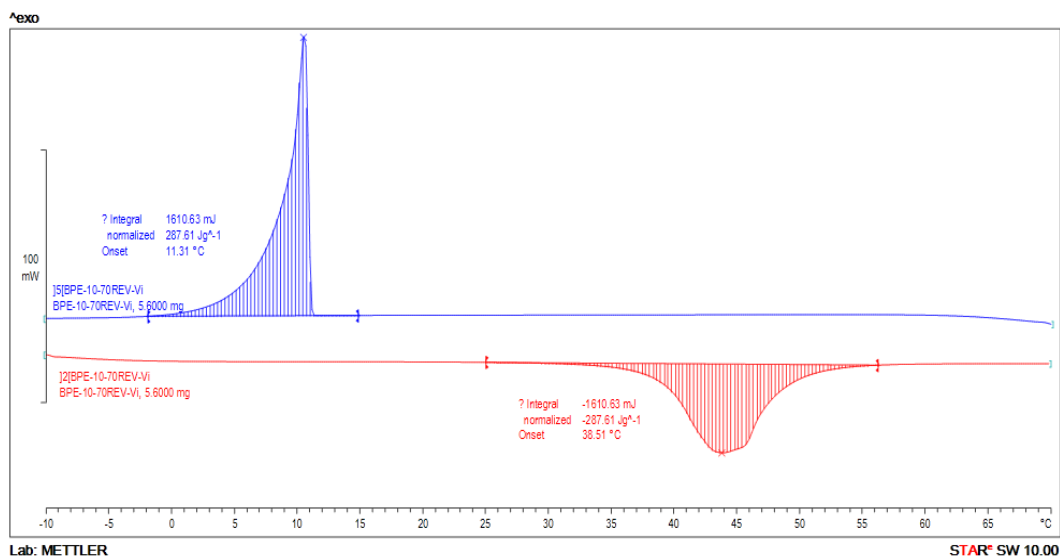


Figure 4.4 Calorigram of benzyl phenyl ether to determine melting behavior (heating –10

to +75 °C below; cooling above).

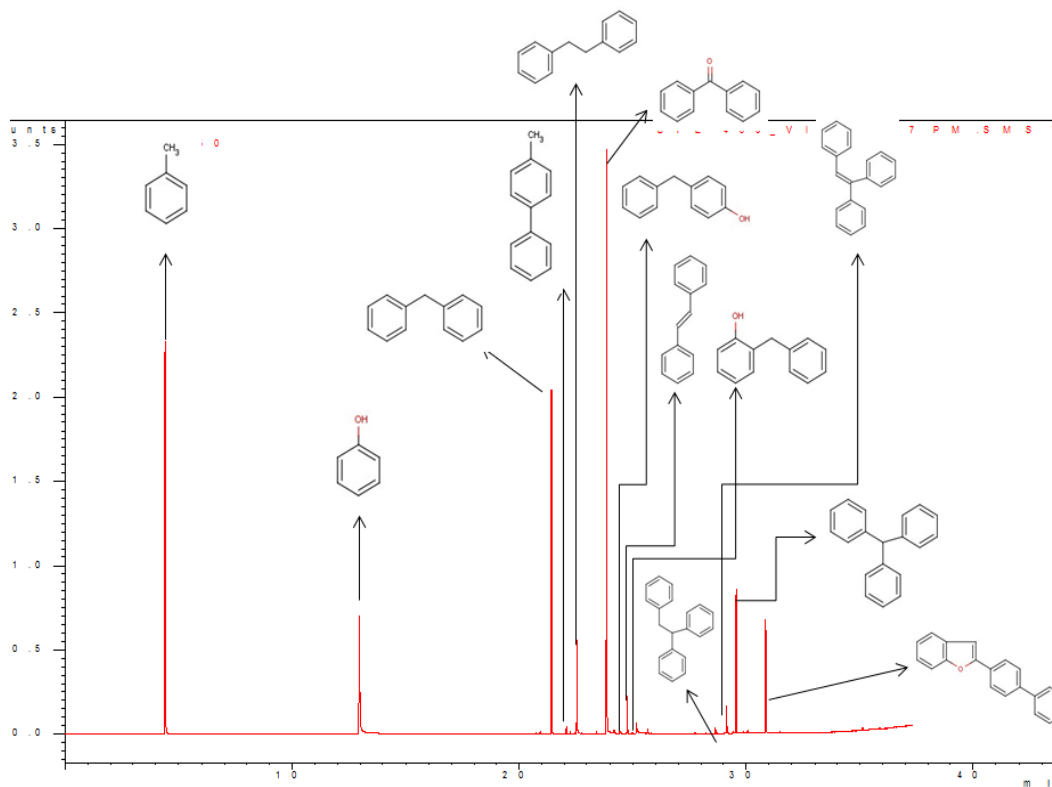


Figure 4.5 Chromatogram of the products obtained from benzyl phenyl ether thermolysis.

4.4.2 Thermal Analysis of Dibenzyl Ether

The following information is obtained from literature, using as reference for this study.

Chemical Name: Dibenzyl ether

CAS Registry Number: 103-50-4

Type of Substance: Isocyclic

Molecular Formula: $C_{14}H_{14}O$

Molecular Weight: 198.265

Melting Point (Wender et al., 1950): 4-5 °C

Boiling Point (Aly et al., 1994): 297 °C

The DSC results are shown as follows. Figure 4.6 is the detailed method for studying dibenzyl ether decomposition and figure 4.8 is the detailed method for studying benzyl phenyl ether melting behavior. The calorigrams of benzyl phenyl ether are shown to illustrate the evaluation of melting point (Figure 4.9) and thermolysis (Figure 4.7).

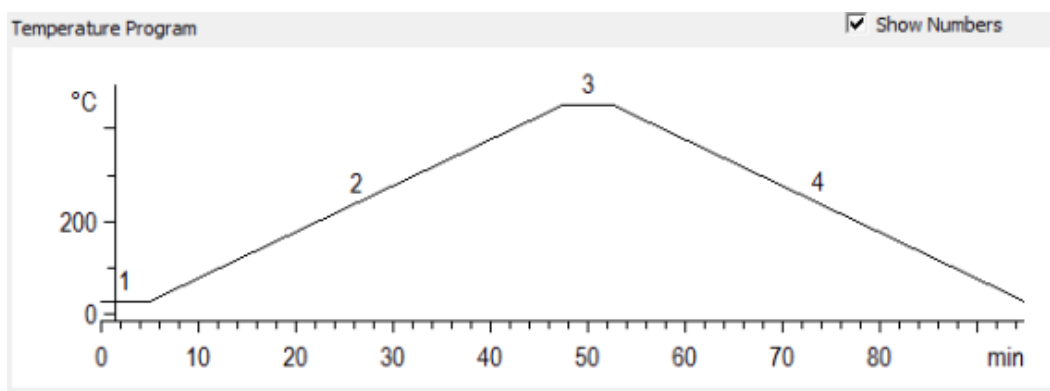


Figure 4.6 Temperature program for dibenzyl ether decomposition. (heating rate 10 °C/min, cooling rate 10 °C/min)

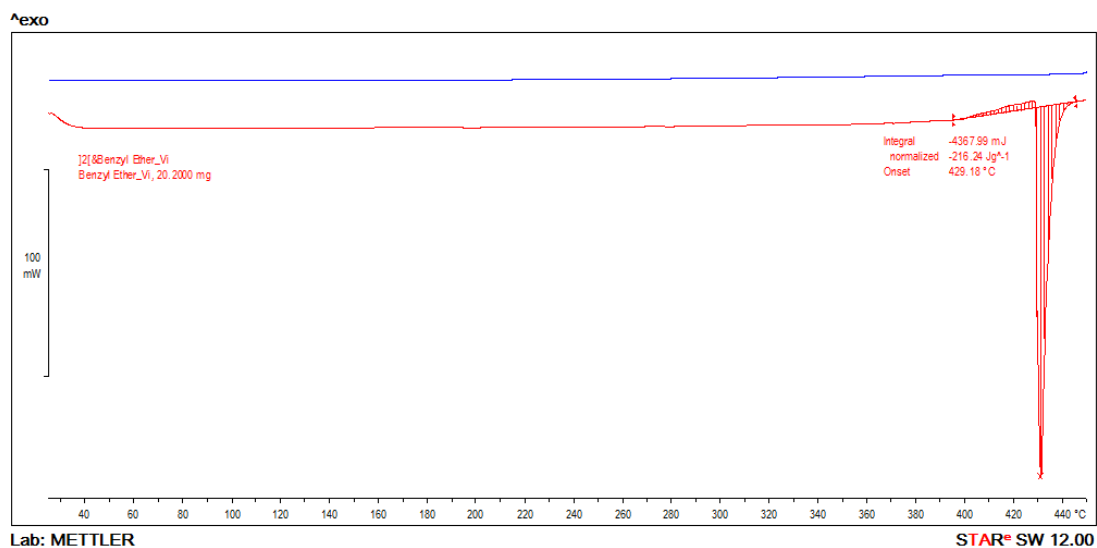


Figure 4.7 Calorigram of dibenzyl ether thermolysis behavior (heating +25 to +450 °C below; cooling above).

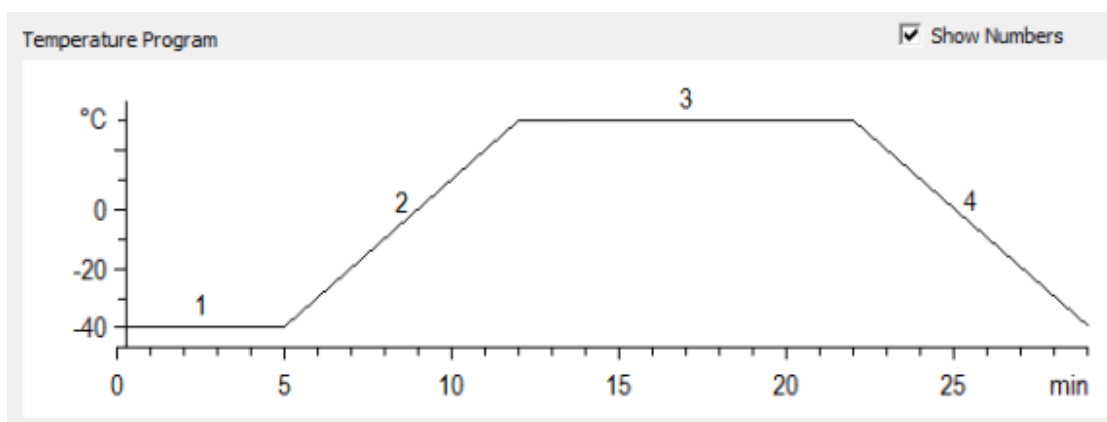


Figure 4.8 Temperature program for dibenzyl ether melting behavior. (heating rate 10 °C/min, cooling rate 10 °C/min)

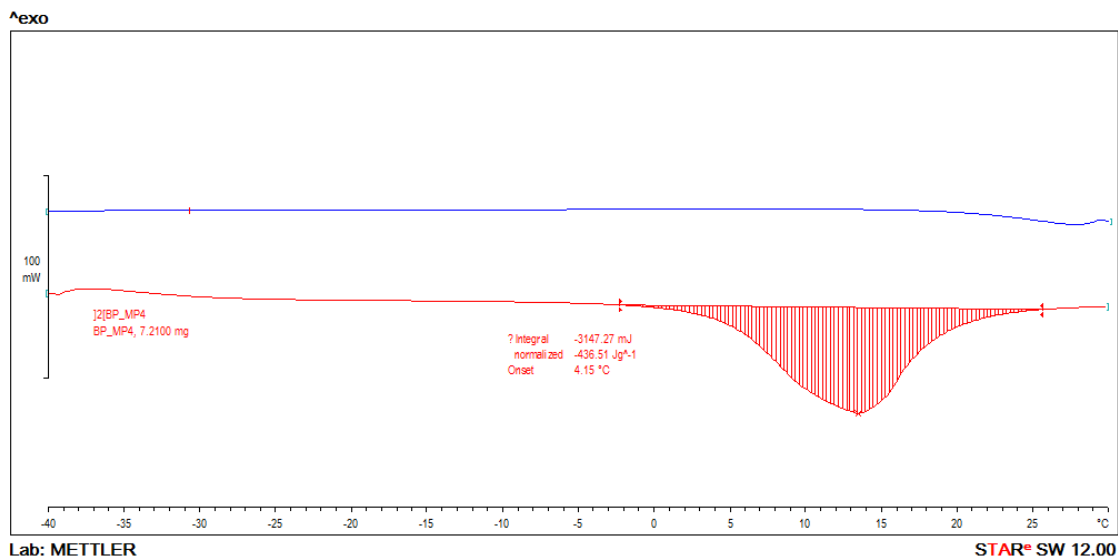


Figure 4.9 Calorigram of benzyl phenyl ether to determine melting behavior (heating –40 to +30 °C below; cooling above).

4.4.3 Thermal Analysis of Diphenyl Ether

The following information is obtained from literature, using as reference for this study.

Chemical Name: Diphenyl ether

CAS Registry Number: 101-84-8

Type of Substance: Isocyclic

Molecular Formula: C₁₂H₁₀O

Molecular Weight: 170.211

Melting Point (Ning and Marc, 2008): 28 °C

Boiling Point (Wiggins et al., 2010): 257 °C

The DSC results are shown as follows. Figure 4.10 is the detailed method for studying diphenyl ether decomposition and figure 4.12 is the detailed method for studying benzyl phenyl ether melting behavior. The calorigrams of benzyl phenyl ether are shown to illustrate the evaluation of melting point (Figure 4.13) and thermolysis (Figure 4.11).

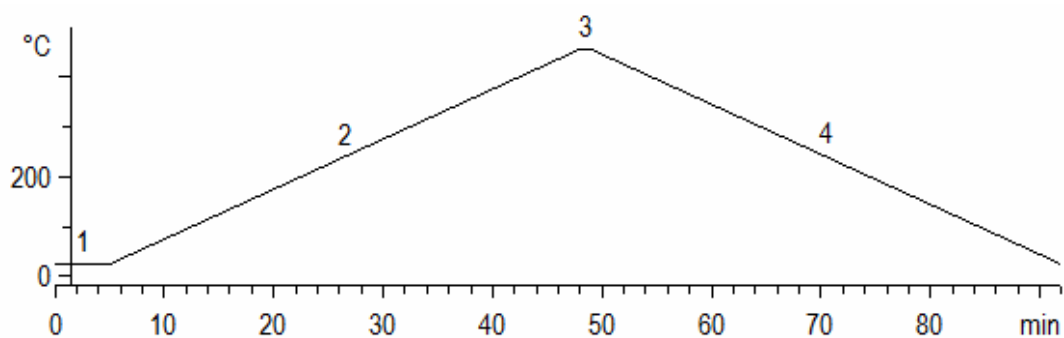


Figure 4.10 Temperature program for diphenyl ether thermal decomposition behavior.

(heating rate 10 °C/min, cooling rate 10 °C/min)

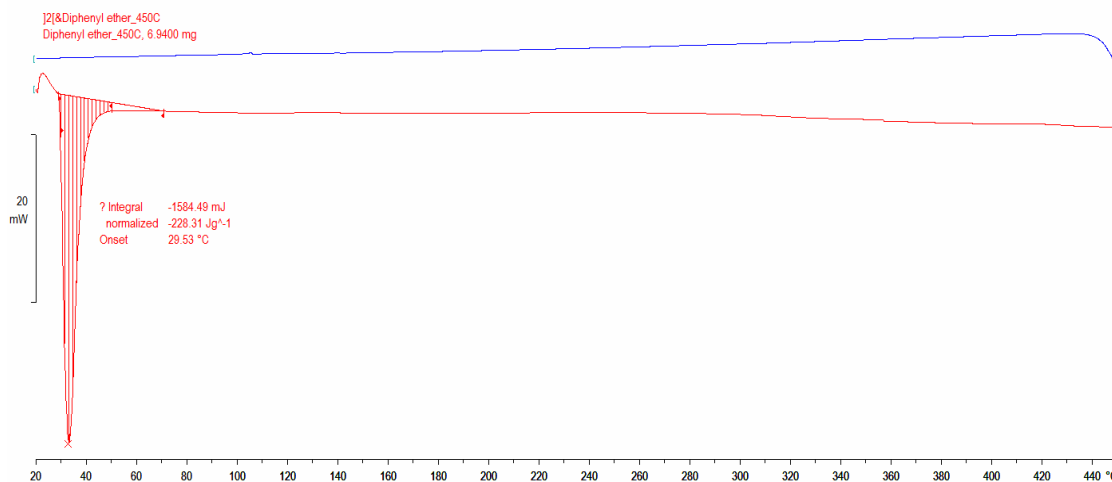


Figure 4.11 Calorigram of diphenyl ether to determine thermal decomposition behavior

(heating 25 to 450 °C below; cooling above).

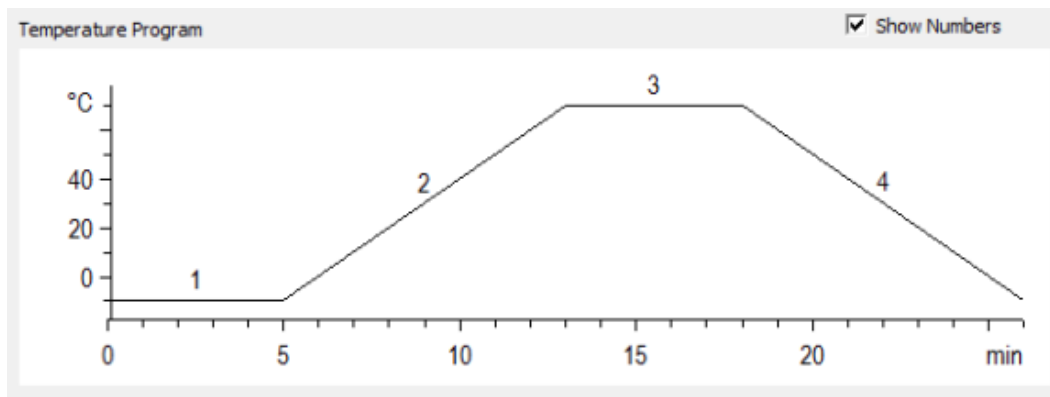


Figure 4.12 Temperature program for diphenyl ether melting behavior. (heating rate 10 °C/min, cooling rate 10 °C/min)

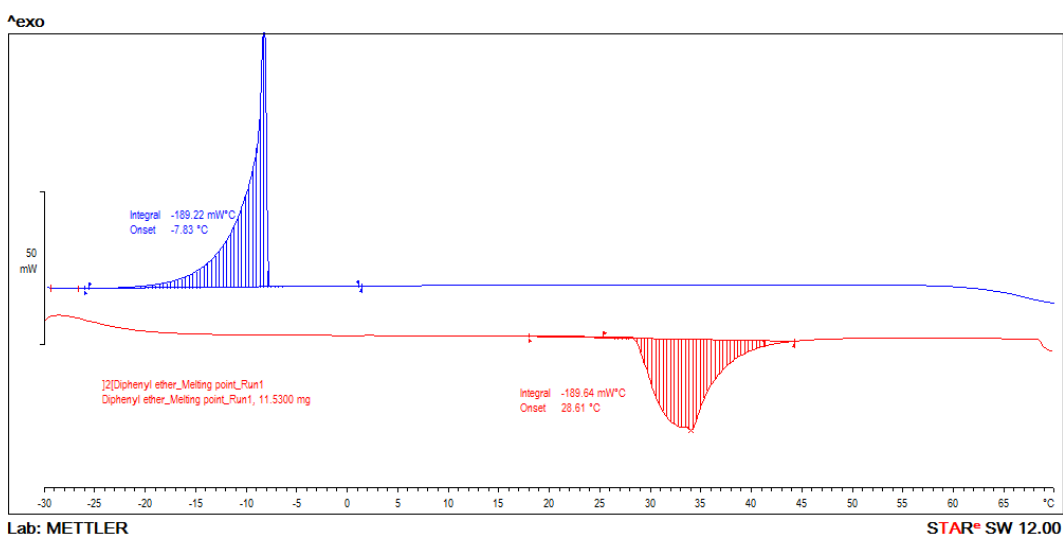


Figure 4.13 Calorigram of diphenyl ether to determine melting behavior (heating -10 to +70 °C below; cooling above).

4.5 Discussion

The melting point data of the ethers investigated is summarized in Table 4.1, which also

lists the onset of thermolysis. Thermolysis (endothermic) could be accompanied by further reaction of the decomposition products, which could also be exothermic in nature.

Table 4.1 Melting Point and Onset of Thermolysis of Ethers

Substance	Melting		Thermolysis	
	(°C)	(J/g)	(°C)	(J/g)
benzyl phenyl ether	38.5	+287.6	357.5	-306.9
diphenyl ether	29.2	+146.4	a	a
dibenzyl ether	4.2	+439.1	420.3	+207.6

^a Compound stable at 450 °C, no thermolysis was observed.

4.5.1 Benzyl phenyl ether

The observed melting point corresponds with the value reported in literature (38.5 °C vs lit. 39-40 °C). The literature value of the melting point was obtained from Reaxys. No enthalpy of melting data was found for comparison.

In tetralin measurable thermolysis was found at 300 °C, but none at 275 °C (Korobkov et al., 1988). Typical reaction times were 15 min and longer. Although not directly comparable, pure α -benzyl naphthyl ether was also found to decompose measurably at <300 °C over a 30 min period (Chawla et al., 1990). These results indicate a 50-75 °C lower temperature for the onset of thermolysis of pure benzyl phenyl ether than in our study (Table 4.1). If thermolysis takes place by a slow initiation followed by rapid propagation, which is typical of some free radical processes, thermolysis at lower temperatures can be explained. The calorimetric investigation increased the temperature at

a fixed rate, which will not reflect an accurate temperature for processes with a meaningful initiation time. This is not the case for reactor-based experiments conducted over an extended period. This explanation must still be verified using isothermal calorimetric investigations. Alternatively, ether bond thermolysis in tetralin was solvent assisted. The thermolysis products (Figure 4.5) are typical of free radical decomposition and addition products. The addition reactions explain the overall exothermic nature of the decomposition (Table 4.1). The PhO–CH₂Ph bond is the most likely bond to rupture; it has the lowest bond dissociation energy (BDE). Phenoxy radicals thus formed are more active subsequent hydrogen for abstraction than benzyl radical (Schlosberg et al., 1983), hence the observed phenolic compounds. However, the significant amount of diphenyl methane indicates that at least some Ph–O bond scission took place. It was reported that aryl alkyl ethers are responsible for the formation of CO during coal pyrolysis (Schlosberg et al., 1983).

4.5.2 Dibenzyl ether

The observed melting point corresponds with the value reported in literature (4.2 °C vs lit. 4 °C). No enthalpy of melting data was found for comparison.

The thermolysis of dibenzyl ether is typical of reactions that follow not only free-radical decomposition, but decompose by a concerted mechanism, with the simultaneous rupture

in the transition state of some bonds and the formation of others (Korobkov et al., 1988). Main products are CO, toluene and benzene (Korobkov et al., 1988). The stability of the products from the concerted decomposition and seemingly limited free radical formation resulted in endothermic decomposition (Table 4.1), with a small amount free addition being possible or taking place.

The thermolysis temperature was higher than anticipated from literature, which reported a high rate of decomposition in tetralin at 350 °C (Korobkov, et al., 1988). This is analogous to the observations for benzyl phenyl ether.

4.5.3 Diphenyl ether

The observed melting point corresponds with the value reported in literature (29.2 °C vs lit. 29 °C). No enthalpy of melting data was found for comparison.

Diphenyl ether was thermally stable at 450 °C, the maximum temperature investigated (Table 4.1). Our observations correspond with the thermal stability of diphenyl ether previously reported by Kamiya et al (1986).

4.6 Conclusions

A calorimetric investigation of the thermolysis of ether bonds relevant to coal liquefaction was undertaken. It was found that diphenyl ether is stable up to 450 °C (5 min). Benzyl

phenyl ether and dibenzyl ether decomposed at 357 and 420 °C respectively. These temperatures are higher than that reported in literature for decomposition over an extended time period in a solvent. The decomposition mechanisms seems to be different and further studies were carried out in chapter 5.

4.7 References

Aly, M. M.; Fahmy, A. M.; Gaber, A. M. and Atalla, A. A. "Deamination of primary amines with benzyl nitrite." *Indian Journal of Chemistry*, 33 (1994): 1139-1143

Chawla, B.; Davis, B. H.; Shi, B.; Guthrie, R. D. "Thermolytic cleavage of selected ether linkages at mild temperatures." *Prepr. Pap.-Am. Chem. Soc., Div. Fuel Chem.* 32 (1990): 387-392.

Kamiya, Y.; Ogata, E.; Goto, K.; Nomim T. "Thermal cracking of coal model diaryl ethers in aromatic solvent." *Fuel* 65 (1986): 586-590

Korobkov, V. Yu.; Grigorieva, E. N.; Bykov, V. I.; Senko, O. V.; Kalechitz, I. V. "Effect of the structure of coal-related model ethers on the rate and mechanism of their thermolysis." *Fuel* 67 (1988): 657-662

Ning, X. and Marc, T. "Copper- or iron-catalyzed arylation of phenols from respectively aryl chlorides and aryl iodides." *Chemistry—A European Journal* 14 (2008): 6037-6039

Schlosberg, R. H.; Szajowski, P. F.; Dupre, G. D.; Danik, J. A.; Kurs, A.; Ashe, T. R.; Olmstead, W. Im. "Pyrolysis studies of organic oxygenates." *Fuel* 62 (1983): 690-694

Shah, S. T. A.; Khan, K. M.; Hussain, H.; Anwar, M. U.; Fecker, M. and Voelter, W. "Cesium fluoride-celite: A solid base for efficient syntheses of aromatic esters and ethers." *Tetrahedron* 61 (2005): 6652-6656

Wender, I.; Levine, R.; Orchin, M. "Chemistry of the oxo and related reactions. II. Hydrogenation." *J. Am. Chem. Soc.* 72 (1950): 4357-4378

Whitehurst, D.; Buttrill, S. E.; Derbyshire, F. J.; Farcasiu, M.; Odoerfer, G. A.; Rudnick, L. R. "New characterization techniques for coal-derived liquids." *Fuel* 61 (1982): 994-1005

Wiggins, K. M.; Hudnall, T. W.; Shen, Q.; Kryger, M. J.; Moore, J. S. and Bielawski, C. W. "mechanical reconfiguration of stereoisomers." *J. Am. Chem. Soc.* 132 (2010): 3256-3257

Yaws, C. L. Yaws' Critical Property Data for Chemical Engineers and Chemists. Knovel
(2012)

Chapter Five: Reaction Pathway of Coal Related Ether Compounds

5.1 Introduction

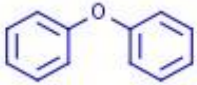
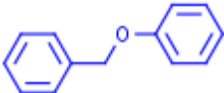
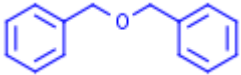
It is known that solvent extraction of coal in the reactive regime is mainly free radical based. What is less clear is how the free radical chemistry takes place, excluding that of hydrogen transfer that is well described. In specific, what is the role and fate of the ethers in coal? Ultimately the ethers are dehydrated, but in the intermediate temperature range the reaction chemistry is more complex. Yet, it is also likely that the way the ethers are decomposed (rate and reactions) determine the product quality and possibly the liquid yield. The objective is to provide a quantitative description of coal ether decomposition and reaction network.

5.2 Experimental chemicals

5.2.1 Coal related ether compounds

Benzyl phenyl ether (98% purity), dibenzyl ether (99% purity), diphenyl ether (99% purity) were purchased from Sigma-Aldrich or Fisher Scientific and used as received (Table 5.1). Reagent-grade acetone and methylene chloride were used in the work-up procedure. All other chemicals used during the experiments were purchased from Fisher Scientific in high purity and used as received. Nitrogen and helium were obtained from Praxair.

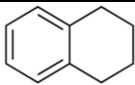
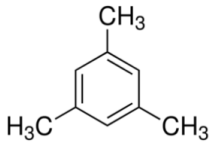
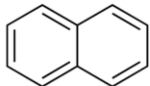
Table 5.1 Detailed information of the ether compounds using for this study

Name	Molecule Structure	MW/(g/mol)	Purity	Company
Diphenyl Ether		170.211	99%	Product of USA Sigma-Aldrich Corp. P24101
Benzyl Phenyl Ether		184.238	99%	Product of USA Sigma-Aldrich Corp. 404284
Benzyl Ether (Dibenzyl ether)		198.265	98%	Product of USA Sigma-Aldrich Corp. 108014

5.2.2 Solvents

Three different solvents were used. 1,2,3,4-tetrahydronaphthalene (tetralin, 99% purity), mesitylene (99% purity) and naphthalene (99% purity) were purchased from Fisher Scientific or Arcos Organics and used as received (Table 5.2). Tetralin was used as hydrogen donor, mesitylene was used as hydrogen shuttler and naphthalene was used as diluent.

Table 5.2 Detailed information of the solvents using for this study

Name	Molecule Structure	MW/(g/mol)	Purity	Company
1,2,3,4-tetrahydronaphthalene (Tetralin)		132.20	99%	Fisher Scientific Company No: T724
mesitylene		120.19	99%	Acros Organics, AC12558-0010
naphthalene		128.17	99%	Acros Organics, AC18090-0010

5.3 Experimental equipment

- Micro reactor

Several micro reactors with same design purchased from Swagelok were used in this study. The schematic of the micro reactor is introduced in figure 5.1. The volume of the micro reactor is 15 mL. The mixture of ether compound and solvent with stainless steel rods occupy approximately 5 mL in volume. The stainless steel micro reactor from Swagelok consists of a 19.05 mm (3/4") outer diameter (OD) stainless steel tube, 76 mm (3") in length, which was joined with a Swagelok reducing union at the top and a Swagelok cap at the bottom.

The 1.6 mm OD (1/16") stainless reactor neck has a length of 15.05cm (6 1/4"). The lower end was joined to the reducing union, and the upper end was joined with a Swagelok severe

service union bonnet needle valve. This valve was located at the top of reactor neck. This design is for operation at severe temperature and pressure condition up to 600°C and 20 MPa. A connector was connected to the needle valve to perform nitrogen-purging step while hooking up with nitrogen cylinder. In the middle of the bracket holder, there is a round hole to attach the whole set-up to the rod and immerse the micro reactor into the sand bath. A K-type thermocouple (ALL Temperature sensor) was inserted in the middle section of the reference micro reactor to track the temperature change inside micro reactor during the experiment.

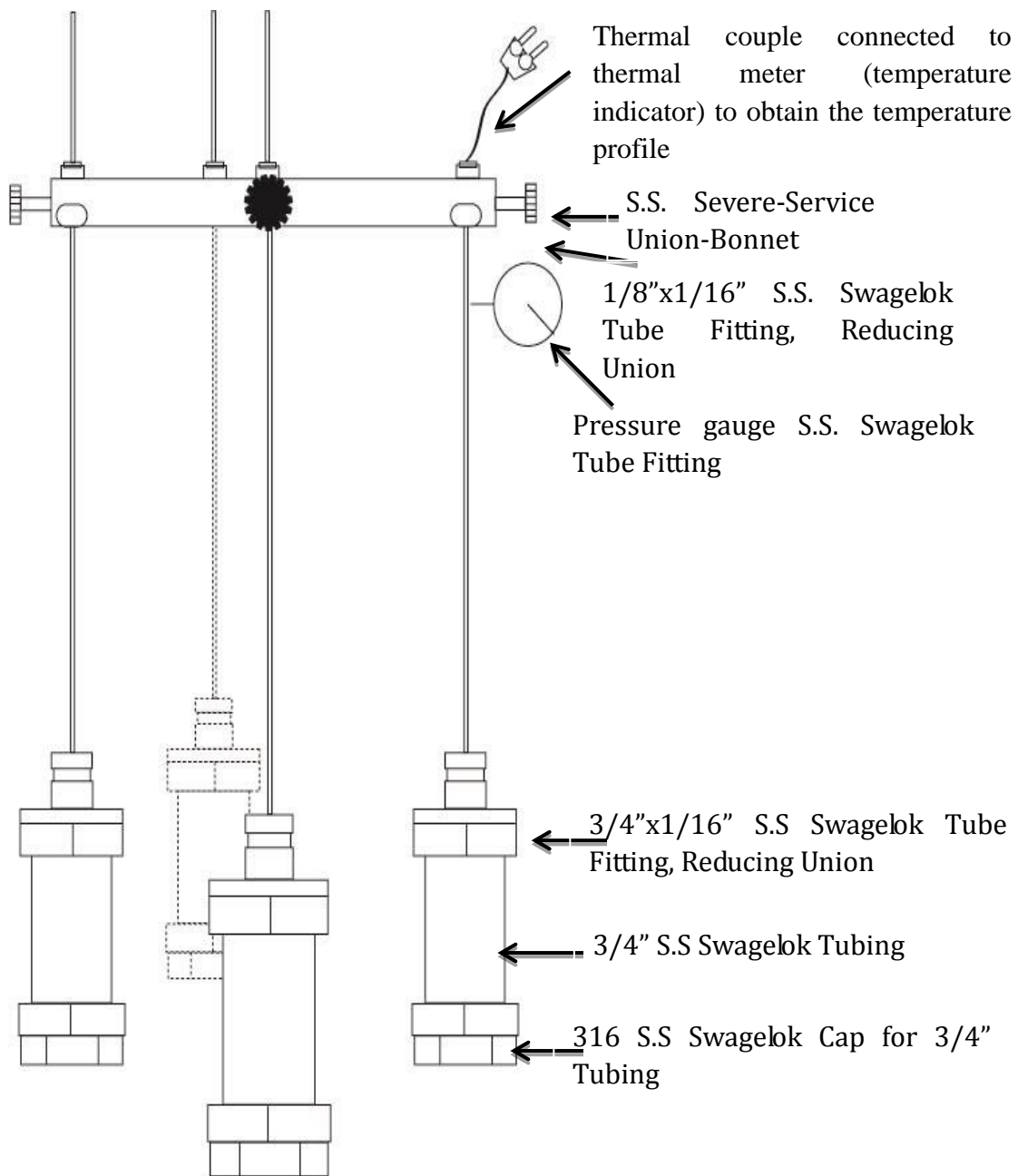


Figure 5.1 Schematic of the micro reactor setup

- Sand bath

Sand bath (Omega, Model No. FSB-3, temperature range from 50 to 600°C) was used in this study. Figure 5.2 showed below was the image of the sand bath with supporting equipment. As we can see in Figure 5.2, sand bath was filled up with silica sand as heat transfer media. Silica sand was fluidized by the air flow to keep the temperature constant in the entire bath. The rate of air flow is very important for the experiments. It affects how sand gets fluidized, also controls the heat transfer rate between sand and micro reactor. Rotameter (Gilmont, D1703) was used to regulate the air flow. A temperature controller (OMRON E5CK) was used to maintain the temperature of sand bath at the set point.

The hole in the middle of micro reactor setup was attached to the rod, the upper part of the micro reactor setup was placed onto the agitator powered by the motor. Before putting the micro reactor setup into sand bath, the parallel branch should be inserted into the guide to maintain the position of the reactor in the middle of the sand bath. Then turn on the motor and plug the thermocouple into the temperature indicator to track the temperature change. The agitator will move the micro reactor setup a distance of 3cm up and down at a frequency of 3 Hz, so that the chemicals can be well mixed during the experiment. For the feed of liquid sample and liquid sample, the mixing was properly done by the agitator, for the feed of solid sample and liquid sample, the diphenyl ether and benzyl phenyl ether both

have a very low melting point (m.p for diphenyl ether is 28 °C, m.p for benzyl phenyl ether is 39 °C – 40 °C), naphthalene as a solvent has a melting point of 80 °C, the mixing of the sample at the preheat stage with agitation is not an issue in this case.

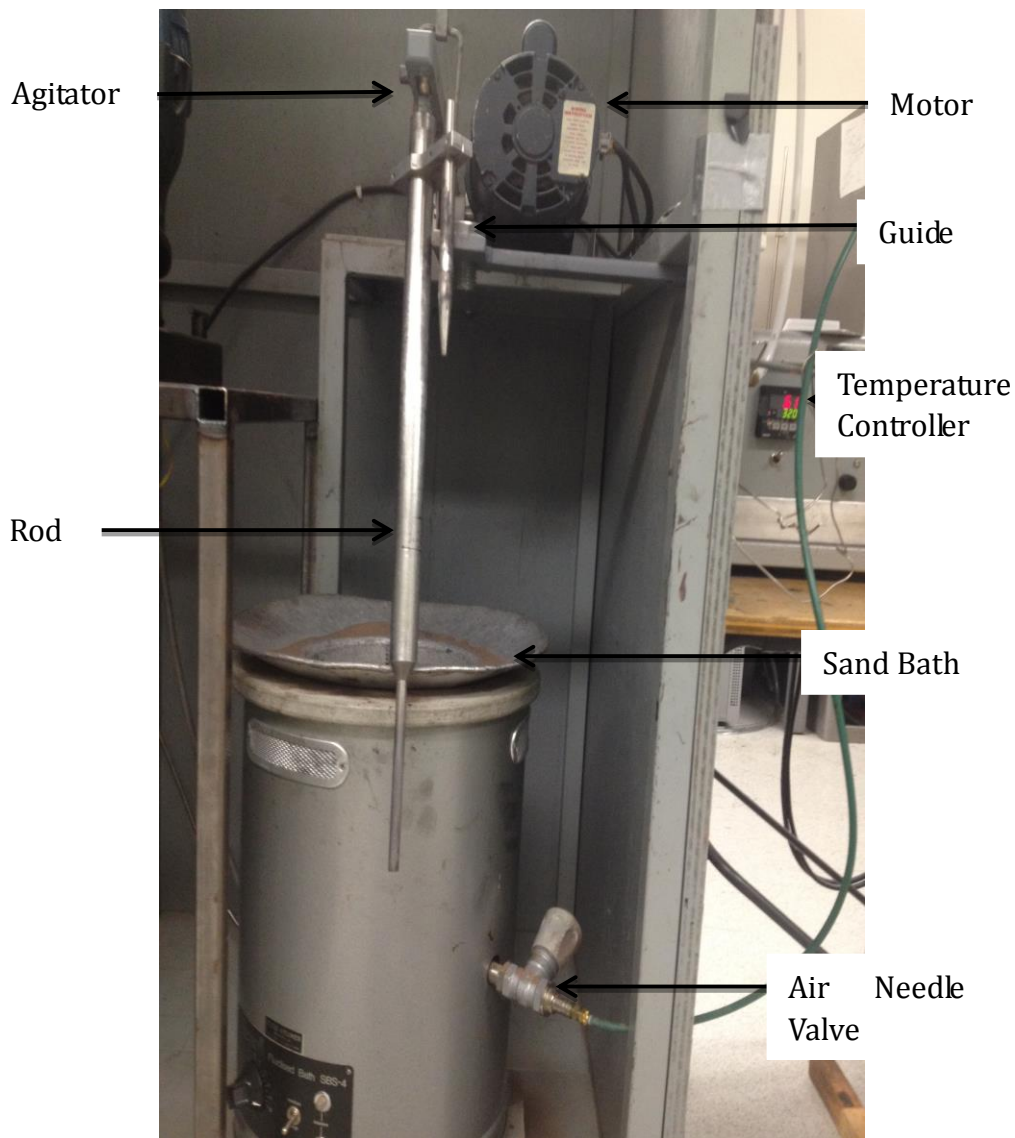


Figure 5.2 Image of the sand bath

- Balance

Three balances were employed for all the weighing in the experiments:

AL104, by METTLER TOLEDO Company, accuracy to 0.1mg, with range 0.1mg to 10000mg; this balance was employed to measure the weight of sample and solvent.

APX 200, by DEVER Instrument Company, accuracy to 0.1mg, with range 0.1mg to 10000mg; this balance was employed to measure the weight of sample and solvent.

CP 622, by Sartorius Company, accuracy to 0.01g, with range 0.01g to 10.0g. This balance was employed to measure the weight of the single micro reactor setup before and after purging and experiments.

5.4 Experimental design

- Ether Samples

Benzyl phenyl ether, Benzyl ether, diphenyl ether were used as model compounds to systemically study the reaction pathways.

- Temperature range

The reactive regime is defined from 300 °C to 450 °C. Reactions at 300 °C, 350 °C, 400°C and 450 °C were carried out.

- Atmosphere and pressure

To match the process from the related industry, nitrogen was used as purging gas and the

whole reaction was carried out under nitrogen atmosphere with the pressure of 40 bar.

- Solvent to sample ratio

The solvent to sample ratio we were using are 1:9, 1:1, 9:1. The solvent to sample ratios that were 1:9 and 9:1 to study the thermal decomposition of ether compounds under extreme solvent environment.

- Holding time

Holding time was 30 minutes for all the experiments.

5.5 Experimental procedure

5.5.1 Reactor Feed and Loading

The ether compounds and solvents were carefully measured then mixed with 5 stainless steel rods. The small stainless steel rods were used to promote mixing of the ether compound and solvent during the reaction.

5.5.2 Reactor sealing and purging with nitrogen

After loading the mixture into the micro reactor, a thin layer of sealant (Silver goop from Swagelok or NeverSeez from Industrial Supply Group, LLC) was applied to the threading of the reactor top and then hand tightened. The sealant we employed was to make sure that micro reactor could be easily opened after high temperature reactions. Then the

hand-tightened reactor was placed in a bench vice and tightened with a wrench.

The reason of purging the reactor with nitrogen was to make sure there is no air left in the reactor so there will be no oxygen and other reactive gas to react with the sample under high pressure and high temperature. The nitrogen purging process is to make sure the experiments was undergo an inert environment.

The fully closed reactor was connected to a nitrogen cylinder for a leak test.

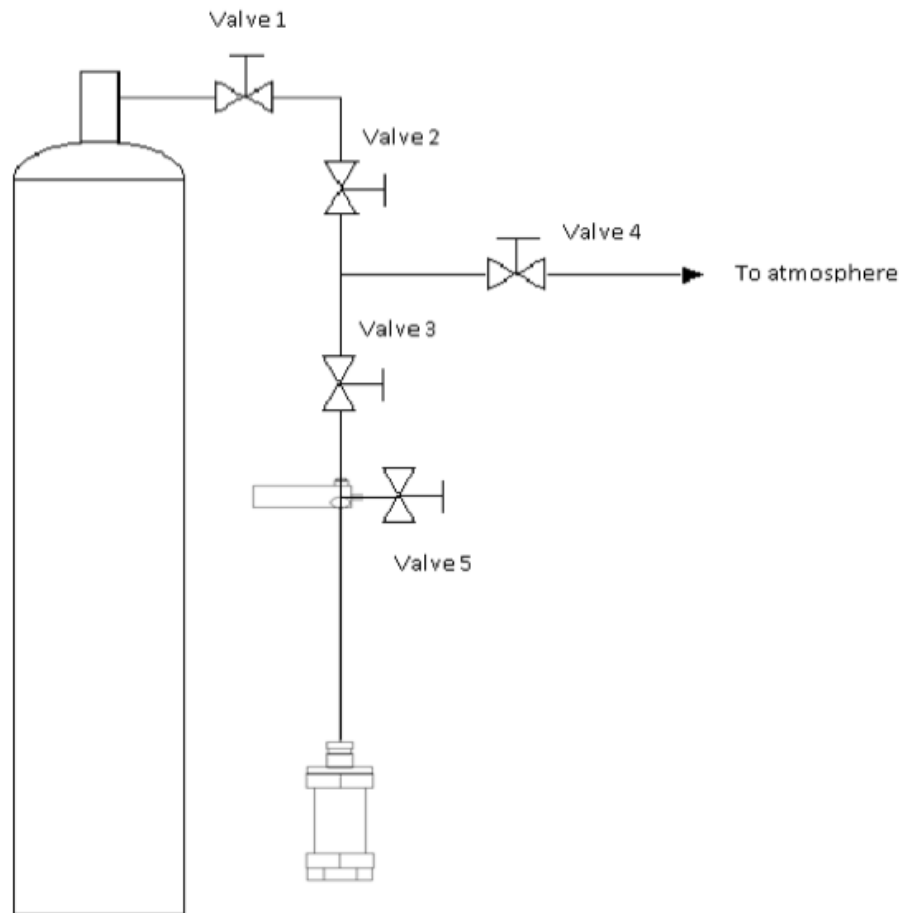


Figure 5.3 Schematic of the nitrogen cylinder setup

Figure 5.3 shows the detailed setup we were using. The standard procedure of leaking test and purging are listed as follows:

- Slowly open the nitrogen cylinder, set the pressure to 40 bar, then open valves 1, 2, 3 and 5, keep valve 4 closed, the nitrogen flows through the line into micro-reactor.
- Apply Snoop (or other leak test liquid) from valve 2 all the way down to the whole reactor, covering all the fittings. Wait for at least two minutes to check if there are any bubbles coming from the threads.
- Usually the bubbles can be found around the reactor which has been used for a few times. This means the reactor was not properly sealed, and it should be taken off, retightened and then restart the whole leak test to see if it is properly sealed. Repeat the leak test until there is no bubble, which means there is no leak, then precede to the next step.
- After the leak test is done and there is no leak, then start to purge the micro-reactor. Before purging the reactor, release the nitrogen inside the reactor first. Close valve 1, 2, slowly open valve 4 and let the gas go to the fume hood through the rubber tube. Then close valve 4. Then open valve 1, 2, 3, 5, let nitrogen flows into reactor again, stay for two minutes. Then close valve 1, 2, and slowly open valve 4. This purging step should be repeated for five times.
- After the purging five times, close valve 5 on the reactor first, then close valve 1, 2, 3,

then open valve 4 to release the gas inside the tubing. Then disconnect the reactor from the set-up.

5.5.3 Reaction

In this study, two stages were included in the reaction sequence. The first stage was the thermal reaction and carried out in the sand bath with heating. The second stage was the cooling interval. The thermal reaction stage was a standard reaction period and to ensure the reaction condition was strictly according to our design. The heating profile was obtained along with the reaction stage. The heating stage was approximately 3 to 4 minutes. After the temperature reached the desired temperature, set the clock to 30 minutes so the reaction time of experiments will strictly be 30 minutes for each. The cooling stage was performed right after 30 minutes of reaction by simply taking out the whole setup from the sand bath to fume hood. The micro reactors were cooled by blowing air to cool down to room temperature. The cooling process mostly took 5 to 6 minutes.

5.5.4 Product Recovery and Analysis

The gas phase products were carefully collected into gas sample bags and liquid phase products were collected from the reactor into 2mL sample vials.

The liquid products were identified on GCMS. This was performed using a Varian CP 3800

equipped with a flame ionization detector (FID) and Saturn 2200 mass selective (MS) detector. The material was separated using a capillary column (30 m × 250 μm). The temperature program used for separation started at 50 °C for 10 min, followed by a +10 °C/min increase from 50 to 320 °C and was then kept isothermally at 320 °C for 10 min.

The gas phase products were injected into an Agilent 7890A gas chromatograph with flame ionization detector (Front FID) and thermal conductivity detector (TCD). The peak areas from the GC-FID chromatograms were related to product mass by employing appropriate FID response factors. A 10' x 0.125" O.D, 80/100 mesh size HayeSep R column was employed for product separation. The temperature programs started at 70 °C, with a holding time of 7 minutes, thereafter the temperatures was increased by 10 °C per minute up to 250 °C and then holds at 250 °C for 2 minutes, then at 30 °C per minute to 30 °C and holding for 8 minutes. After 1.75 minutes, the remaining compounds were then traverse into a parallel line and into a thermal conductivity detector and then a flame ionization detector. Total time is 41 minutes.

All the results from GC-MS were characterized and cross checked with two different databases to ensure the accuracy. The first database we were using was NIST Standard Reference Database (Data Version: NIST 11, Software Version 2.0g). The second database was AMSDIS (Automated Mass Spectral Deconvolution & Identification System).

Quantitative product mass fractions were determined from GC calibration factors derived from standard samples of known compositions. Response factors (Nel, et al., 2009) of linear ethers were applied to the product spectra (Table 5.3).

Table 5.3 Experimentally determined GC-FID response factors of linear ethers

Compound	Response factor
di- <i>n</i> -propyl ether	0.695±0.005
di- <i>n</i> -butyl ether	0.803±0.003
di- <i>n</i> -pentyl ether	0.856±0.010
di- <i>n</i> -hexyl ether	0.878±0.007
di- <i>n</i> -octyl ether	0.906±0.008

5.5.5 Validation of Experimental Method

Temperature Profile

To validate the experimental methods, the heating profiles of micro reactor during experiment were obtained.

The procedure was described as follows: first insert a thermocouple inside the reference micro reactor. The thermocouple was inserted through a modified 1/4" x 1/16" cap union which installed at the top part of the micro reactor. The reference reactor was closed with no feed inside. To obtain the signals from the thermocouple, the thermocouple was connected to a device quipped with analysis software. For the all temperature profiles, the setup was the same.

There were four different temperatures needed for the experiments. Figure 5.4 to Figure 5.7 were the temperature profiles at 300 °C, 350 °C, 400 °C and 450 °C. As an example, Figure 5.4 shows the temperature of the micro reactor as a function of time starting from 0 min, when the micro reactor was put into sand bath and the agitation was begun. The set point of the temperature controller was higher than the actual temperature because from the temperature calibration of the sand bath, it shows that the deviation of the sand bath was 10 °C lower than the set point at 300 °C, 9 °C lower than the set point at 350 °C and 400 °C, 8 °C lower than the set point at 450 °C. The temperature of micro reactor was above 295 °C within 170 s, and then the micro reactor reached a steady temperature at 300.4 °C. After 30 minutes of reaction, the micro reactor was taken out to quench under air flow to stop the reaction.

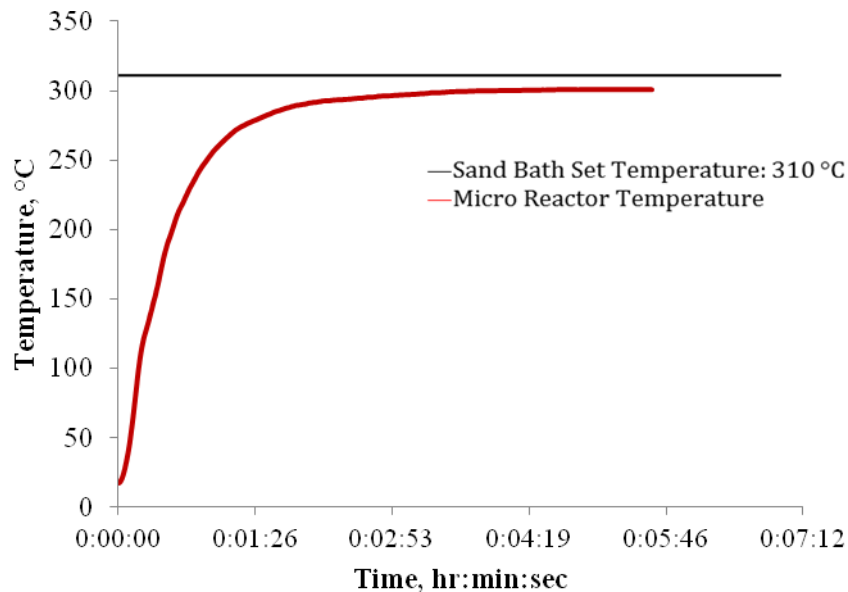


Figure 5.4 Internal reactor temperature as a function of time for a reaction with a sand bath set-point of 300 °C

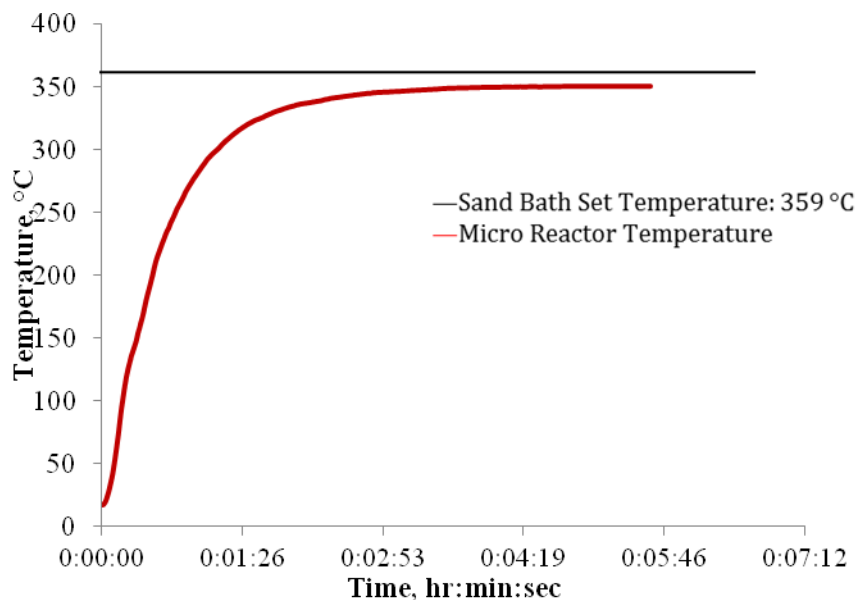


Figure 5.5 Internal reactor temperature as a function of time for a reaction with a sand bath set-point of 350 °C

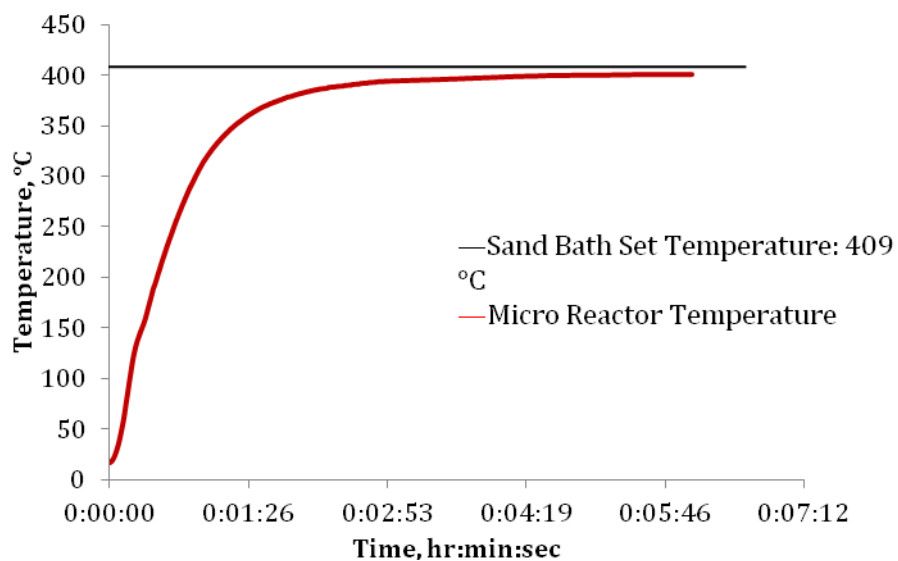


Figure 5.6 Internal reactor temperature as a function of time for a reaction with a sand bath

set-point of 400 °C

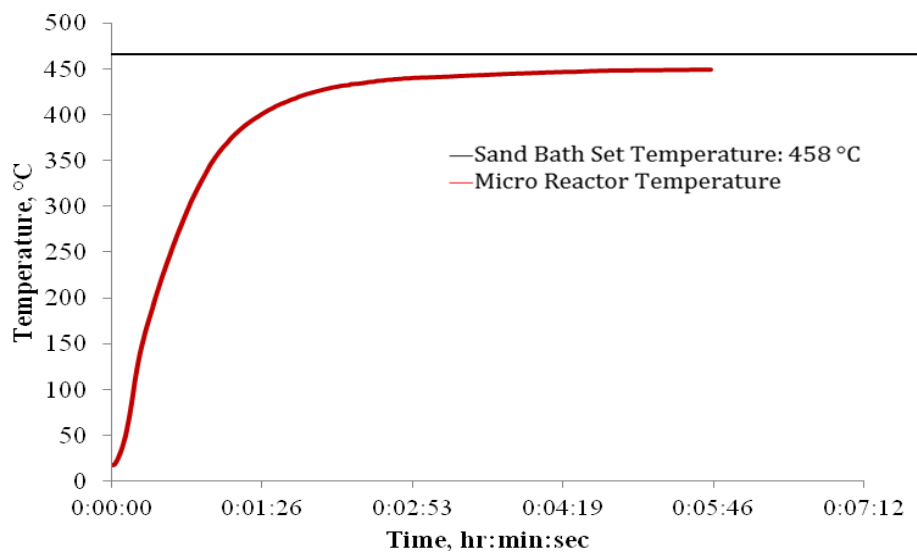


Figure 5.7 Internal reactor temperature as a function of time for a reaction with a sand bath

set-point of 450 °C

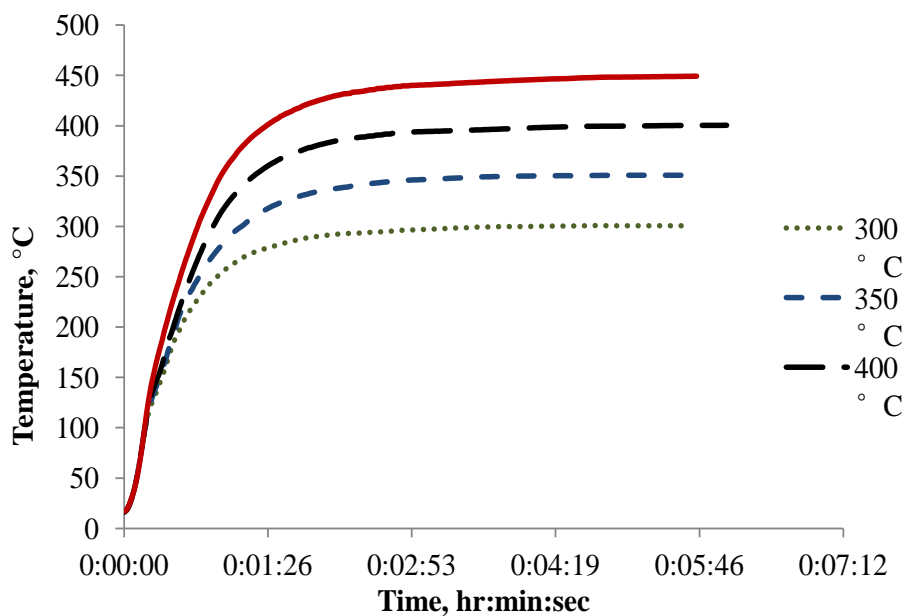


Figure 5.8 Overall comparison of the temperature profile

Mass Balance

Table 5.3 shows a sample mass balance of the reactions of DBE at 450°C. Runs with most reasonable results were chosen for mass balance calculations. Gas product yield was calculated by subtracting weight of the gas released by the nitrogen added.

Four weight measurements were done for each experiment as follows:

$W_{\text{setup+sample}}$: The weight of the setup and the sample loaded inside

$W_{\text{setup+sample+nitrogen}}$: The weight of the setup with sample after purging with N_2

$W_{\text{setup after experiment}}$: The weight of the setup right after the cool down process (with gas products)

$W_{\text{setup after experiment gas release}}$: The weight of the setup after the cool down process (after release the gas products to gas bag)

$$W_{\text{setup+sample+nitrogen}} - W_{\text{setup+sample}} = W_{\text{nitrogen}} \quad 5-1$$

$$W_{\text{setup after experiment gas release}} - W_{\text{setup after experiment}} = W_{\text{nitrogen with gas products}} \quad 5-2$$

$$W_{\text{nitrogen with gas products}} - W_{\text{nitrogen}} = W_{\text{gas products}} \quad 5-3$$

The mass of the gas was calculated using 5-1, 5-2 and 5-3.

Liquid product was calculated by subtracting the total weight of reactor after the reaction by the weight of the reactor. The weight of the feed was measured before the feed was added to the reactor. As shown in the table, if we assume nitrogen is inert, then the total product should have the same weight of the feed. The runs in the table agreed within 10%

error. Sometimes the total product is more than the feed, but sometimes is lower. There are several reasons for the observation. Firstly, when the total product is more than the feed, the reason could be that some sand stuck with the reactor when the reactor was taken out from the sand bath. Even with thorough clean of the sand, some sands can still contribute to weight increase of the total weight of reactor. Secondly, significant amount grease was applied to the reactors before they were put into the sand bath and some ingredients in the grease were evaporable when heated. Hence the total weight of the reactor after could also be lower than before the reaction. Lastly, other reasons such as human error could also contribute to the results. In conclusion, the amount of reactants in the reactor was too little to provide good mass balance because any trivial influences during the experiments could have large effect to the results.

Table 5.4 Sample mass balance of DBE reacted with different solvents at 350 °C with different ratios.

DBE to Solvent Ratio	Liquid Product	Standard Deviation	Gas Product	Standard Deviation	Total Product	Feed
9:1 with Tetralin	0.817	0.045	0.220	0.017	1.037	0.995
	0.802		0.210		1.012	0.991
	0.795		0.202		0.995	0.984
9:1 with Mesitylene	0.868	0.054	0.206	0.029	1.074	1.008
	0.850		0.200		1.050	1.005
	0.895		0.227		1.122	1.124
9:1 with Naphthalene	0.764	0.021	0.228	0.021	0.992	1.009
	0.705		0.210		0.915	0.910
	0.741		0.205		0.946	0.950
1:1 with Tetralin	0.880	0.087	0.111	0.036	0.991	1.003
	0.905		0.132		1.037	1.025
	0.850		0.107		0.987	1.002
1:1 with Mesitylene	0.828	0.034	0.226	0.045	1.054	1.000
	0.814		0.220		1.034	1.024
	0.874		0.254		1.128	1.130
1:1 with Naphthalene	0.910	0.021	0.200	0.023	1.110	1.080
	0.950		0.224		1.174	1.154
	0.947		0.214		1.161	1.054
1:9 with Tetralin	0.943	0.041	0.049	0.054	0.992	1.003
	0.914		0.038		0.952	0.988
	0.901		0.039		0.940	0.968
1:9 with Mesitylene	0.882	0.054	0.086	0.087	0.988	1.003
	0.854		0.074		0.928	1.000
	0.814		0.059		0.873	0.907
1:9 with Naphthalene	0.929	0.026	0.086	0.019	1.015	0.999
	0.917		0.081		0.998	0.995
	0.902		0.080		0.982	0.968

*All the experiments were triplicated under the same reaction condition and standard deviation of gas products and liquid products were reported

Figure 5.9 to 5.11 show more visualized results of the sample mass balance. Despite we already concluded mass balance in this study give little value, there is still some observation might be useful. First of all, reaction with tetralin normally yielded the least gas product in this case. The methylene and naphthalene gave almost the same gas product. Secondly, in the case when solvent was excess, least gas product were formed. Same

results were observed when BPE was reactant.

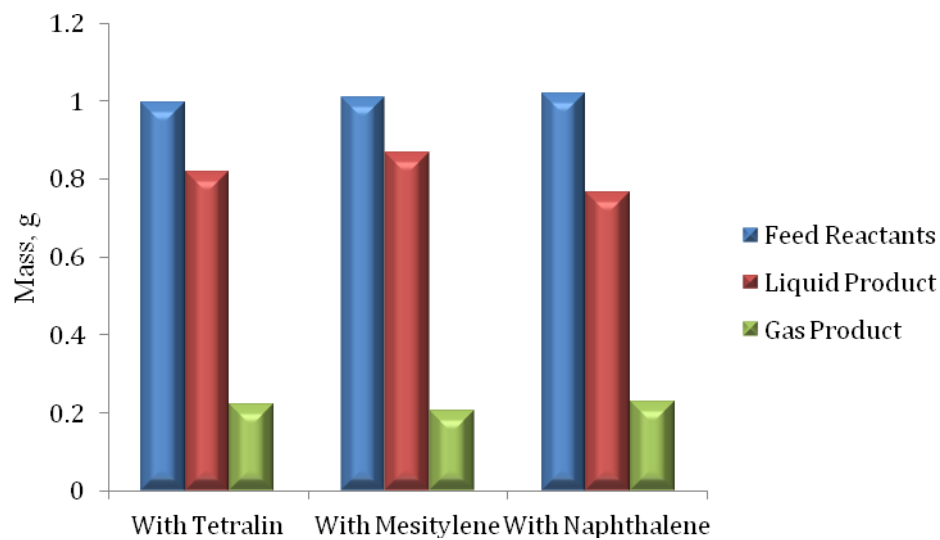


Figure 5.9 Mass balance of DBE reacted with different solvents at 350 °C with DBE:Solvent=9:1.

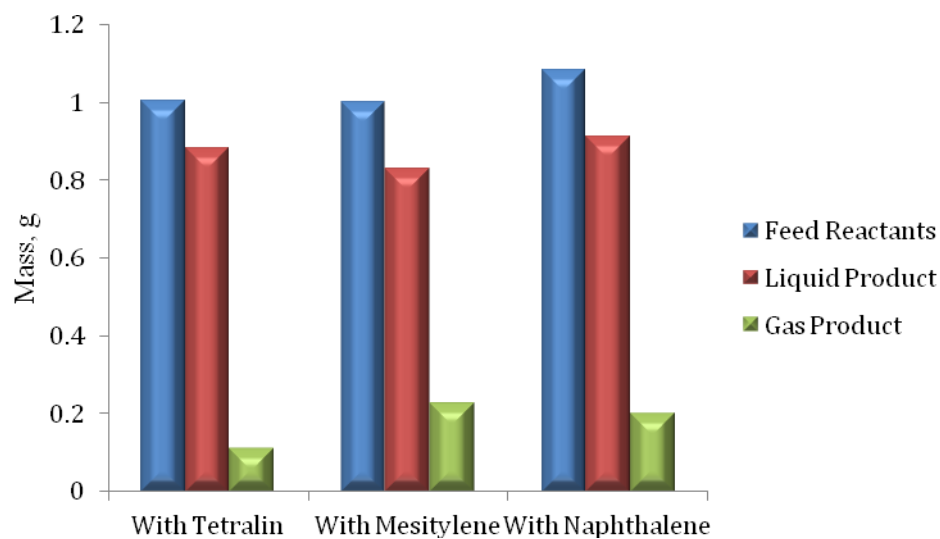


Figure 5.10 Mass balance of DBE reacted with different solvents at 350 °C with DBE:Solvent=1:1

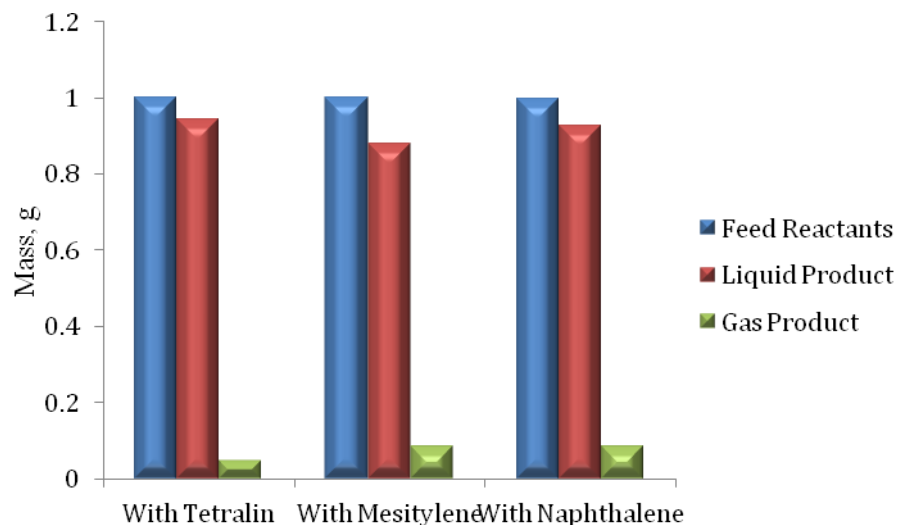


Figure 5.11 Mass balance of DBE reacted with different solvents at 350 °C with DBE:Solvent=1:9

Standard Deviation

All the experiments were triplicated under the same reaction conditions to obtain the standard deviation. Figure 5.12 and 5.15 are the comparison of products chromatographs of three different reactors performing the same reaction. It shows great repeatability of the experiments. The GC results were measured by GC-FID (before corrected with response factors).

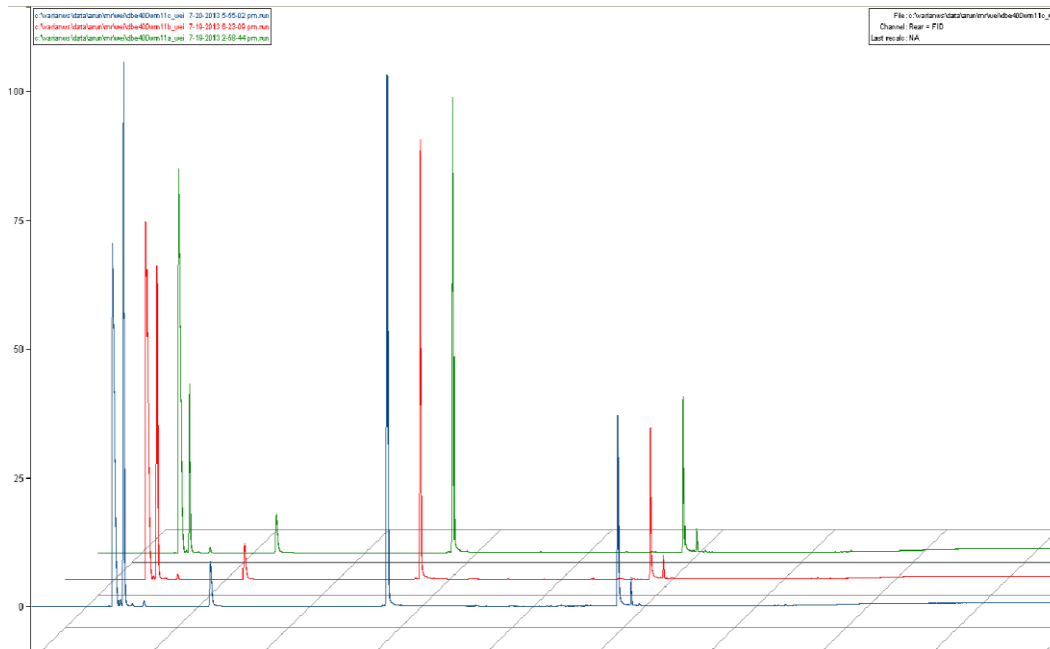


Figure 5.12 Triplicated experiments of DBE with mesitylene at 400 °C with ratio 1: 1. GC-MS data obtained for comparison and standard deviation calculation.

Table 5.5 Triplicated experiments of DBE with mesitylene at 400 °C with ratio 1: 1, three runs were carried out in the exact same experimental condition.

Retention Time /min	Reacted Composition			Average Composition	Standard Deviation
	Run1	Run2	Run3		
4.414	0.5130	0.5146	0.5262	0.5179	0.0072
12.329	0.0257	0.0278	0.0232	0.0256	0.0023
12.551	0.3872	0.3785	0.3950	0.3869	0.0083
24.071	0.0655	0.0695	0.0488	0.0613	0.0110
24.678	0.0087	0.0094	0.0068	0.0083	0.0013

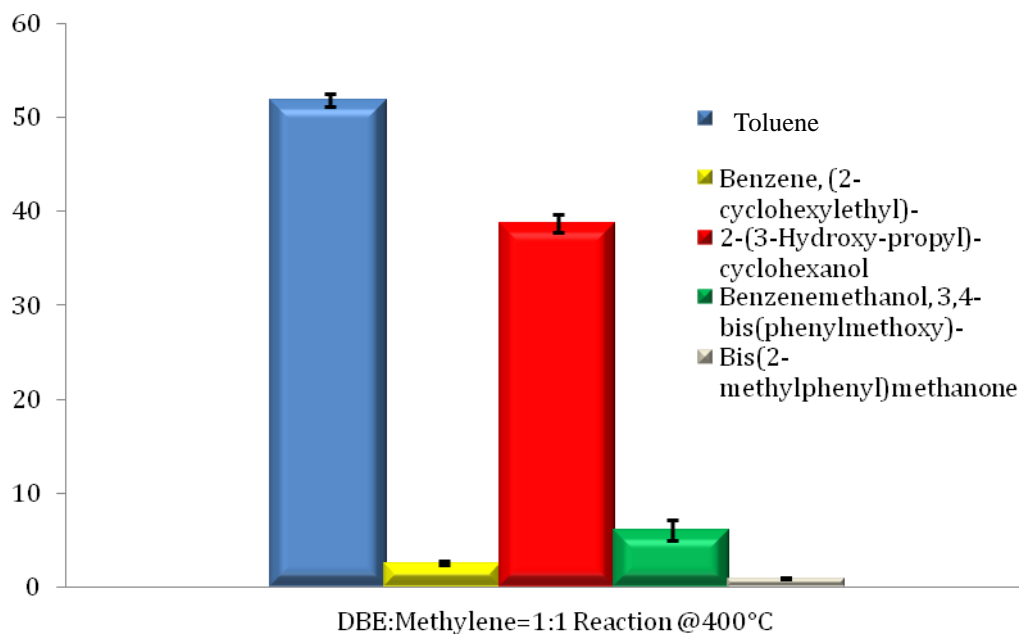


Figure 5.13 Products distribution of DBE with mesitylene at 400 °C with ratio 1:1

Table 5.6 Triplicated experiments of DBE with tetralin at 400 °C with ratio 1: 1, three runs were carried out in the exact same experimental condition.

Retention Time /min	Reacted Composition			Average Composition	Standard Deviation
	Run1	Run2	Run3		
4.414	0.7715	0.7583	0.7814	0.7704	0.0116
12.329	0.0220	0.0210	0.0209	0.0213	0.0006
17.274	0.1397	0.1427	0.1253	0.1359	0.0093
27.129	0.0090	0.0084	0.0093	0.0089	0.0005
27.414	0.0174	0.0163	0.0167	0.0168	0.0006
27.931	0.0072	0.0071	0.0093	0.0079	0.0012

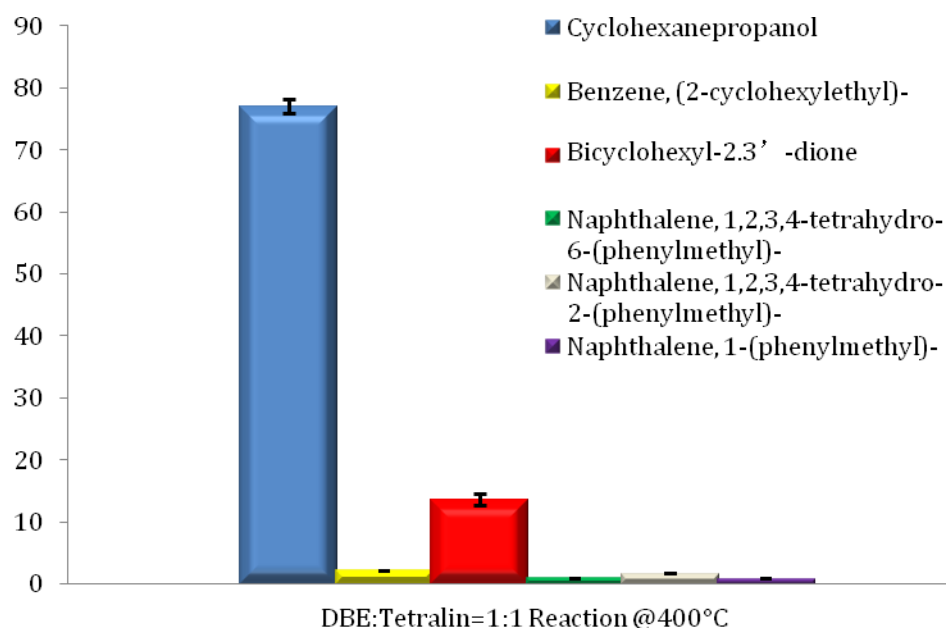


Figure 5.14. Products distribution of DBE with tetralin at 400 °C with ratio 1:1

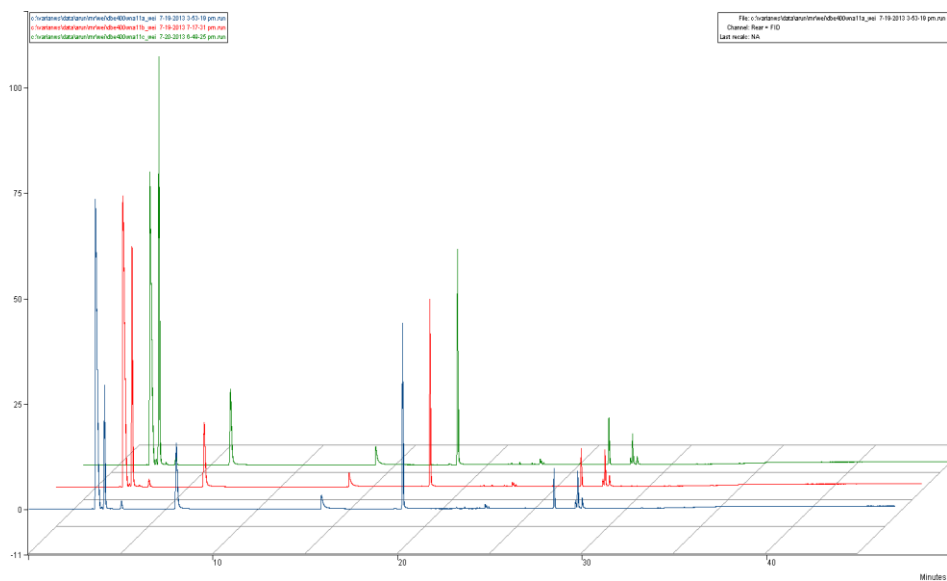


Figure 5.15 . Triplicated experiments of DBE with mesitylene at 400 °C with ratio 1: 1.

GC-MS data obtained for comparison and standard deviation calculation.

Table 5.7 Triplicated experiments of DBE with naphthalene at 400 °C with ratio 1: 1, three runs were carried out in the exact same experimental condition.

Retention Time /min	Reacted Composition			Average Composition	Standard Deviation
	Run1	Run2	Run3		
4.414	0.7564	0.7449	0.7566	0.7526	0.0067
12.329	0.0327	0.0368	0.0294	0.0330	0.0037
17.744	0.1738	0.1857	0.1891	0.1829	0.0080
26.368	0.0175	0.0164	0.0154	0.0164	0.0011
27.687	0.0087	0.0094	0.0084	0.0088	0.0005

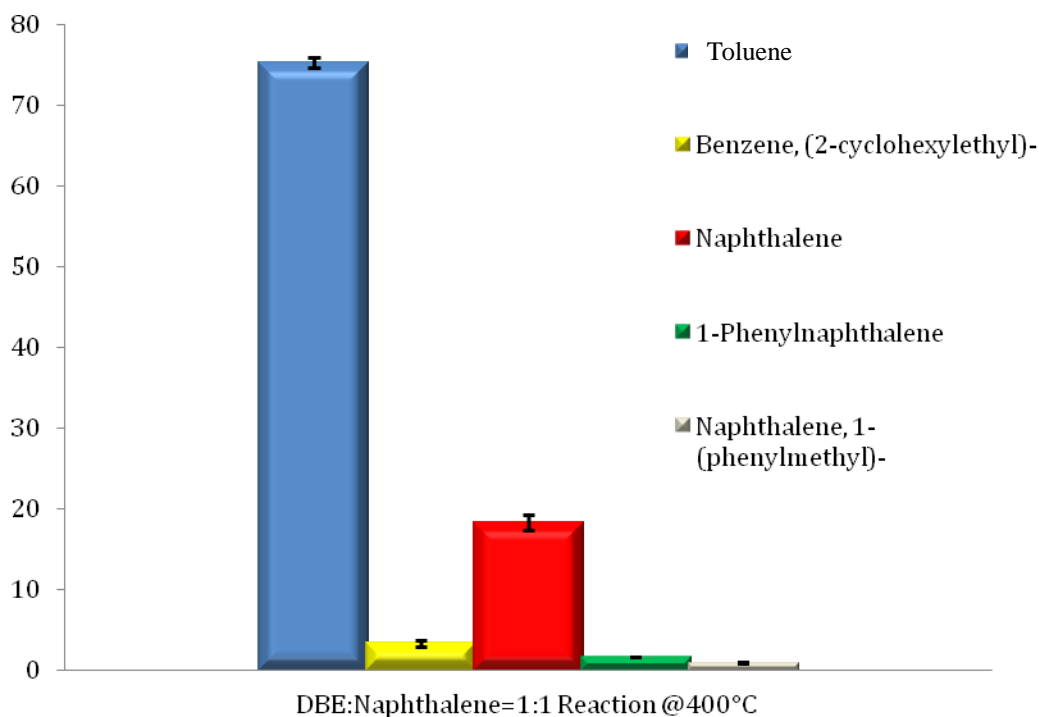


Figure 5.16 Products distribution of DBE with naphthalene at 400 C with ratio 1:1

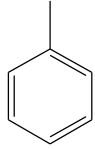
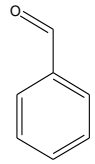
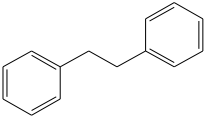
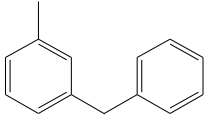
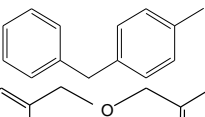
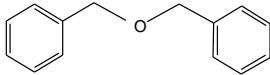
5.6 Results

5.6.1 Reaction Network Pure Dibenzyl Ether (DBE)

If pure dibenzyl ether was reacted at 300 °C, the GC-MS only showed one peak appeared at retention time of 24.067min.(Appendix A) This represented dibenzyl ether. Detailed scanning peaks were included Appendix A. The temperature was too low to let DBE to decompose.

Once the temperature reached 350 °C, DBE started to decompose. Major product are tabulated in Table 5.8. Based on the information provided by GC-MS a reaction network can be easily proposed, which is shown in Figure 5.17. During the reaction, DBE first underwent an Alpha scission, and the free radicals that contained oxygen atom formed compound D2 in the table. If we look at the mole fraction of compound D2, it was about half of the total product, which was reasonable. The rest of the free radicals ether gained hydrogen to form toluene or formed compound D3, D4, D5 in the table. There might be other isomers similar to compounds 4 and 5, because their peaks were so close that it was very hard to distinguish the isomers. The C: H: O: Aromatics in DBE is 14:14:1:2, whereas in the product, it was 14.0:14.5:0.97:2.1. The proposed results can be considered accurate because the error was within 5%.

Table 5.8 Reaction product of DBE at 350 °C

Compound	Weight Fraction, %	Molecular Weight	Mole Fraction, %	Formula	Aromatic
D 1 	29.98	92	37.30	C ₇ H ₈	1
D 2 	41.82	106	45.16	C ₇ H ₆ O	1
D 3 	4.21	182	2.65	C ₁₄ H ₁₄	2
D 4 	4.75	182	2.99	C ₁₄ H ₁₄	2
D 5 	4.09	182	2.57	C ₁₄ H ₁₄	2
D 0 	16.16	198	9.34	C ₁₄ H ₁₄ O	2

Reaction Network of Pure DBE

300°C

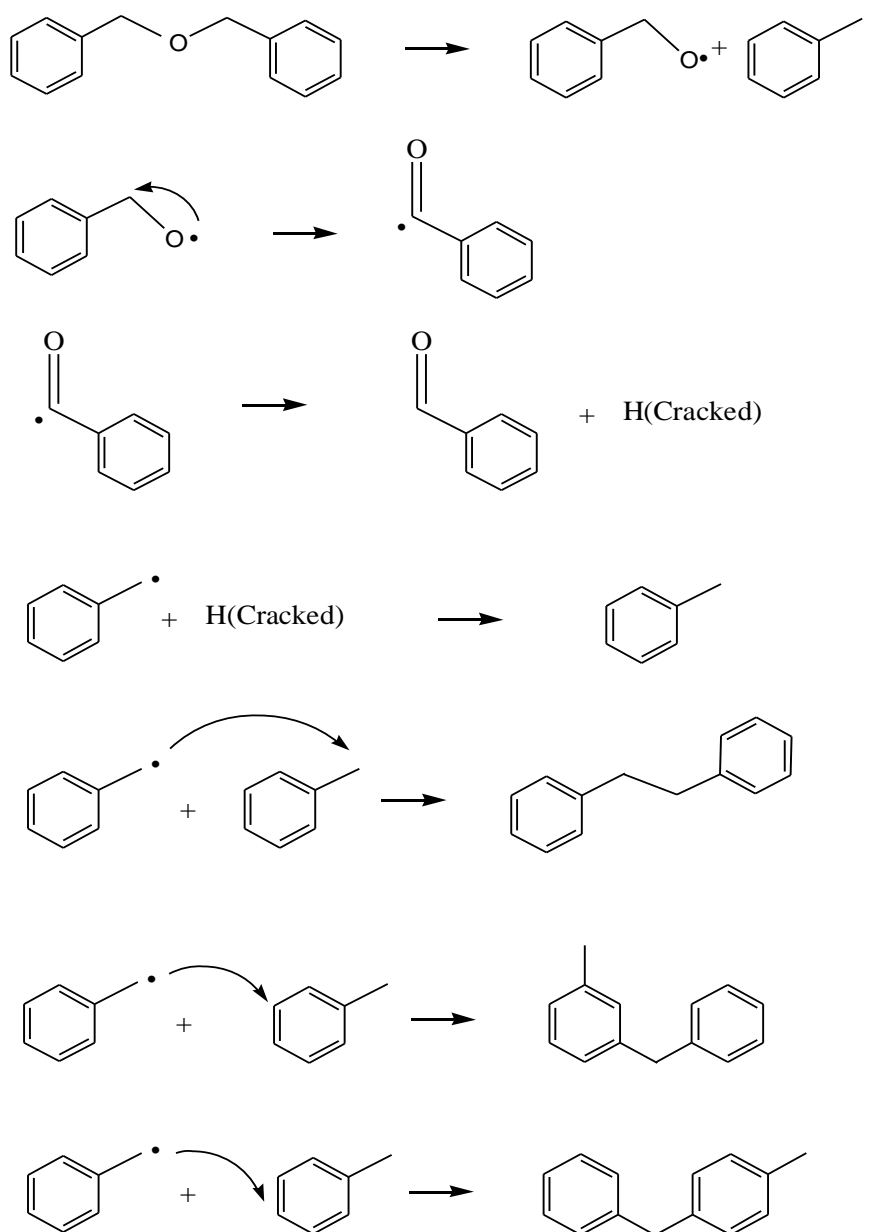
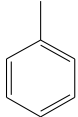
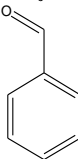
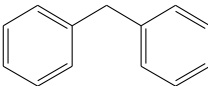
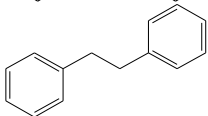
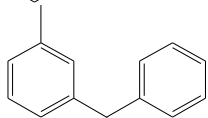
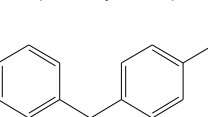
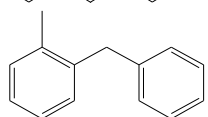


Figure 5.17 reaction network of pure DBE at 350 °C.

Major components formed during 400 °C reaction were tabulated in Table 5.9. The products were similar to when at 350 °C. However, much more product such as D3, D4, D5,

D7 (D7 is similar to D3, D4, D5) were formed and accordingly, much less toluene could be found in the product. This observation makes sense because according to Figure 5.18, compound D3, D4, D5 were formed by toluene and its free radicals. Toluene and its free radicals were formed by the part of DBE without oxygen after Alpha scission. If we calculate C: H: O: Aromatics in this case, which is 14:13.6:0.46:2.2, the result shows that significant amount of oxygen is missing. That could be due to the formation of carbon monoxide and water. The gas analysis was not done in this case and further investigation needs to be done, Carbon monoxide could form during the cracking of compound D2, and the rest free radical went to form D6 with toluene free radical. Most of the feed was reacted in this case, which showed that DBE was not very stable under thermolysis. Beta scission could also occur at this temperature, detailed network is included in Figure 5.18. Further investigation is needed to verify the reaction network.

Table 5.9 Reaction product of DBE at 400 °C

Name	Weight Fraction, %	Molecular Weight	Mole Fraction, %	Formula	Aromatics	
D1		3.99	92	6.49	C ₇ H ₈	1
D2		23.66	106	33.40	C ₇ H ₆ O	1
D6		9.19	168	8.19	C ₁₄ H ₁₄	2
D3		17.23	182	14.17	C ₁₃ H ₁₂	2
D4		9.89	182	8.13	C ₁₄ H ₁₄	2
D5		18.09	182	14.87	C ₁₄ H ₁₄	2
D7		17.95	182	14.76	C ₁₄ H ₁₄	2

Additional Reaction at 400 °C

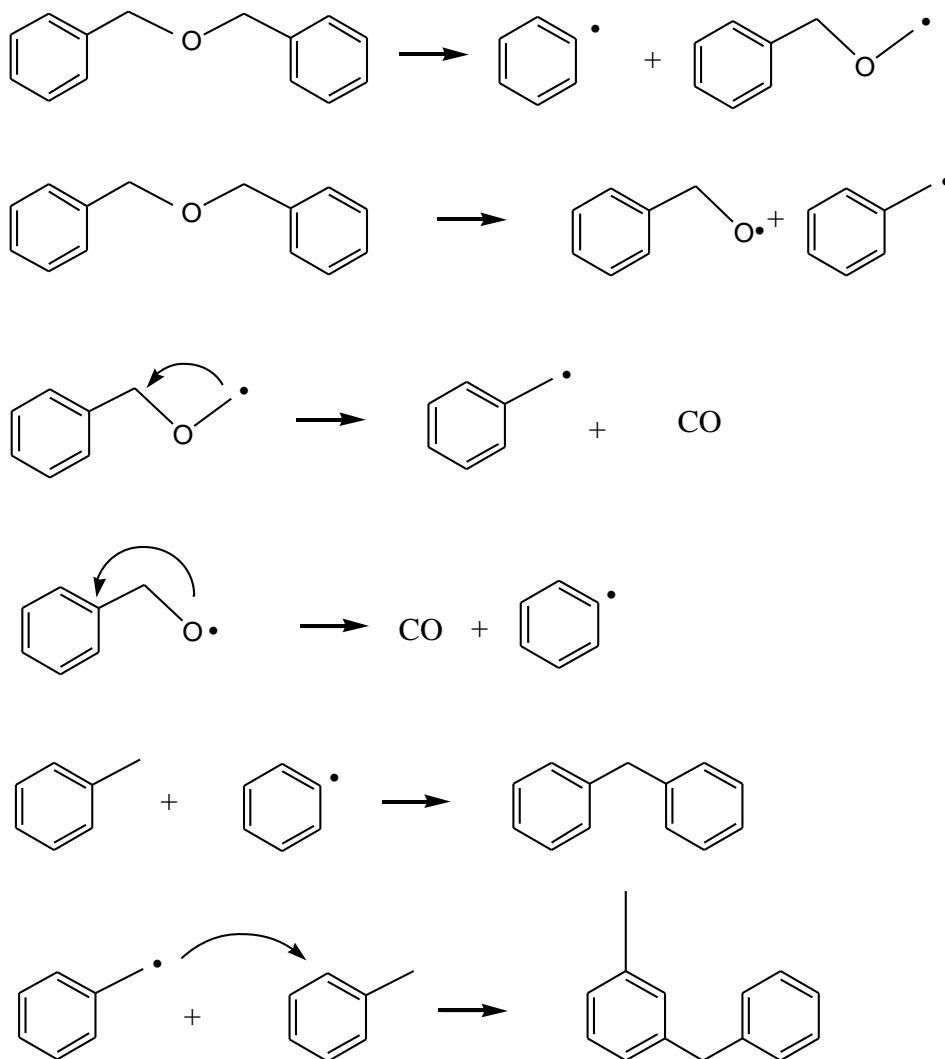
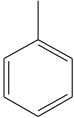
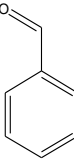
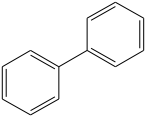
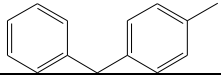


Figure 5.18. Additional reaction of pure DBE at 400 °C

If the temperature was further increased to 450 °C, instead of forming compound D3, D4, D5 and D7, much more toluene was formed. Major product of DBE reacted at 450 °C was tabulated in Table 5.10. The percentage of toluene seemed not so reasonable. However, according to the GC-MS peak shown in Appendix A, there were small peaks in the large

molecule region, and their intensities were too low to be considered as significant. Since these tabulated molecules were the most abundant products, many products were missing in the table. At 450 °C, polymerization could occur since the product after reaction had dark color, and those missing products had various chemical structures and could hardly be identified by GC-MS. Hydrogen free radicals could form during the polymerization. Therefore, instead of forming compound D7, D4, D5, a lot of toluene was formed during the reaction. The C: H: O: Aromatic was calculated to be 14:15.2:0.1:2.0. The data showed that a lot of oxygen originally carried by DBE was not in the product. If we take a look at compound D8, it could be formed by two D2 molecules losing carbon monoxide, and the rest two aromatic free radicals combined together. Detailed network is included in Figure 5.19.

Table 5.10 Reaction product of DBE at 450 °C

	Name	Weight Fraction, %	Molecular Weight	Mole Fraction, %	Formula	Aromatics
D 1		46.41	92	83.19	C ₇ H ₈	1
D 2		7.32	106	6.92	C ₇ H ₆ O	1
D 8		9.39	154	6.11	C ₁₂ H ₁₀	2
D 5		6.87	182	3.78	C ₁₄ H ₁₄	2

Additional Reactions for DBE at 450 °C

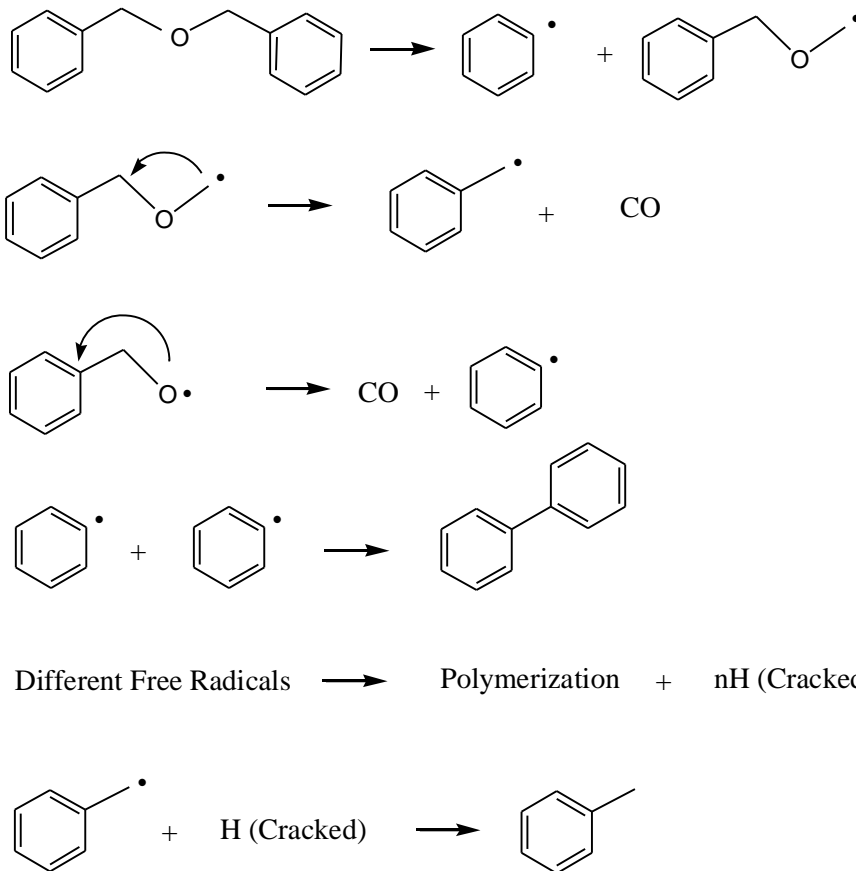


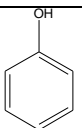
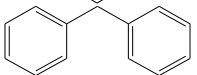
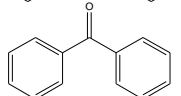
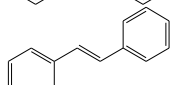
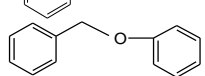
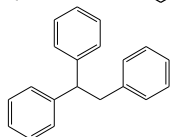
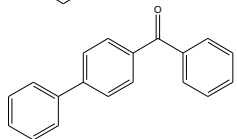
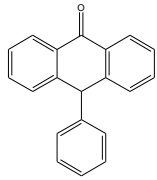
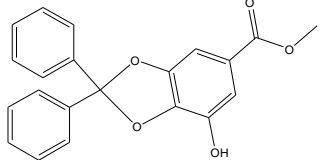
Figure 5.19 Additional reactions of DBE at 450 °C

5.6.2 Reaction Network Pure Benzyl Phenyl Ether (BPE)

If pure Benzyl Phenyl ether was reacted at 300 °C, the GC-MS only showed one peak appeared at retention time of 23.147min. This represented BPE. Detailed scanning peaks were included Appendix A. The temperature was too low to let BPE to decompose.

Similar with DBE, BPE started to decompose at 300 °C. Major components are tabulated in Table 5.11. Different from DBE decomposition, BPE underwent both Alpha and Beta scission. Free radical formed by Alpha scission gained a hydrogen atom to form phenol. This mechanism was similar with the toluene formation for DBE; the only difference was that there was oxygen in the molecule. The rest of the products were basically the rearrangement of the free radicals formed after Alpha and Beta scission. Compound B8 was a complicated product, and it was chosen because it contained the key functional groups that most likely could form in the reaction. Product D2 and B2 had similarity, which implied that C=O was likely to form during the reaction. Surprisingly, different from DBE reactions, the amount of toluene formed in the reaction was not significant. The reason could be that hydrogen free radicals were hydrogen and oxygen had higher dipole moment so that phenol was formed, and not enough hydrogen free radicals could be provided at this relatively low temperature. So B4, B5, B6, B7 formed instead. The C: H: O: Aromatics in BPE was 13: 12: 1: 2. The ratio from the product was calculated to be 13: 11: 0.9: 2. The error was within 10%. The product was slightly lack of hydrogen and oxygen, there might very little water formed, further investigation is needed.

Table 5.11 Reaction product of BPE at 350 °C

Name	Weight Fraction, %	Molecular Weight	Mole Fraction, %	Formula	Aromatics
 B1	19.44	94	35.23	C ₆ H ₆ O	1
 B2	12.2	168	12.37	C ₁₃ H ₁₂	2
 B3	19.16	182	17.93	C ₁₃ H ₁₀ O	2
 B4	5.6	180	5.30	C ₁₄ H ₁₂	2
 B0	6.06	184	5.61	C ₁₃ H ₁₂ O	2
 B5	8.59	258	5.67	C ₂₀ H ₁₈	3
 B6	11.93	258	7.88	C ₁₉ H ₁₄ O	3
 B7	11.84	270	7.47	C ₂₀ H ₁₄ O	3
 B8	5.2	348	2.55	C ₂₁ H ₁₆ O ₅	3

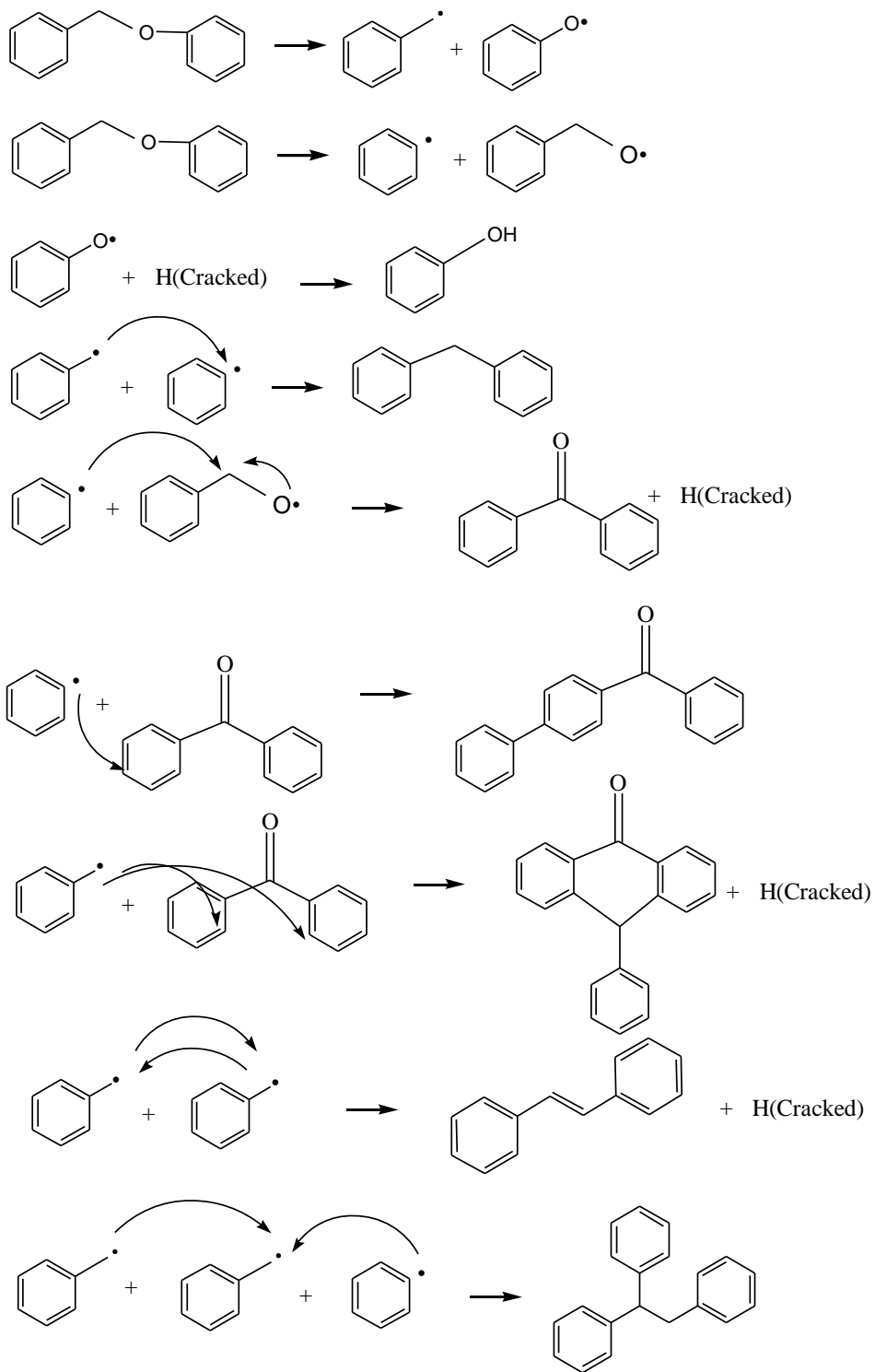


Figure 5.20, reaction network of pure BPE at 350 °C.

Major product of pure BPE reacted at 400 °C were tabulated in Table 5.21. The Product was very similar to when it was at 350 °C. Significant amount of toluene started to form at this temperature. This observation confirmed our previous statements that once the temperature was high enough, more hydrogen free radicals could be released to form toluene. Moreover, the fraction of phenol stayed almost the same, which explained that hydrogen would likely first combine oxygen to form hydroxyl group. Same as the previous reaction, similar product such as B3, B6, B7 consisted more than 40% of total product. Hence, it can be concluded that BPE had high intensity to lose hydrogen to form carbon oxygen double bonds during thermolysis. The C: H: O: Aromatics ratio was 13:11.3:0.8: 2. Same as previous reaction, hydrogen and oxygen was slightly less than what they supposed to be because their might be water formed. Furthermore, different from DBE, there was always significant amount of BPE left unreacted.

Table 5.12 Reaction product of BPE at 400 °C

Name	Weight Fraction, %	Molecular Weight	Mole Fraction, %	Formula	Aromatics
D1	8.63	92	14.74	C ₇ H ₈	1
B1	17.20	94	28.75	C ₆ H ₆ O	1
B2	13.45	168	12.58	C ₁₃ H ₁₂	2
B0	6.11	184	5.27	C ₁₃ H ₁₂ O	2
B3	17.81	182	15.37	C ₁₃ H ₁₀ O	2
B4	5.11	180	4.46	C ₁₄ H ₁₂	2
B5	3.72	256	2.41	C ₂₀ H ₁₆	3
B10	2.3	258	1.40	C ₂₀ H ₁₈	3
B6	11.89	258	7.24	C ₁₉ H ₁₄ O	3
B7	11.92	270	6.93	C ₂₀ H ₁₄ O	3
B8	1.86	348	0.83	C ₂₁ H ₁₆ O ₅	3

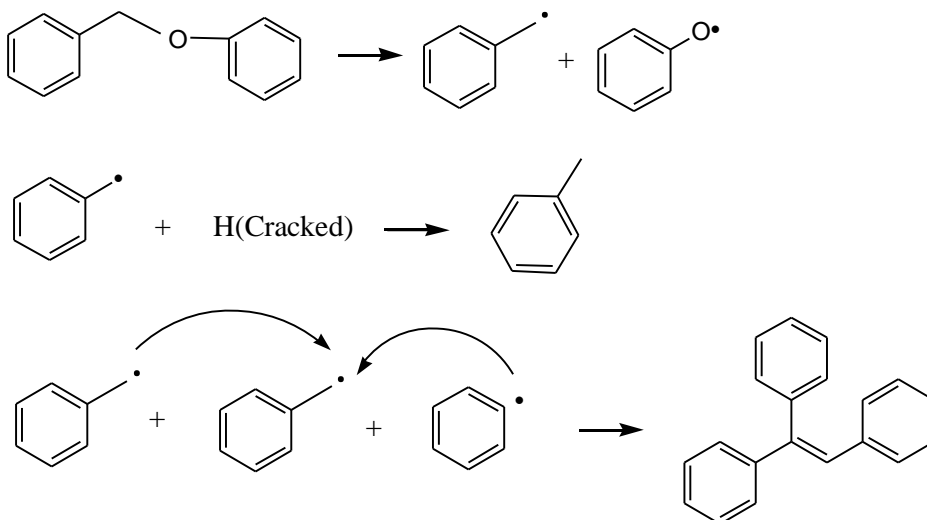
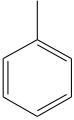
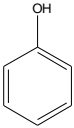
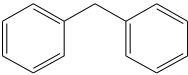
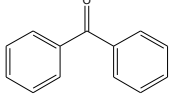
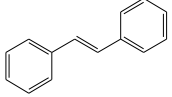
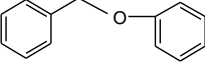


Figure 5.21 Additional reactions of DBE at 400 °C

Major product formed in after 450 °C reaction was tabulated in Table 5.13. Same as DBE at 450 °C, polymerization occurred at this temperature, and the exact chemical compound can hardly be identified. Meanwhile, a lot of hydrogen free radicals were released, and significant amount of toluene was formed due to the hydrogen support. This also caused the decrease of product B6 and B7. Instead of combine with B3, toluene free radical gained hydrogen to form toluene. The ratio of C: H: O: Aromatics at this temperature was 13: 12: 0.7: 2. As previously stated, many polymerized molecules were not included. Hence, this number might not be as accurate as the previous ones.

Table 5.13 Reaction product of BPE at 450 °C

Name	Weight Fraction, %	Molecular Weight	Mole Fraction, %	Formula	Aromatics	
D1		23.13	92	33.36	C ₇ H ₈	1
B1		18.61	94	26.27	C ₆ H ₆ O	1
B2		19.08	168	15.07	C ₁₃ H ₁₂	2
B3		16.23	182	11.83	C ₁₃ H ₁₀ O	2
B4		2.85	180	2.10	C ₁₄ H ₁₂	2
B0		5.66	184	4.08	C ₁₃ H ₁₂ O	2

5.6.3 Reaction of dibenzyl ether with Solvents

DBE Reacted with Solvent at 300 °C

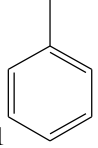
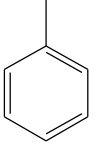
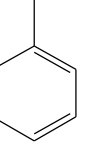
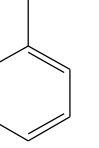
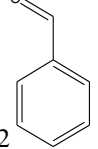
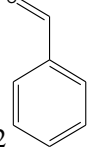
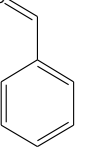
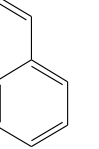
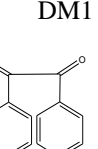
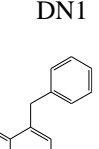
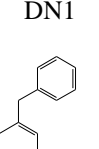
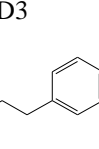
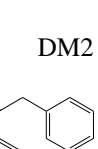
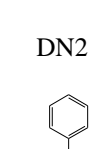
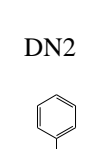
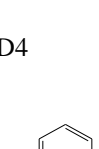
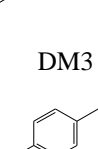
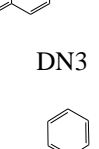
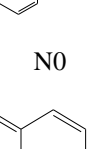
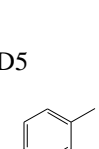
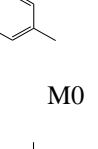
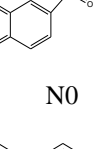
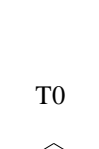
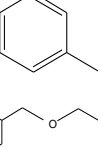
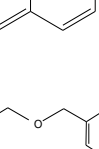
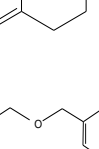
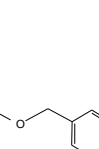
According to the GC-MS plots attached in Appendix A, only the solvent peaks (naphthalene, mesitylene, or tetralin) and DBE peaks appeared. The observation again confirmed that 300 °C is too low for the reaction to occur.

DBE Reacted with Solvent at 350 °C

Reaction at 350°C is what we are going to focus on since there were not many side reactions or polymerization, and the temperature was high enough to let the reaction to

occur. The purpose of adding solvent to the feed is to investigate whether the solvents are hydrogen donor, hydrogen shutter, or diluents during the reaction. Since it is hard to provide the exact weight percentage of each product with each solvent, we only going to provide approximate molar fractions. The most abundant and most representative products were selected, there might be similar structure formed. Among all the ratios, DBE: Solvent= 9: 1 has provided most obvious observation. Major products were tabulated in Table 5.14.

Table 5.14 Major products of DBE with solvents

wMesitylene	Mole%	wNaphthalene	Mole%	wTetralin	Mole%	Pure	Mole%
	39		40		45		37
D1		D1		D1		D1	
	37		41		43		45
D2		D2		D2		D2	
	3		2		1		2
DM1		DN1		DN1		D3	
	2		2		1		3
DM2		DN2		DN2		D4	
	2		2		2		3
DM3		DN3		N0		D5	
	5		3		4	-	
M0		N0		T0			
	3		5		4		9

In the hypothesis, we assumed that, mesitylene is a hydrogen shuttler. In fact, based on the products, it was both a hydrogen shuttler and hydrogen donor. For example, structure DM3 was formed by mesitylene free radical and toluene. A methyl group donated a hydrogen atom at this time. However, based on the amount of mesitylene left unreacted, and product DM1, DM2, Mesitylene was possibly a good hydrogen shuttler. An interesting observation was that the cracked free radicals with oxygen atoms had higher intensity to combine with each other with the presence of mesitylene. Product DM1 and DM2 could hardly be detected once other solvents were used. Detailed explanation needs further investigation. Proposed network is included in Figure 5.22. As indicated in previous sections, toluene was a very good indicator that it only formed when sufficient hydrogen could be provided.

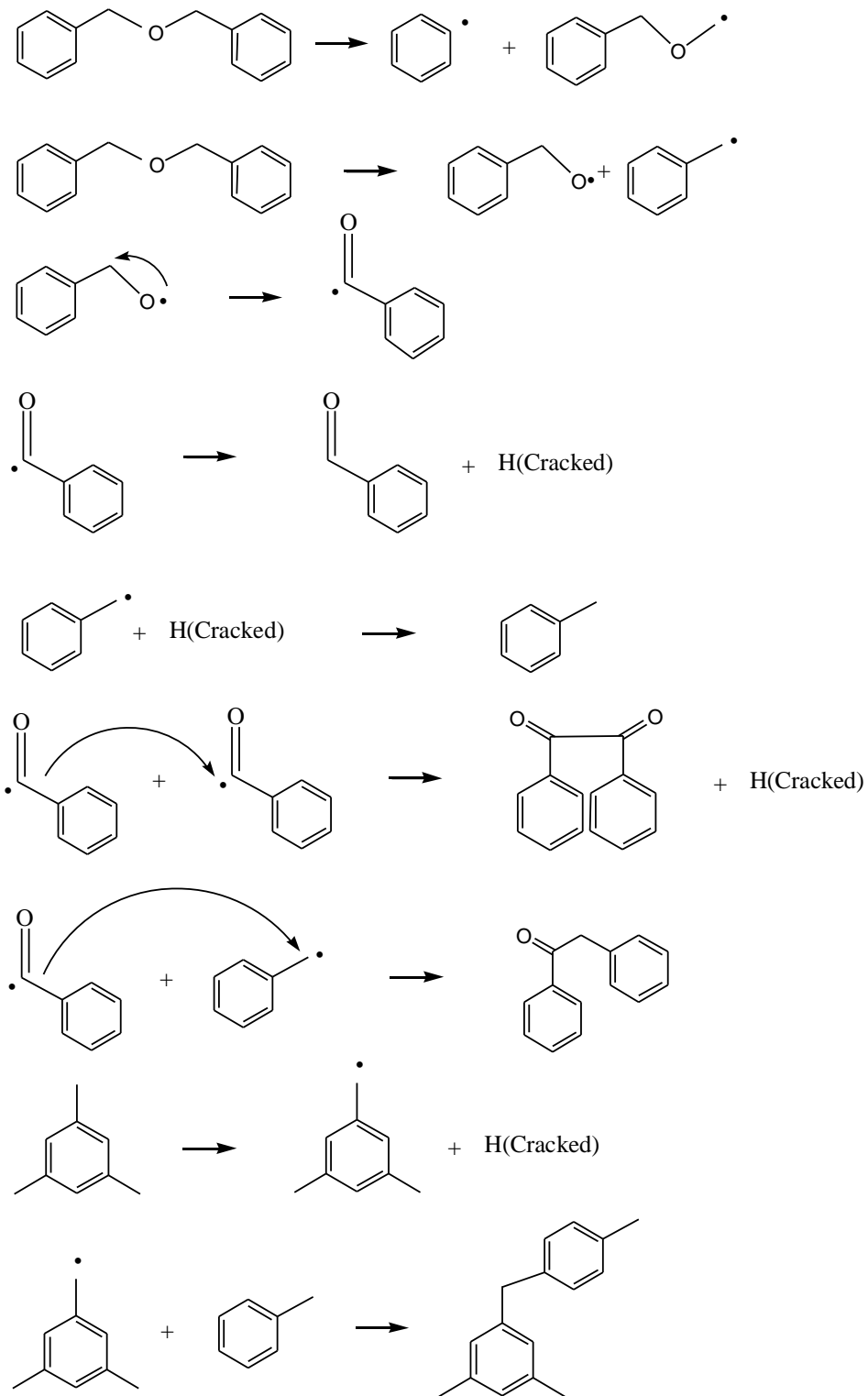


Figure 5.22 Reaction network of DBE with Mesitylene at 350 °C

Since naphthalene is constructed by two benzene rings, which is very stable, it is first assumed that it would only act as a diluent during the reaction instead of participating in the reaction network. However, different from what was expected, naphthalene was a good hydrogen donor. First of all, toluene formed during the reaction was higher than that formed when only DBE was the feed. This indicated some hydrogen was provided. Instead of forming D4, D5, toluene free radicals preferred to react with naphthalene. Hence significant amount of structure DN1 and DN2 formed. Nevertheless, naphthalene was a poor hydrogen donor when compare to tetralin, which will be introduced in the following section.

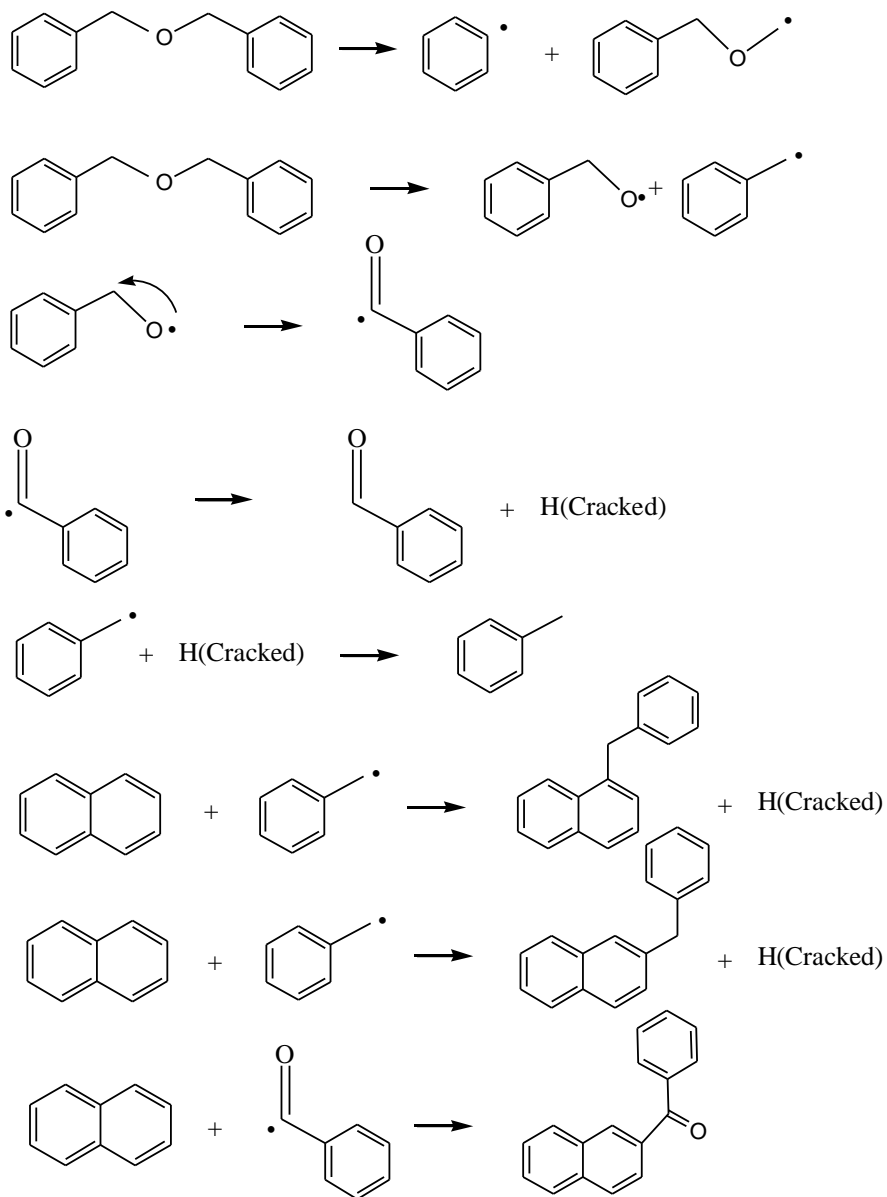


Figure 5.23 Reaction network of DBE with naphthalene at 350 °C

Among all the solvents used in the study, tetralin had the highest toluene yield. Naphthalene was detected in the product. Therefore, we can assume that the cycloalkane in tetralin structure performed as excellent hydrogen donor so that four hydrogen atoms could

once the cycloalkane became aromatics. There were also DN1 and DN2 formed during the reaction. Most toluene formed in this case compare to when other solvents were used.

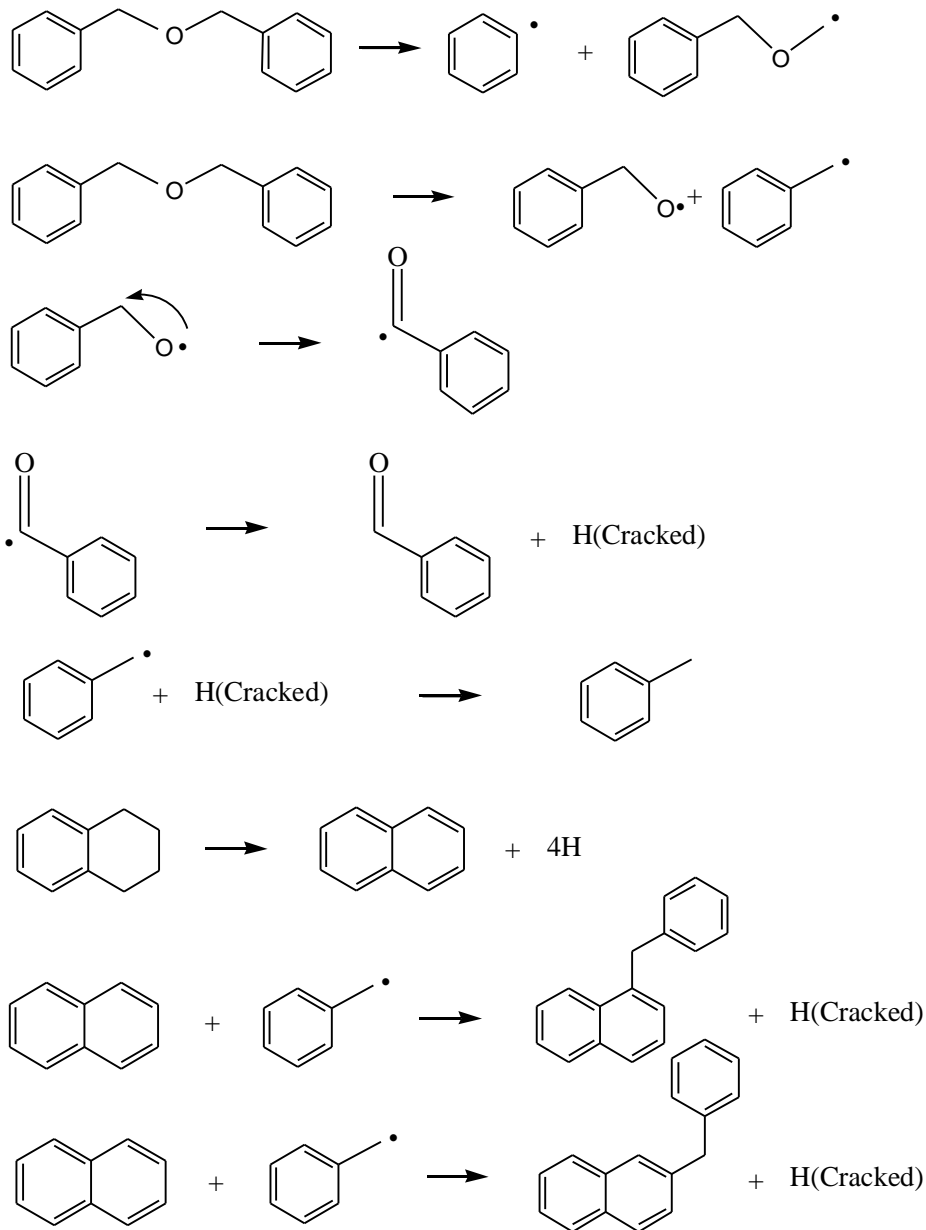


Figure 5.24 Reaction network of DBE with tetralin at 350 °C

Compare reactions with solvents and without solvents, first of all, solvents were always

involved in the reaction network. Secondly, higher conversion of DBE was observed. To further investigate this phenomenon, investigation on reaction kinetics should be carried out. Thirdly, with the appearance of solvents, there was always more toluene formed since more hydrogen could be provided somehow.

DBE Reacted with Solvent at 400 °C

Similar products were formed after the reaction temperature reached 400 °C, and more side reaction occurred (Much more small peaks in GC-MS graphs). For the case of DBE: solvent = 9:1. The approximate molar ratios of toluene product for DBE after reaction were 15%, 13%, 27%, 7% for with mesitylene, with naphthalene, with tetralin, and pure DBE feed, respectively. At this temperature, the effect of hydrogen donor became more and more obvious and effective. For example, every tetralin molecule could donate four hydrogen atoms and then became Naphthalene. Hence the yield of toluene was much higher than the other cases. Toluene free radicals also selectively preferred to interact with naphthalene and mesitylene hence much less compounds such as D3, D4, D5, D6, D7 were formed during the reaction. Again, 400 °C was an interesting temperature that can suppress the formation of toluene compare to 350 °C and 450 °C. Detailed mechanism should be investigated by further experiments.

DBE Reacted with Solvent at 450 °C

At 450 °C, large number of side reactions occurred, and it was very difficult to identify each compound one by one. For the case of DBE: solvent = 9: 1, the molar ratio of toluene in the product was all around 30%, which was much lower than the case of only pure DBE was the feed. This observation was in contradiction with the statement that saying the higher temperature, the more hydrogen would likely to be released to form. One reason could be that the appearance of solvent suppressed the side reactions and polymerization, so that most products could be included in the integration. Another reason could be that even with excessive amount hydrogen, toluene free radical would like to interact with the solvents, and the products were included in the integration. The approximate molar fraction of DM3, DN1+DN2 in naphthalene, DN1+DN2 in tetralin were found to be 5%, 6%, 4%, respectively. Furthermore, same as the situation of pure DBE feed, the amount total oxygen in the product was low. The reason could be that carbon monoxide formed. Significant amount of D6 and D8 were found in the product, which meant benzene free radical formed. Benzene free radical could only be released by Beta scission, which could potentially lose the oxygen.

5.6.4 Reaction of benzyl phenyl ether with solvents

BPE reacted with solvent at 300 °C

At 300 °C, there were only two peaks in GC-MS plots; one was BPE, and the other peak was the solvent. The reaction temperature was too low for any reaction to occur. It agreed with the results gained when pure BPE was the feed.

BPE reacted with solvent at 350 °C

Once again, BPE also started to decompose at 350 °C, and at this temperature, there were not many side reactions or polymerization. Therefore, reactions and products at 350 °C were what we were focusing on. Major components Different from DBE reacted with solvents were tabulated in Table 5.15. Again, the ratio of BPE: Solvents= 9:1 was used because it provided most obvious spectra in GC-MS. Once BPE was reacted with solvents, the conversion of BPE was decreased at 350 °C. Conversion of BPE with Naphthalene was especially low. Based on the reaction network proposed previously, product B1 (phenol) was mainly because of Alpha scission, whereas product B3 was mainly because of Beta scission. Base on the products tabulated in Table 5.15, the amount of B3 remained almost the same, but the amount of B1 was suppressed more than 50%. It is worthwhile to carry out kinetics experiments to look at how that presence of solvents influencing the activation energy of Alpha scissions of BPE.

Table 5.15 Major products of BPE with solvents at 350 °C

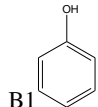
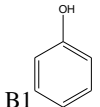
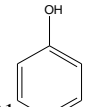
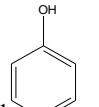
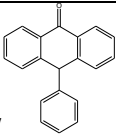
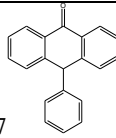
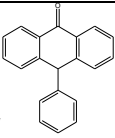
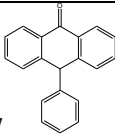
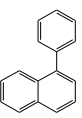
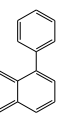
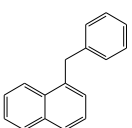
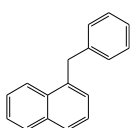
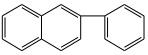
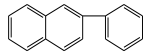
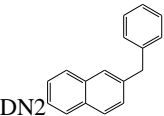
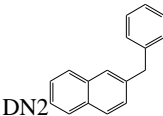
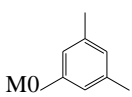
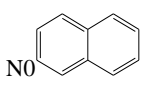
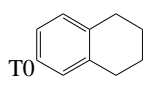
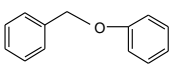
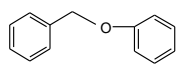
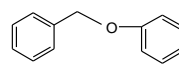
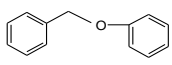
wMesitylen	Mole	wNaphthalene	Mole	wTetralin	Mole	Pure	Mole
e	%		%		%		%
	12		7		19		0
	16		9		17		35
	5		2		4		12
							
							
							
							
							
							
							
							
							
							
							
							
							
							
							
							
							
							
							
							
							
							
							
							
							
							
							
							
							
							
							
							
							
							
							
							
							
							
							
							
							
							
							
							
							
							
							
							
							
							
							
							
							
							
							
							
							
							
							
							

Table 5.16 Major products of BPE with solvents at 350 °C (Cont.)

	1		1		1		7
--			1		1	--	
--			1		2	--	
--			1		2	--	
--			1		2	--	
	16		14		8	--	
	24		40		19		6

When mesitylene was the solvent, major products were almost the same as when pure BPE was the feed. The biggest difference was there were significant amount of toluene formed. As previously stated, hydrogen atoms had higher selectivity to combine with oxygen to form phenol. During the formation of B3, B4, B5, B7, there were always hydrogen released but the amount just sufficient to be provided to form phenol. Hence there was no toluene

formed. However, once Alpha scission was significantly lowered, toluene started to form. No new product was formed that contained the functional groups from mesitylene. Therefore, during the reaction, mesitylene might act as hydrogen shutter. Additional reaction network to pure BPE is included in Figure 5.25.

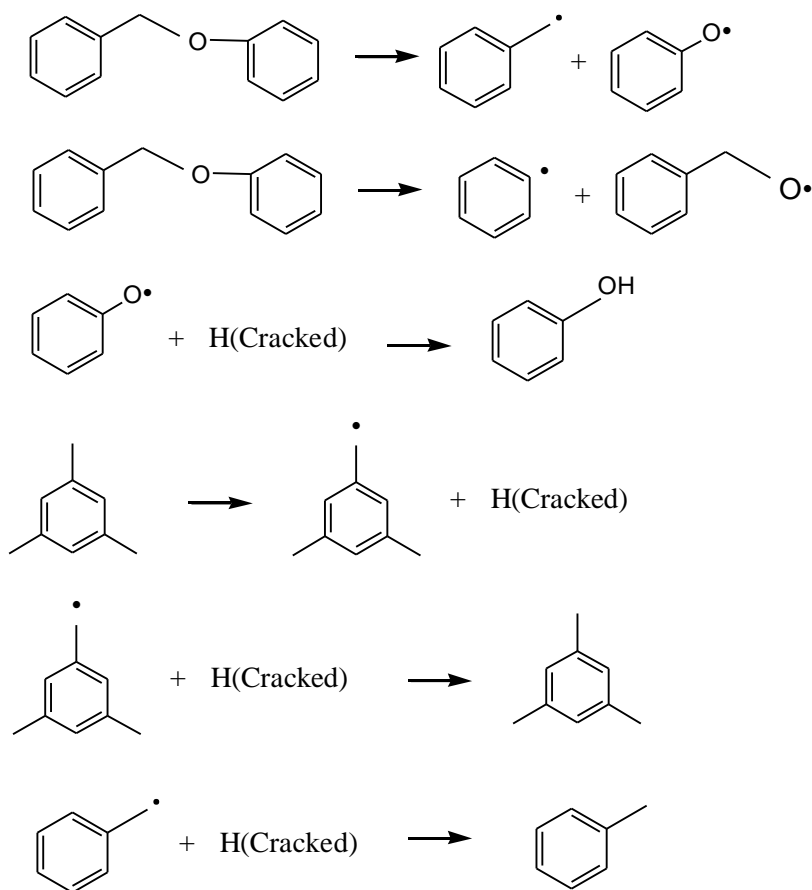


Figure 5.25 Additional reaction network of BPE with mesitylene at 350 °C

BPE reaction with naphthalene had very low conversion. The reason needs further

investigation. Unlike mesitylene, naphthalene participated in the reaction network. Naphthalene actually reacted to form BN1, BN2, DN1, and DN2, depended on how many carbon atoms were attached with aromatic ring in the free radicals. Therefore, here naphthalene was considered as weak hydrogen donor. There was also toluene formed because Alpha scission was also low and sufficient hydrogen was provided. Additional reaction network to pure BPE in this case was included in Figure 5.26.

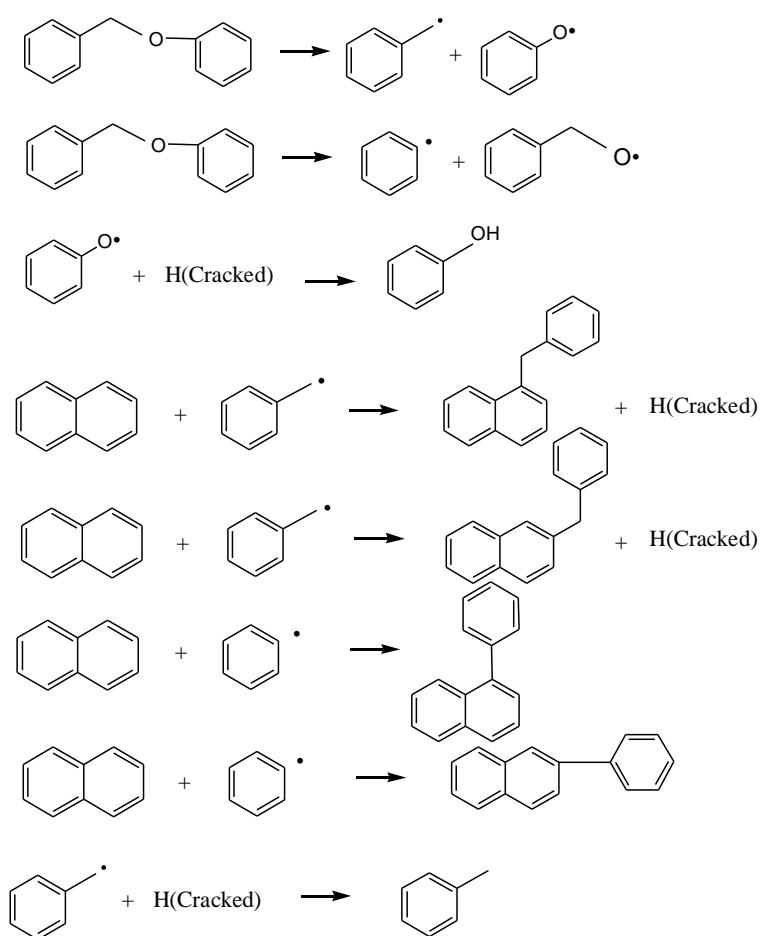


Figure 5.26. Additional reaction network of BPE with naphthalene at 350 °C

For tetralin at 350 °C, the products were very similar with BPE with naphthalene. However,

the conversion was slightly higher than with naphthalene. Same as proposed in DBE reaction networks, tetralin atom first lost four hydrogen atoms became naphthalene, and then alkyl free radicals were likely to combine with the naphthalene. Since tetralin could provide the most hydrogen among the three solvents, the amount of B4, B5, B6, and B7 formed was decreased since toluene free radical no longer needed to react with B3.

BPE reacted with solvent at 400 °C

At 400 °C, more side reactions occurred, but the most abundant products stayed the same as when the reaction temperature was 350 °C. The conversion of BPE became higher but still not as high as its pure form, especially when with naphthalene, there was about 20mole% of BPE left. The amount of toluene formed with mesitylene, naphthalene, and tetralin increased to 18%, 12%, 21% respectively, while the amount of structure B3 stayed almost the same, which means there Alpha scission became more severe whereas Beta scission stayed almost the same.

BPE reacted with solvent at 450 °C

Once the temperature reached 450 °C, major products of all the reactions still stayed almost the same with a lot of noises. The conversion of BPE was still as high as its pure form. Compare the amount of toluene structure B3 formed in the case, there were more toluene

formed than B3. This implied that Alpha scission became more important than Beta scission.

Chapter Six Conclusions and Recommendations

6.1 Conclusions

- Cp value of industrial used solvent (coal liquids) was measured and can be used as reference for industrial research. The DSC calorigram of coal digestion was obtained. A baseline was established after the subtraction of solvent effects. Several heat effects were measured and explained.
- The melting behaviors and thermal decomposition of model ether compounds were studied by DSC. The value from this study is highly consistent with the literature and can be used as a reference in further study
- The reaction pathways of pure model ether compounds were studied to compare with theoretical reaction chain mechanism. Proposed reaction mechanism of benzyl phenyl ether and dibenzyl ether were showed in Chapter 5. It showed that the whole reaction was not as simple as the theoretical reaction mechanism, during the whole reaction; additional elementary reactions were take place. Both pure DBE and pure BPE started to decompose at 350 °C. DBE mainly underwent Beta scission and BPE had both Alpha and Beta scission. At higher temperature, more side reactions and polymerization occurred. The higher reaction temperature, the more toluene formed, since the formation of toluene required hydrogen, and hydrogen was more severely cracked at higher temperature. large molecules. The reaction pathways of

Tetralin, mesitylene and naphthalene were used as solvents. When the ether: solvent ratio equaled 9:1, the products provided most obvious results. The conversion of DBE stayed almost the same, whereas the conversion of BPE was lower when solvents were added, especially with naphthalene. With all the solvents, both DBE and BPE had higher toluene yield, which meant more hydrogen gained during the reaction. All the solvents could act as hydrogen donor, while tetralin had the best performance. Mesitylene could be both hydrogen shuttler and hydrogen donor; however, detailed mechanisms need further investigation. Detailed report can be found in Chapter 5.

6.2 Recommendations for future study

- For thermal decomposition study of coal-related ether compounds, melting points and decomposition temperatures for model compounds were obtained as a context to fill in. For diphenyl ether decomposition, the decomposition temperature is higher than 450 °C, which exceeds the limitation for our experimental setup. For further study the thermal decomposition temperature of diphenyl ether, new High Pressure crucibles for DSC can be applied to complete this blank.
- For reaction pathways of coal-related ether model compounds, the experimental methods we were using were micro-reactor setup and this setup is not ideal for

study fundamental chemistry. The reactor is very consumable under high temperature and high pressure. To confirm the results and conclusions we got from this study, molecular simulation, as a very novel and effective method, should be used to calculate the transition energy of each reaction. Material Studio should be employed for further study of reaction pathways.

- Further study of different coal samples should be carried out in the same experimental conditions. The fundamental chemistry we obtained can be compared and in this way, it is more applicable for improving the coal liquefaction process.